الجمهورية الجزائرية الديمقراطية الشعبية
وزارة التعليم العالي و البحث العلمي

NATIONAL HIGHER SCHOOL FOR HYDRAULICS
"The MujahidAbdellah ARBAOUI"

المدرسة الوطنية العليا للري
"المجاهد عبد الله عرباوي"
ⴰⵢⵙⵙⴰⵏ ⴰⵢⵏⵏⴰⵍ ⵉⵎⵉⵣⵡⴰⵔⵏ ⵏ ⵜⵙⵙⵓⵏⵉⵜ

MEMOIRE DE FIN D'ETUDES

Pour l'obtention du diplôme d'Ingénieur d'Etat en Hydraulique

Option: AMÉNAGEMENT ET OUVRAGES HYDROTECHNIQUES

THEME :

ETUDE DE FAISABILITE D'UN BARRAGE EN TERRE OULED TAOUI (W. AÏN TÉMOUCHENT)

Présenté par :
LAHCEN Abdelaziz Bilal Fayçal

Devant les membres du jury

Nom et Prénoms	Grade	Qualité
HADJ SADOK Ahmed	Professeur	Président
ZAIBAK Issam	M.A.A	Examinateur
BOUZIANE Mamar	M.A.A	Examinateur
BOURI Djamel Eddine	M.C. B	Promoteur

Session juillet 2024

الجمهورية الجزائرية الديمقراطية الشعبية
وزارة التعليم العالي و البحث العلمي

NATIONAL HIGHER SCHOOL FOR HYDRAULICS
"The MujahidAbdellah ARBAOUI"

المدرسة الوطنية العليا للري
"المجاهد عبد الله عرباوي"

END-OF-STUDIES MEMORY

For obtaining the State Engineering Diploma in Hydraulics

Option: **HYDROTECHNICAL PLANNING AND STRUCTURES**

THEME :

FEASIBILITY STUDY OF AN EARTH DAM OULED TAOUI (AÏN TÉMOUCHENT PROVINCE)

Presented by:
LAHCEN Abdelaziz Bilal Fayçal

Before the members of the jury

Last name and First names	Grade	Quality
HADJ SADOK Ahmed	Professor	President
ZAIBAK Issam	M.A.A	Examiner
BOUZIANE Mamar	M.A.A	Examiner
BOURI Djamel Eddine	M.C. B	Supervisor

Session July 2024

Acknowledgements

بِسۡمِ ٱللَّهِ ٱلرَّحۡمَٰنِ ٱلرَّحِيمِ

I express my deepest gratitude and heartfelt thanks to Allah for granting me the strength, wisdom, and perseverance to complete this work. His blessings have guided me throughout this journey, and I am humbled by His grace.

I extend my sincere gratitude to my supervisor BOURI Djamel Eddine, for his invaluable guidance and unwavering support during the past six months. His expertise and commitment to advancing our nation, Algeria, have been instrumental in shaping this work. I am especially thankful for his assistance and insightful guidance related to Plaxis V20 modeling.

This thesis represents the work of a student from the National Higher School of Hydraulics in Blida (ENSH). I am deeply grateful to the researchers at the school who have demonstrated their commitment to advancing scientific research in Algeria. Their insightful scientific articles have significantly contributed to my understanding of various topics: BENLAOUKLI Bachir, HADJ SADOK Ahmed, MEDDI Mohamed, MIHOUBI Mustapha Kamel, TOUAIBIA Bénina & ZEROUAL Ayoub.

Furthermore, I would like to express my gratitude to the professors, administrative staff, and workers at the National Higher School of Hydraulics throughout my academic journey.

I want to show my gratitude to ANBT company for administrative facilities specially the head of engineering department BOUCHAIR Azedine .

Lastly, I extend my sincere appreciation to my uncle, LAHCEN Fayçal, whose unwavering support has been invaluable throughout this scholarly endeavor.

LAHCEN Abdelaziz Bilal Fayçal

Blida, June 2024

الإهداءات

إلى أمي الحبيبة، غريب ن:

رغم أن المسافة تفصلنا في هذا اليوم المهم، إلا أن حبك ودعمك كانا القوة الثابتة التي تدفعني للأمام. تضحياتك وإيمانك الراسخ بي جعلا هذا الإنجاز ممكنًا. هذا النجاح هو لك بقدر ما هو لي.

إلى ذكرى والدي الحبيب، لحسن أحمد:

أبي، رغم أنك غادرتنا في عام 2020 بعد معركة مع سرطان الرئة، إلا أن روحك لا تزال حية في كل ما أفعله. حكمتك وقوتك وحبك يستمرون في توجيهي. أتمنى أن أكون قد جعلتك فخورًا.

إلى أخي، لحسن علي:

منذ عام 2019، فرقتنا المسافة، مع وجودك في اليونان وأنا هنا. لكن اعلم أنك دائمًا في أفكاري. صمودك يلهمني يوميًا.

إلى أخي معاذ وأخواتي ج و ع:

كان دعمكم وحبكم مرساتي خلال هذه الرحلة. شكرًا لكم على كونكم مشجعيّ وقوتي.

إلى أصدقائي الأعزاء، عمار, سفيان, ياسين ويونس :

كانت صداقتكم مصدر فرح ودعم طوال هذه الرحلة الصعبة. شكرًا لكم على الضحك والتشجيع، وعلى وجودكم معي في السراء والضراء.

شكر خاص لـ بن سعيد يونس:

كان توجيهك وإرشادك ودعمك لا يقدر بثمن.

هذا الإنجاز هو شهادة على الحب والدعم والإلهام الذي تلقيته من كل واحد منكم. شكرا لكم على كونكم جزءًا من رحلتي.

: ملخص

تركز هذه الأطروحة على التقييم التفصيلي لمشروع سد ترابي، بدءا بتحليل معمق لمنطقة الدراسة. تم إجراء دراسة هيدرولوجية دقيقة لفهم الظروف الهيدرولوجية المحلية. تضمن الجزء المركزي من الدراسة استخدام برنامج بلاكسيس للنمذجة العددية لسلوك السد تحت مختلف الأحمال، مطبقا نموذج موهر-كولومب وطريقة تخفيض التماسك لحساب عامل الأمان. شمل التحليل السيناريوهات الثابتة والديناميكية قبل ملء السد، بالإضافة إلى آثار ارتفاع مستويات المياه الجوفية حتى الوصول إلى مستوى الملء الأمثل.بالتوازي مع ذلك، تم إجراء تحليل مبتكر للصور الفضائية، باستخدام تقنيات التعلم الآلي مع بايثون، لتقييم التأثيرات المحتملة لتغير المناخ على النهر . مكنت هذه المقاربة من الكشف عن التغيرات المحتملة في مجاري المياه وتحديد كمياتها، مما وفر معلومات حاسمة لإدارة الموارد المائية المستقبلية والتكيف مع التغيرات البيئية.من خلال دمج هذه التحليلات الجيوتقنية والهيدرولوجية وتحليل الصور الفضائية المختلفة، توفر هذه الدراسة أساسا متينا لتصميم وإدارة السد بشكل مستدام، .مع الأخذ بعين الاعتبار التحديات الحالية والمستقبلية المتعلقة بالمناخ والبيئة

.

.

Abstract:

This thesis focuses on the detailed assessment of an earth dam project, beginning with an in-depth analysis of the study area. A rigorous hydrological study was conducted to understand local hydrological conditions. The central part of the study involved using Plaxis software for numerical modeling of the dam's behavior under various loads, applying the Mohr-Coulomb model and the cohesion reduction method to calculate the safety factor. The analysis covered static and dynamic scenarios before dam filling, as well as the effects of rising groundwater levels up to optimal filling. Simultaneously, an innovative analysis of satellite images was undertaken, utilizing machine learning techniques with Python to assess potential impacts of climate change on the nearby river. This approach detected and quantified potential variations in watercourses, providing crucial insights for future water resource management and adaptation to environmental changes. By integrating these various geotechnical, hydrological, and satellite imaging analyses, this study provides a robust foundation for sustainable dam design and management, addressing current and future challenges related to climate and environmental changes.

Résumé :

Ce mémoire se concentre sur l'évaluation détaillée d'un projet de barrage en terre, en commençant par une analyse approfondie de la zone d'étude. Une étude hydrologique rigoureuse a été menée pour comprendre les conditions hydrologiques locales. La partie centrale de l'étude a impliqué l'utilisation du logiciel Plaxis pour modéliser numériquement le comportement du barrage sous différentes charges, en appliquant le modèle de Mohr-Coulomb et la méthode de réduction de la cohésion pour calculer le facteur de sécurité. L'analyse a couvert les scénarios statiques et dynamiques avant le remplissage du barrage, ainsi que les effets de la montée du niveau de la nappe phréatique jusqu'à l'atteinte du niveau de remplissage optimal. En parallèle, une analyse innovante des images satellite a été entreprise, exploitant les techniques d'apprentissage automatique avec Python, pour évaluer les impacts potentiels du changement climatique sur la rivière voisine. Cette approche a permis de détecter et de quantifier les variations éventuelles des cours d'eau, offrant ainsi des informations cruciales pour la gestion future des ressources en eau et l'adaptation aux changements environnementaux. En intégrant ces différentes analyses géotechniques, hydrologiques et d'imagerie satellite, cette étude fournit une base solide pour la conception et la gestion durables du barrage, en tenant compte des défis actuels et futurs liés au climat et à l'environnement.

Contents

Tables list

Figures list

THE LIST OF PLANS

General Introduction

General introduction:

In response to the global demand for sustainable water management and infrastructure development, earth dams stand out as vital components of hydraulic engineering. These dams, constructed primarily from locally available materials such as soil and rock, play pivotal roles in regulating rivers, storing water, and generating hydroelectric power. Their construction offers cost-effectiveness and environmental benefits by minimizing material transportation and integrating seamlessly into diverse landscapes.

The present study focuses on the execution of the Oued Ouizert dam in the Oueled Taoui commune of Ain Témouchent Wilaya. It involves a comprehensive analysis encompassing geological, geotechnical, and structural aspects to assess the feasibility of constructing the dam in this region. The chosen site has been meticulously evaluated for its geological and geotechnical suitability, ensuring minimal risk to foundations and anchoring systems.

The design of the dam integrates innovative approaches, utilizing locally available materials through meticulous optimization studies. This approach guarantees stability under various load conditions, as demonstrated through advanced geotechnical modeling using Plaxis software. The study includes the application of the Mohr-Coulomb model and the C phi reduction method to calculate safety factors under static and dynamic conditions before and during dam filling.

Moreover, the study addresses the significant challenges posed by climate change, particularly the anticipated impacts on declining river water levels. It emphasizes the importance of alternative water management strategies and thorough environmental assessments to mitigate risks and ensure sustainable development.

By leveraging theoretical knowledge and advanced technologies such as Plaxis software and Python-based machine learning for satellite image analysis, this research provides a comprehensive framework for the design and execution of the Oued Ouizert dam. It aims to contribute valuable insights into the sustainable development of water infrastructure, integrating scientific rigor with technological innovation to address current and future challenges effectively.

Chapter I:
PRESENTATION OF THE STUDY AREA

Part 1: Presentation of the study area

1.Introduction:

To construct dams, it is necessary to carry out in-depth topographic, geological, and geotechnical studies in order to ensure the safety of the project.

Before starting the preliminary design, the main criteria for choosing the site and the type of dam must be defined. In some cases, several types of dams can be considered.

The costs must then be compared in order to choose the best solution.

This chapter presents the work to be done to select a potential site, the axis of the dike and its ancillary structures, and to characterize the geotechnical quality of the foundation soil, construction materials, and the permeability of the dam soils.

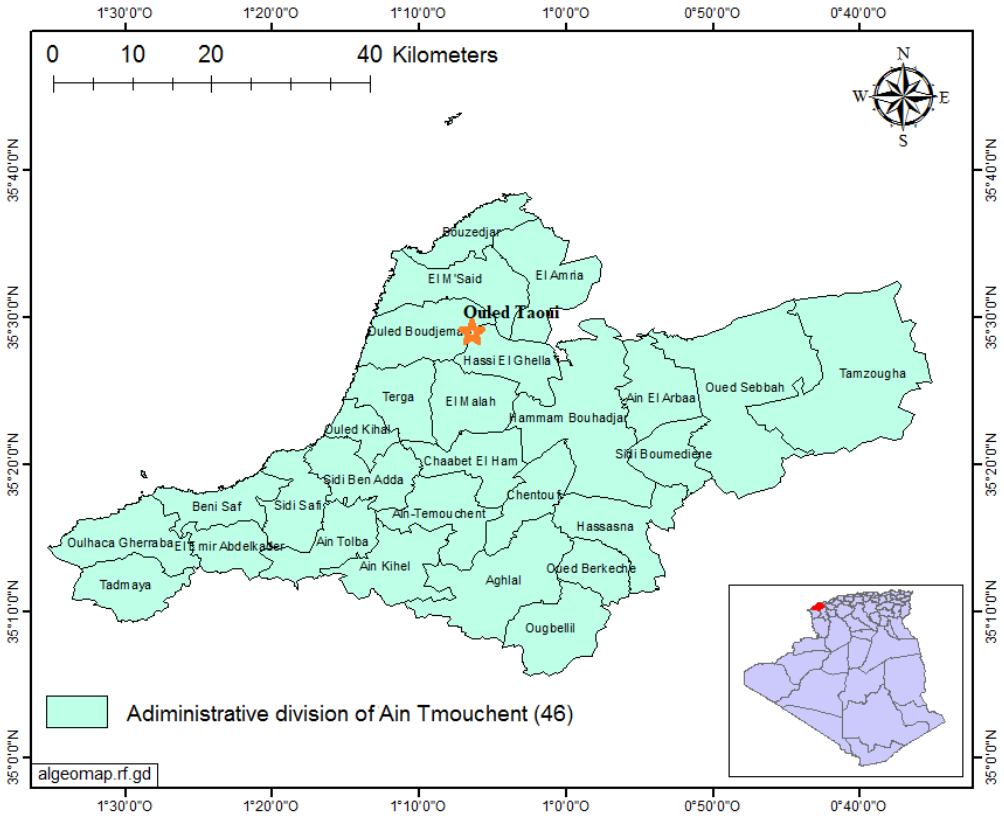

Figure I.1: Adiministrative map shows the position of the commune of Ouled Taoui in the wilaya of Ain Temouchent**.** Source: algeomap.rf.gd

2. Geographic Situation:

The future hill dam on Oued Ouizert is located in the commune of Ouled Taoui in the wilaya of Ain Temouchent approximately 1 km as the crow flies northeast of the chief town of the commune.

The axis of the reservoir is located on the Lourmel staff map No. 180 at the following Lambert coordinates:

X: 153.00 km Y: 248.30 km Z: 66.00 m

Access to the site is via a track about 1 km from the town of Ouled Taoui, on the left of the road conneting it to Hassi El Ghella.

3. Natural Regional Framework:

From a socio-economic point of view, the region studied is essentially an agricultural region.

Indeed, in the past the region experienced great development in vine cultivation, particularly along the banks of the Rio Salado and the large Sebkha, whose predominant silty soils were well suited to this type of cultivation.

During on-site reconnaissance, observations on current cultural traditions, supported by our various interviews with farmers in the region, show two agricultural trends in the downstream areas representing the plain. The land located in the Ouled Taoui region is mainly devoted to market gardening, essentially producing tomatoes, peppers, onions, and green beans, while the trend in the Ouled Boudjemaa region leans much more towards cereal cultivation.

Finally, from a purely technical point of view, knowing the nature of the land in the region, essentially represented by limestones, sandstones, and silty sands, we can affirm that the types of crops best suited to the region are:

- For soils consisting of limestone scree (hillsides and feet of hills), vine cultivation would be the best adapted.
- The silty lands (Ouled Boudjemaa which are not subject to capping) are most suitable for cereal cultivation along with beet and potato cultivation.
- The Oued Taoui region, much richer in calcareous and sandy-silty soils, would be best suited for market gardening in general and especially potato cultivation.

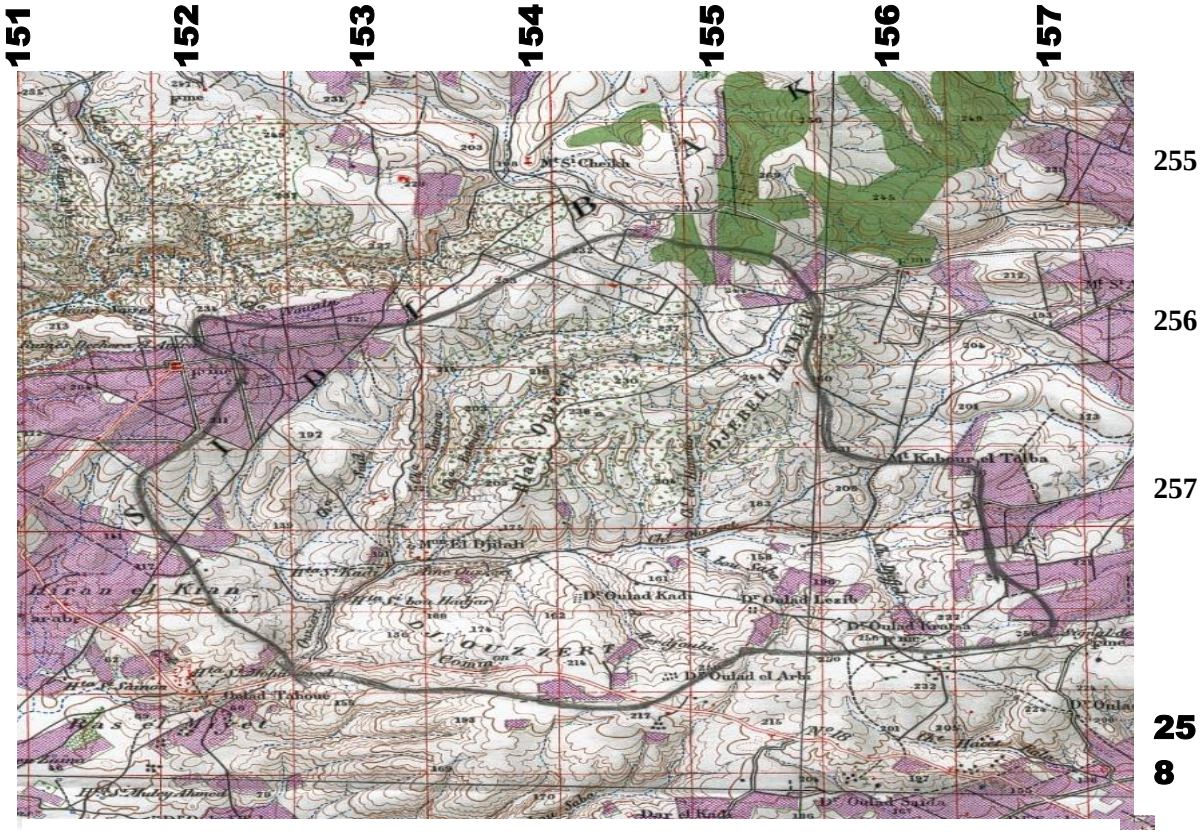

Figure I.2: Extract from Ordnance survey map N° 180 LOURMEL

Source : ABH

4. Hydrological Overview:

The characteristics of the watershed are:

- Area: 26.26 km2
- Perimeter of the watershed: 22 km
- Length of the thalweg: 7 km
- Average altitude: 183 m
- Compactness index: 1.20
- Thalweg slope: 2.4%

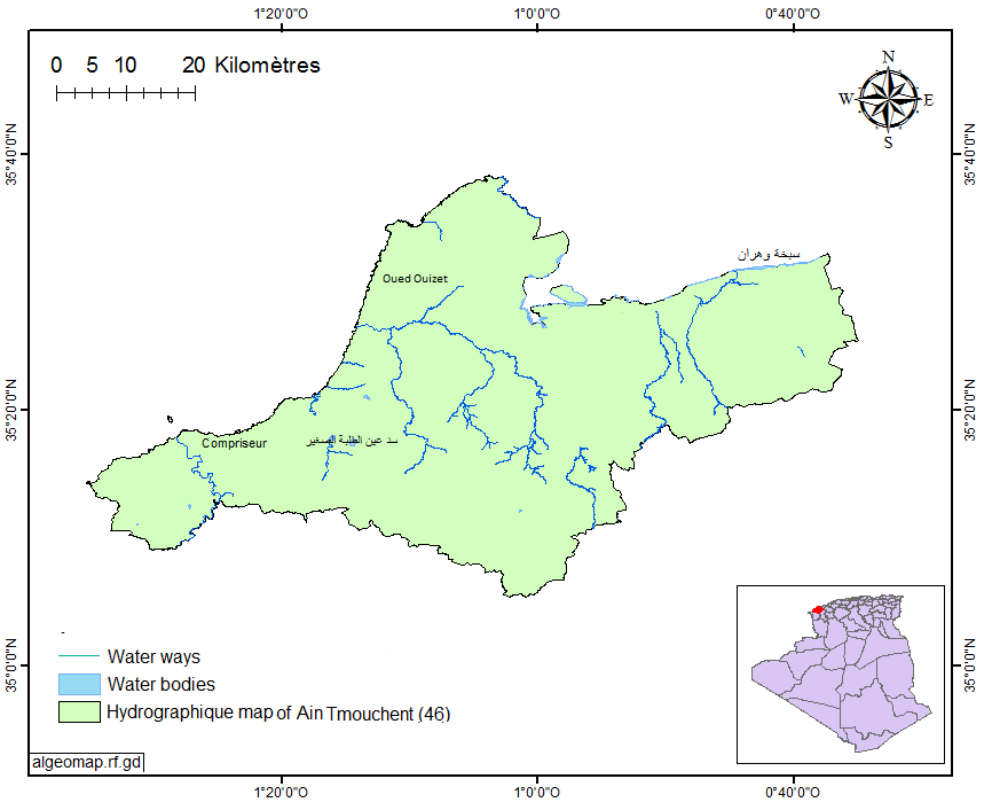

Figure I.3 : Hydrographic map of Ain Temouchent (Water ways) .

Source : algeomap.rf.gd

The characteristics of the wadi regime are:

- Concentration time: 4.0 h
- Average annual rainfall: 388 mm
- Average maximum precipitation: 44.14 mm
- Average annual inflow: 1.1 hm3
- 80% frequency inflow: 0.50 hm3
- Centennial flood flow: 76 m3/s
- Centennial flood volume: 0.912 hm3
- Solid inflow: 11250 T/year

5. Geological Overview:

According to the geological map of the region "Lourmel No. 180", and the on-site reconnaissance, the main geological formations forming the Oued Ouizert watershed are white limestones, which are the majority distribution in the basin, followed by alluvial deposits in the form of red marly sandstones, sandstones, and sands.

In the downstream terraces, clay pockets have been observed, however their availability in the necessary quantity and quality must be confirmed by the geotechnical study.

Finally, let us note that the quality of the predominant quarry outcrops in the reservoir area cannot be used as riprap due to their friability.

From a seismic point of view, the study region can be classified as zone II, i.e. an area with a fairly high seismic risk with a seismic acceleration of around 0.20g.

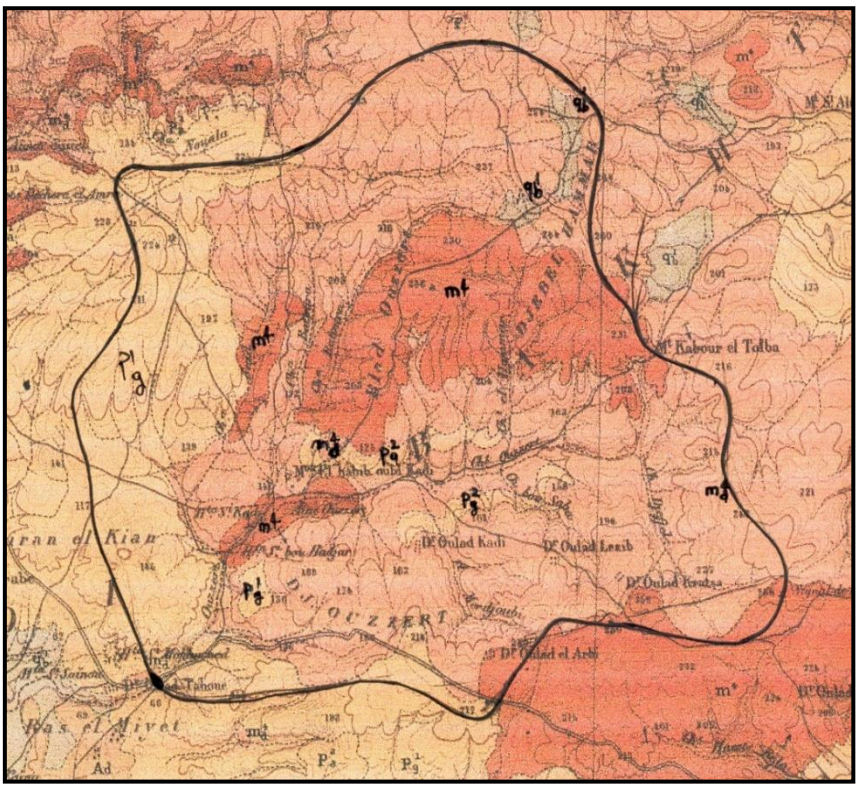

Figure I.4: Watershed of the Ouizert River Extract from Geological Map No. 180 Lourmel, scale: 1/50,000. Source : ABH .

LEGEND

m4: Massive white limestones (Upper Sahelian).

m4d: Chalky limestones.

p1g: Sandstones and helical sands.

6.Dam Type:

While awaiting the conclusions of the geological investigations, it is possible to consider at the current stage, taking into account:

- Available materials and their proximity
- Nature of the foundations
- Height of the dike
- Safety of the dam and downstream infrastructure

We are going to study: Heterogeneous Dike (clay core and alluvial shell)

Part 2: Hydrochemical study area

1. Issues related to water chemistry:

Given the modest size of the Ouizert river basin (barely 26 km2), where the future Ouled Taoui reservoir will be built, specialized institutions like ANRH do not have any data on water quality.

Chemical analysis of surface water must be conducted over several years due to variability in concentrations of components like chlorides, sulfates, carbonates, etc., which depends on fluctuating flow rates. However, ANRH only performs such frequent water analyzes for large rivers with hydrometric stations. During our visits to the reservoir site, the absence of flow in the Ouizert river prevented sample collection for analysis.

The flow rates of the Ouizert river, like other rivers, change significantly throughout a hydrological year. It experiences varying degrees of flooding during rainfall and is dry on other days. Therefore, analyzing a sample from any rainy episode alone cannot provide reliable data on water quality.

2. Theoretical evaluation of water quality:

analyzing periodically collected water samples Besides over several hydrological years (as done for rivers with gauging stations), it's common for studies of hillside reservoirs intended for irrigation to analyze geological formations within the watershed and chemical soil analysis of the riverbed to detect any materials that could alter water quality. After evaporation and infiltration, traces of soluble salts remain on and within the soil.

Water quality for irrigation purposes is not subject to the strict standards applied to drinking water. Generally, measurements focus on elements like carbonates, chlorides, and sulfates, whose excess can be harmful to agriculture.

3. Searching for sources of water quality alteration:

The main factors influencing water’s chemical composition and quality are:

- Domestic and industrial waste
- Agriculture (use of fertilizers and manure)
- The geological nature of the formations crossed

The absence of urban or industrial areas within the Ouizert river basin eliminates the risk of water pollution by elements such as chlorine, silicates, sulfur, fluorine, copper, zinc, manganese, nickel, chrome, detergents, hydrocarbons, etc. Also, the lack of intensive or large-scale

agriculture protects the water from contamination by nitrates, sulfates, phosphates, nitrogen, etc.

The only elements that can enter the water composition are those related to the solubility and erosion of geological formations crossed, which are generally:

- Carbonates (CaCO3) from sedimentary rocks such as clayey soils, marl, chalk, and limestone.
- Chlorides (NaCl…) mainly from gypsums, saline clays, salty loams, and sylvinite (raw quarry salt).
- Sulfates (SO4) which can come from gypsums (hydrated calcium sulfate) and anhydrite (anhydrous calcium sulfate).

The Ouizert river basin is mostly composed of white limestones, chalky limestones, sandstones, sands, and sandy marls. No presence of saline soils such as gypsums, clays, and salty loams is detected (this type of soil is concentrated in the large Sebkha).

4. Results of soil chemical analyses:

Chemical analyses performed on samples from drillings and excavations gave the following results:

Carbonates:

Right bank and riverbed: A concentration of CaCO3 around ***12.2%,*** indicating a clayey predominance.

Right bank**:** A concentration of carbonates varying between ***33.48*** and ***62.65%,*** revealing a more limestone tendency.

Carbonates are generally insoluble (except in the presence of water charged with carbon dioxide) and have physical characteristics favorable to agriculture.

Chlorides:

The analyses for chloride percentage evaluation were negative as no trace was detected in all examined samples, most of which concerned drilling S1 in the riverbed.

Sulfates:

The analyses for sulfate percentage evaluation were negative as no trace was detected in all examined samples, most of which concerned drilling S1 in the riverbed.

Note: Generally, chlorides and sulfates are products mainly from industrial and agricultural discharges where they are used on a large scale in textile industries and farms as fertilizers. These two activities are completely absent within the Ouizert river basin limits.

5. Results of water chemical analyses:

Water samples collected during the first week of November 2003 (first rains) were subjected to laboratory analyses to determine their chemical potability. However, the absence of significant flow in the riverbed led us to confirm the results of the water analysis taken from the residual flow in the riverbed by analyzing a sample from the aquifer taken from a well located in the basin.

The analysis of the results allows us to draw the following conclusion:

An excessive concentration of soluble salts in water can have toxic effects on plants. Chlorides, especially Sodium Chloride (NaCl), cannot be tolerated in the nutrient solution at levels higher than 5 g/l. Their presence in soil is less significant as they can be removed by leaching.

The analyses reveal 1.2 g/l of NaCl in the aquifer and 0.243 g/l in the river, which is well below the tolerated maximum.

The difference in concentration between well water and river water can be explained by the influence of the nearby salty Sebkha on the aquifer at Ouizert river.

Sulfates, which have medium toxicity, contribute to increasing water's concentration in soluble salts; therefore, they cannot be tolerated in irrigation water at high rates.

In any case, the total Chlorides - Sulfates should not be tolerated at rates > 8 - 10 g/l in irrigation water. In this case, this sum is very low (see appendix).

For bicarbonates ($NaHCO_3$, $Ca(HCO)_2$, $Mg(CO_3)_2$…), which at high levels in irrigation water tend to precipitate Calcium and Magnesium, thus reducing Sodium absorption from water, they are only proscribed at high rates exceeding Chlorides and Sulfates tolerance.

Table I.01 : Water chemical analysis result **.**

The sample / Parameters		Well	River (wadi)
PH		6.8	6.7
Total hardness		38.5 °F	48 °F
Alkametric strength	**TAC**	31.66 °F	33.33 °F
	TA	none	none
Chlorides		745.5 mg/l	274.5 mg/l
NaCl		1228.5 mg/l	243.36 mg/l
Sulfates SO_4^{2-}		160.17 mg/l	82.64 mg/l
H_2SO_4		163.52 mg/l	133.32 mg/l
NaOH		253.28 mg/l	279.97 mg/l
$NaHCO_3$		532 mg/l	166.51 mg/l
$CaCO_3$		316.16 mg/l	259.43 mg/l
$Ca(HCO_3)_2$		512.89 mg/l	339.94 mg/l
$Mg(HCO_3)_2$		462.24 mg/l	234.04 mg/l

6.Conclusion:

Based on the water analysis results, it is easy to deduce that the water from the future dam on Taoui river is usable for irrigation purposes.

Chapter II: Hydrological Study

Part I: Hydrological study of the watershed

1.Introduction:

Hydrology is the science that studies terrestrial waters, their origin, movement and distribution on our planet, their physical and chemical properties, their interactions with the physical and biological environment and their influence on human activities..

This definition of hydrology makes it a multidisciplinary science involving:

- Meteorology and climatology: study of rainfall and its return to the atmosphere.
- Geography, geology and pedology: analysis of the basin's hydrological behavior.
- Hydraulics: measurement and study of free-surface flows.
- Statistics: data processing, simulations, etc.
- Numerical calculation: flood propagation, models, etc.
- Computing: as a working tool for numerical calculation, data storage, etc.
- Chemistry, biology, cartography, physics, mathematics, RO, etc.

2.Definition of a watershed:

The watershed of a watercourse can therefore be defined as all the land on which all the water feeding the watercourse flows, infiltrates and runs.

It's an area in which all water flows converge towards a single point, the basin's outlet. So every drop of water that falls into this territory delimited by natural boundaries flows towards the watercourse or its tributaries, then downstream towards its outlet.

3.Presentation of the watershed:

This study focuses on the Oued Ouizert watershed, located in the Ouled Taoui commune, wilaya of Ain Témouchent.

The Oued Ouizert watershed is part of the large hydrological basin of the Oranese coast, code 04, with its outlet located in the commune of Ouled Taoui - Wilaya de Ain Témouchent.

The axis of the future dam, which will represent the outlet of the Oued Ouizert watershed and limit the surface area drained, is located at Lambert coordinates

X : 153.00 km ; Y : 248.30 km ; Z : 66 m

The Oued Ouizert watershed, with its gentle relief and rounded shape, rises from altitudes of around 264 NGA to reach values close to 66 NGA at its outlet..

Finally, it is worth noting that the watershed has a moderately developed vegetation cover, consisting mainly of scrub with a few shrubs along the watercourse.

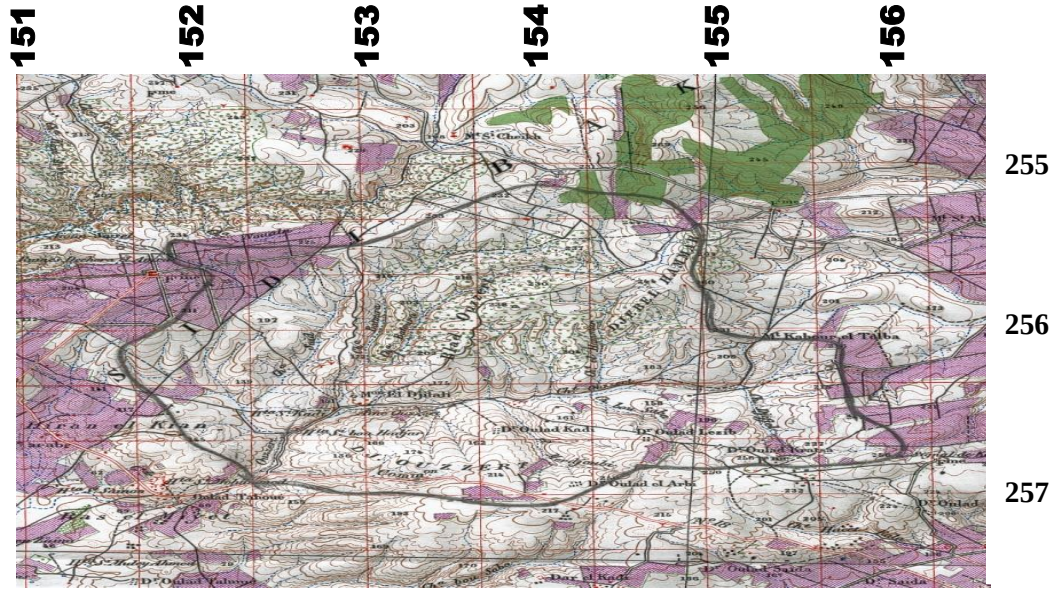

Figure II.1: Extract from Ordnance survey map N° 180 LOURMEL

Echelle 1 /50.000 è . Source : ABH.

4.Morphometric characteristics of the watershed:

The area, perimeter and length of the watershed's thalweg were determined using AutoCad 2000 software, after digitizing the 1:50,000 Lourmel major survey map and delineating the watershed contour.

Surface area:

The surface area of the watershed is:

$$S_{bv} = 26.26 km^2$$

Perimeter:

The perimeter of the watershed is:

$$P_{bv} = 22.00 km$$

Length of main thalweg:

The main Thalweg is:

$$L = 7.00 km$$

Compactness index:

There are a number of parameters that serve to describe the shape of a drainage basin, such as the Gravelius compactness index which is defined as the ratio between the perimeter of the watershed and the perimeter (or circumference) of the circle with the same surface area as this basin. The closer this coefficient approaches 1, the more compact the watershed shape will be. It will be elongated otherwise.

$$K_c = K_G = \frac{P}{2\pi R} = \frac{P}{2\pi\sqrt{\frac{A}{\pi}}} = \frac{P}{2\sqrt{\pi . A}} = \frac{1}{2\sqrt{\pi}}\frac{P}{\sqrt{A}} = 0.28\frac{P}{\sqrt{A}}$$

K_C = Gravelius coefficient.

P = watershed perimeter (km).

A = watershed area (km^2).

$$K_c = 1.2.$$

Result: K_c>1,128 so our basin is then "**elongated**"

Equivalent rectangle:

The concept of the equivalent rectangle, introduced by Roche (1963), makes it easy to compare watersheds with regard to the influence of their characteristics on flow.

The rectangular watershed is the result of a geometric transformation of the real watershed, in which the same surface area, perimeter (or the same K_C) and therefore consequently the same hypsometric distribution are preserved.

If L and B represent the length and width respectively of the equivalent rectangle, then :

$$L = \frac{K_G \cdot \sqrt{A}}{1.12} \cdot \left[1 + \sqrt{1 - \left(\frac{1.12}{K_G}\right)^2}\right] \quad K_G \geq 1.12$$

$$B = \frac{K_G \cdot \sqrt{A}}{1.12} \cdot \left[1 - \sqrt{1 - \left(\frac{1.12}{K_G}\right)^2}\right] \quad K_G \geq 1.12$$

Where:

L = the lenght of the equivalent rectangle

(km);

B = the width of the equivalent rectangle

(km);

K_G = Gravelius compactness index

A = the area of the watershed (km^2).

P = the perimeter of the wtershed (km).

L = 7.5 km; B = 3.5 km

$S_{rectangle}$= 7.5*3.5 = 26.25 km^2

$P_{rectangle}$= 2*(7.5+3.5) = 22 km

Result: We can clearly see that by making this geometric transformation, the surface area and perimeter of our watershed are relatively preserved..

Table II.01: Summary table of watershed characteristics

DESIGNATION		SYMBOLE	UNITE	VALUES
Surface		S	Km^2	26.26
Perimetre of the watershed		P	Km	22.00
Length of the main thalweg		L	Km	7.00
Altitude	Average	H_{moy}	M	183
Altitude	Max	H_{max}	M	264
Altitude	Min	H_{min}	M	66
Drainage density		D	Km/km^2	1.13
Campactness index		K c	-	1.2
Equivalent rectangle		L	Km	7.5
		B	Km	3. 5
Slope of the thalweg		I	%	2.4

5.Hydrographic Characteristics:

5.1. Relief:

: The influence of relief on flow is easily understood, as many hydrometeorological parameters vary with altitude (precipitation, temperatures, etc.) and the morphology of the basin. In addition, the slope influences the flow speed. The relief is also determined by the following indices or characteristics:

5.2. The Hypsometric Curve:

The relief of the watershed is often characterized by the hypsometric curve. This represents the distribution of the surface of the watershed according to its altitude.

It carries on the abscissa the surface (or the percentage of surface) of the watershed which is above (or below) the altitude represented on the ordinate.

The following table indicates the distribution of surfaces according to the coasts.

Table II.2: Distribution of surfaces according to the coasts.

N°	Coast (m)	Hi (m)	Si (km²)	Si / S (%)	Si / SCum (%)
1	264 : 250	257	0.30	1.14	1.14
2	250 : 200	225	9.69	36.90	38.04
3	200 : 150	175	10.66	40.59	78.63
4	150 : 100	125	4.87	18.55	97.18
5	100 : 66	83	0.74	2.82	100

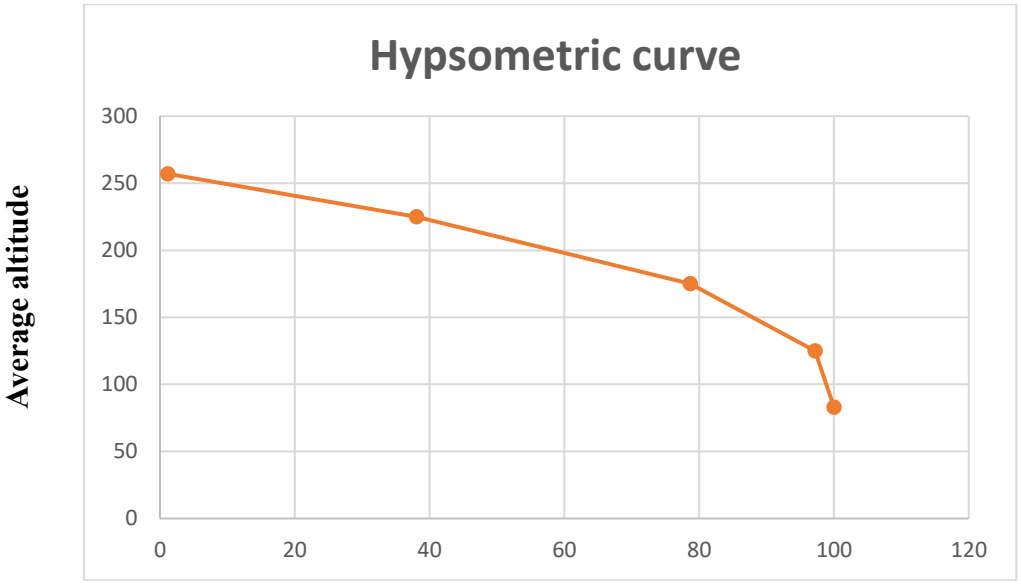

Figure II.2: Hypsometric curve.

From hypsometric curve we get:

H_{max}= 267 m.

H_{min}= 83 m.

The altitude $H_{5\%}$ = 250 m.

The altitude $H_{95\%}$ = 130 m.

The median altitude $H_{50\%}$ =218 m.

The average altitude H_{moy} = 183 m.

Result:

From the shape of the hypsometric curve, we can conclude that our watershed has a slope that is somewhat steep for low altitudes, while for high altitudes we observe a relatively gentle slope.

5.3. Global slope index :

The global slope index is considered to be a good evaluative index of the relief of the watershed, it is determined as follows:

$$I_g = D/L = 6 \text{ (m/km)} = 0.006 = 0.6\%.$$

Where:

I_g = global slope index (m/km).

D = the difference in altitude H5% -H95% = 120 m.

L = Length of equivalent rectangle (km).

Note: Based on the result obtained and the table below, we can conclude the characteristic of the watershed slope.

Table II-3: Relief classes with their descriptions.

Descriptions	Slopes in m/km
Low slope	2 < Ig < 5
Moderate slope	5 < Ig < 10
Quite steep slope	20 < Ig < 50

Source : USBR.

Result: As Ig=6 (m/km) our watershed has a moderate slope.

5.4. Average slope index:

The average slope is an important characteristic that informs about the topography of the basin. It is considered as an independent variable. It gives a good indication of the travel time of direct runoff, therefore on the concentration time, and directly influences the point flow during a shower.

The average slope is then given by the following relation**:**

$$I = D*L/A$$

Where: I = average slope of the watershed (m/km);

∑l = totale length of contour lines (km).

D = constant altitude difference between two contour lines (m).

A = total area of the watershed drainage (km^2).

$$I = 18.2$$

Result: We clearly see that the watershed has a slope that is relatively gentle.

5.5. Longitudinal profile of the watercourse:

Represents the altimetric variation of the bottom of the watercourse in relation to the distance to the outlet.

This representation becomes interesting when we plot the secondary watercourses of a watershed, which can then be easily compared with each other and with the main watercourse**.**

. The longitudinal profile of a watercourse allows to define its average slope.

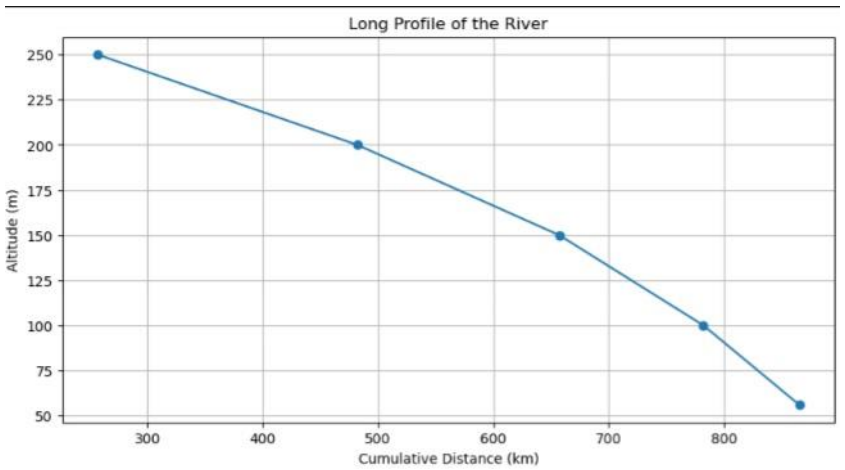

Figure II.3: Longitudinal profile of the watercourse

Result: We observe from the longitudinal profile of the watercourse that it has a relatively steep slope.

5.6. The concentration time Tc:

The concentration time **Tc** of the waters on a watershed is defined as the maximum duration necessary for a drop of water to travel the hydrological path between the furthest point of the basin and the outlet of the latter.

Several formulas for determining the concentration time have been developed, the most common are:

GIANDOTTI formula:

$$T_c = 0.6615.L^{0.77}.I^{-0.385} = 4.15 heures$$

KIRPICH formula:

$$T_c = \frac{4\sqrt{S} + 1.5L}{0.8\sqrt{H_{moy} - H_{\min}}} = 3.58 heures$$

Improved PASSINI formula:

$$T_c = \left[\frac{4\sqrt[3]{\sqrt{S.L}}}{\sqrt{I}}\right]^{0.75} = 4.47 heures$$

With:

- S: watershed area in Km².
- L: length of the main thalweg in Km.
- I: slope of the Thalweg in percent for Kirpitch and per thousand for Passini.
- H : Elevation in m.
- Hmoy: Average altitude of the watershed.
- Hmin: Minimum altitude of the watershed.

Given that the average value of the three methods is 4.07 hours, and considering that it is not necessary in practice to estimate the concentration time of a watershed with very high precision, we will use the following value for our subsequent calculations:

Tc = 4.0 hours

5.7. Runoff speed:

It is given by the following formula:

$$V_r = L/T_c = 1.75 \text{ km/h}$$

Where:

L: is the length of the main talweg; L = 7 km.

T_c: is concentration time of the flow; T_c = 4 hours.

5.8. Drainage density:

The drainage density, introduced by Horton, is the total length of the hydrographic network per unit area of the watershed:

$$D_d = \frac{\sum l_i}{A}$$

Where:

D_d = drainage density (km^{-1})

∑l = total length of the watercourses in the basin = 29.26 km.

A = area of the watershed= 26.26 km^2.

$$D_d = 1.13 km^{-1}$$

Result:

A lower drainage density, like 1.13km-1, is preferable as it generally indicates a less rugged terrain and potentially more stable to support the dam structure. Moreover, with fewer watercourses to manage, there could be less risk of erosion or dam overflow.

6.Climate:

The climatic conditions that prevail in the study region will be described by the measurements and observations available at the nearest measurement stations and sites.

Thus, for the Oued Ouizert reservoir, the climatic characteristics in question can be approximated by the measurements made at the Es Senia, Oran, and Sarno dam stations.

6.1.Temperatures:

Generally, the climate of the region is Mediterranean, characterized by a hot, dry summer and a relatively mild winter.

The average temperature in this region is around 16.2°C, generally, the coldest months are December and January with temperatures oscillating between 10°C and 11°C..

As for the hottest months, it is certain that the months of July and August are quite designated with temperatures of the order of 23°C to 25°C, and a maximum monthly average temperature of the order of 29.4°C recorded at Oran IHFR.

The average and extreme temperatures of the Oran IHFR station are summarized below:

Table II-4: The average and extreme temperatures of the Oran IHFR station.

T° C	Sep	Oct	Nov	Dec	Jan	Feb	Mar	Apr	May	Jun	Jul	Aug	Year
Avg	21.5	17.0	13.3	10.6	10.4	11.4	12.0	13.5	16.8	19.8	23.1	24.4	**16.2**
Max	27.1	22.5	19.0	16.0	16.1	16.0	16.4	17.5	20.9	23.6	27.2	29.4	**21.0**
Min	15.8	11.6	8.3	5.3	4.7	6.8	7.5	9.2	12.5	15.8	19.0	19.4	**11.3**

Source: NRH.

6.2. Evaporation :

The determination of the evaporation of the water surface of the Oued Ouizert reservoir will be estimated according to the measurements made on a tray at the Sarno dam given the absence of measurements in the

region. These measurements were made over a period of 19 years spanning 1978 and 1996 with however a few missing years.

The following table gives the evaporation on the water surface:

Table II-5: The evaporation on the water surface

Mois	Sep	Oct	Nov	Dec	Jan	Feb	Mar	Apr	May	Jun	Jul	Aug	Year
E (mm)	126.2	69.6	40.1	29.4	27.0	34.3	62.0	91.5	123.4	169.7	205.3	184.4	**1165.8**
%	10.8	6.0	3.4	2.5	2.3	2.9	5.3	7.8	10.6	14.6	17.6	15.8	**100**

Source: NRH.

6.3. Wind regime :

To get an idea of the wind regime in the region, we have used the measurements made at the Es Sénia station, which is considered more representative due to its proximity to the study region.

The prevailing winds in the region are from the West and Northwest, their annual frequency is represented in the following table:

Table II-6: The annual frequeny of winds

Direction	N	N.E	E	S.E	S	S.W	W	N.W
Frequency (%)	11.4	7.4	5.9	2.7	5.2	10.7	11.6	18.1

Source: NRH.

The average maximum wind speed is of the order of 24 m/s, and an average minimum of about 6.5 m/s.

Part II: Study of Precipitation :

1. Introduction:

Precipitation is a very important element of the hydrological cycle. The study of precipitation involves determining the average annual rainfall, extreme and frequent rains, and the monthly distribution of average rainfall.

The recorded precipitation from four stations located near the Oued Ouizert watersheds was provided by the National Agency for Water Resources (ANRH) and the National Office of Meteorology (O.N.M).

The recommended method for filling monthly gaps are:

- The rainfall of the low water months (July and August) was considered null by comparison with the data of the series 04 02 03.
- For the months where a good correlation could be obtained, the gaps were filled by reconstructing the missing data.
- For cases where the correlation was not satisfactory, the gaps were filled by the interannual average of the missing month.

2.Presentation and Critique of Data:

The rain gauge stations that we have studied and which are distributed around the Oued Ouizert watershed are represented with their characteristics in the following table:

Table II-7: The rain gauge stations

Station	Code	Altitude (m)	Coordinates	
			X	Y
El Malah Mitidja	04 02 10	80	156.59	241.94
Terga	04 02 18	38	148.50	242.75
Hassi El Ghella	04 04 14	167	160.50	248.76
Lourmel	04 04 28	115	163.44	254.22

However, the stations of El Malah, Lourmel, and Terga are no longer operational, so it was agreed to consider the Hassi El Ghella station as the reference station, and to use the Oued Berkeche station (04 02 03) whose observations are quite well provided, to fill in some monthly gaps.

3.Quality of the Rainfall Series:

The obtained rain gauge station, considered as the reference station, has a sufficient observation series, but however, it has some interruptions and gaps (1967-1974; 1980-1995; 1997-2009).

It was not deemed useful to consider the part of the series prior to 1967 as it is located in a period of abundant rainfall and the trend since 1986 is towards drought (source: ANRH report, rainfall map of northern Algeria).

Attempts to fill annual gaps with data from the series of station 04 02 03 were in vain since the correlation coefficient hardly exceeds 0.76.

Result :

- The average annual rainfall for the period 1967 – 2009 is 388 mm
- The average annual rainfall according to the rainfall map of northern Algeria is 400 mm.

The differences not being very significant, we will consider the rainfall of the series 1967/2009 which is very close to the average.

$$\mathbf{P_o = 388\ mm}$$

The monthly distribution of precipitation is as follows:

Table II-8: The monthly distribution of precipitation

Month	Sep	Oct	Nov	Dec	Jan	Feb	Mar	Apr	May	Jun	Jul	Aug	Year
P (mm)	9.77	32.77	53.03	66.98	48.25	56.21	48.81	35.77	22.62	7.51	2.55	2.86	**388**
%	2.52	8.45	13.67	17.26	12.44	14.50	12.58	9.22	5.83	1.94	0.66	0.74	**100**

Source: NRH.

3.1. Choice of the Representative Rain Gauge Station:

The choice of a representative rain gauge station will allow us to have a series of rainfall data, with which we can study the variability of precipitation over time and also determine extreme rains.

The representative station that was chosen is that of Hassi El Ghella whose ANRH code is 04 04 14 since it offers the longest observation series (1967-2009) and whose average annual precipitation is closest to that of the watershed (700 mm). Therefore, all the following estimates will be based on the data from this station.

3.1.1. Average annual rainfall:

Average annual rainfall is estimated at 388 mm.

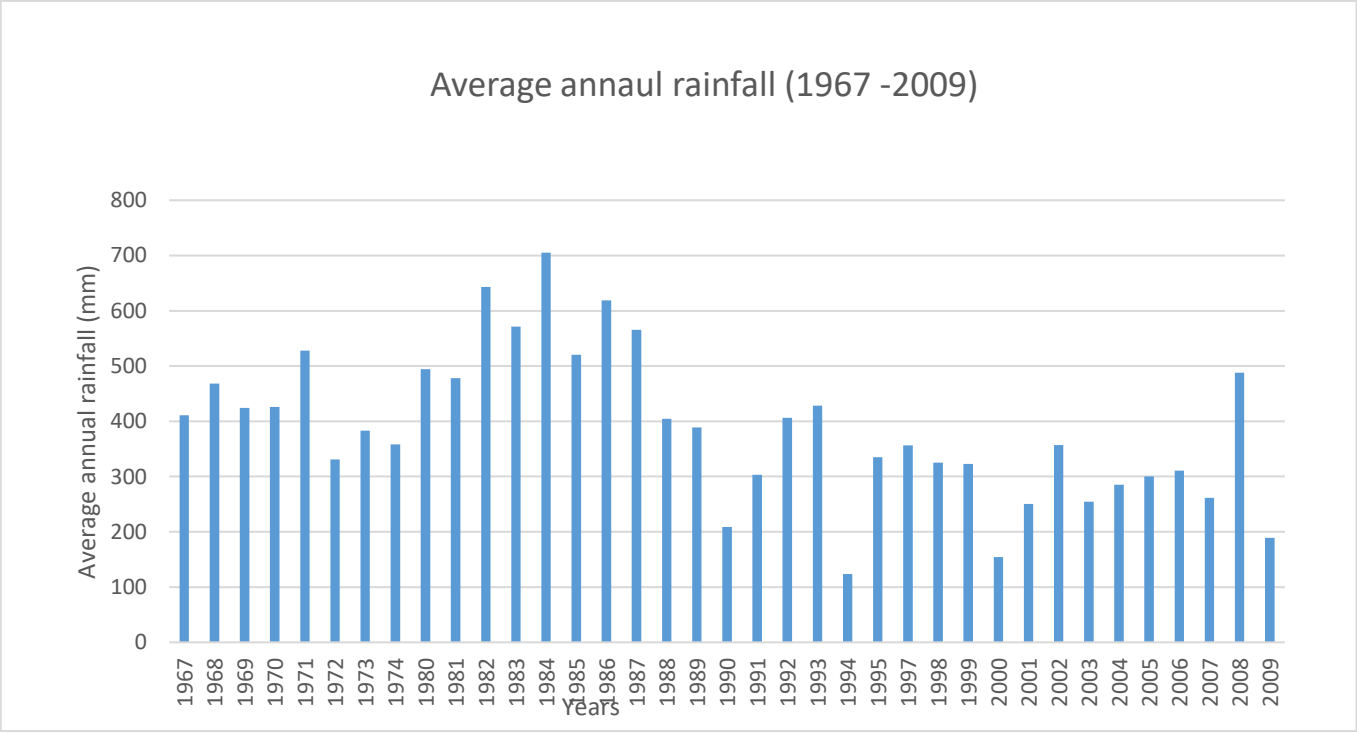

Figure II.4: Distribution of annual rainfall 1967-2009.

3.1.2. Average monthly rainfall :

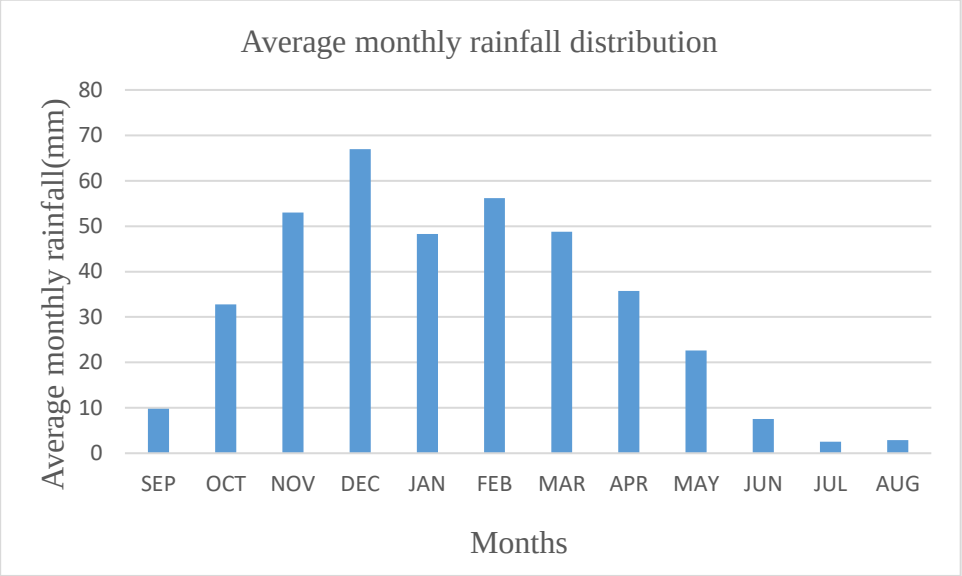

Figure II.5: The distribution of average monthly rainfall from 1967-2009.

4.Maximum Daily Rains:

To better understand the extreme nature of the flow, it is necessary to go down to a smaller time scale in the analysis of precipitation, this is the scale of maximum daily rains. Protection against water damage also requires an interest in maximum annual daily rains.

This study consists of determining the probable maximum precipitation in a day for different return periods. To achieve this, we have used statistical laws to establish an adjustment of the studied precipitation series.

The following table shows the maximum annual daily rains observed at the Hassi El Ghella rain gauge station.

TableII-9: Maximum Daily Rains (1967-2009).

Année	P_j max	Année	P_j max
1967	52.5	1990	48.2
1968	13.8	1991	53
1969	71.3	1992	70.9
1970	39.1	1993	50
1971	25.2	1994	95.9
1972	55.6	1995	39
1973	26.2	1996	38.4
1974	30.2	1997	36.2
1975	33.4	1998	43
1976	28	1999	78.3
1977	29.1	2000	36.1
1978	50.3	2001	25.3
1979	27.4	2002	42.5
1980	41.9	2003	36.3
1981	29.5	2004	114.1
1982	142	2005	66
1983	53	2006	46.6
1984	97.6	2007	70.7
1985	60	2008	50.5
1986	52.3	2009	53.4
1987	21		
1988	72.6		
1989	63		

Source: NRH.

N: Size of the series = 43; This means there are 43 data points in the series.

Xmoy: The average of the series = 51.38; This is the mean value of all the data points in the series.

σ : Standard deviation = 25.67; This measures the amount of variation or dispersion in the data set. A low standard deviation indicates that the data points tend to be close to the mean, while a high standard deviation indicates that the data points are spread out over a wider range.

4.1. Homogeneity test on the series of maximum daily rainfall:

Samples are said to be homogeneous if they are characterized by the same probability law and the same parameters, the collected data are then considered as extracted from the same population.

There are several tests to check the homogeneity of data series, in this case we will use the Wilcoxon test.

In hydrology, this means that the conditions that prevailed during the collection of data, or the occurrence of the considered phenomenon (rain, evaporation, etc.) have not changed throughout the duration of the collection, or in other words that there has not been an extraordinary phenomenon that could have modified the considered hydrological data (change of site of the measuring station, construction of a dam upstream, urbanization etc…).

We divide the rainfall series into two series X and Y such that N1 and N2 represent the sizes of these two sub-series.

Then we rank the values in ascending order from 1 to n and we note the ranks R (xi) of the elements of the first subset and R (yi) of the elements of the second subset in the original sample.

We noticed after plotting the graph of daily rainfall over the years that there is a break in 1986 as shown in the following graph.

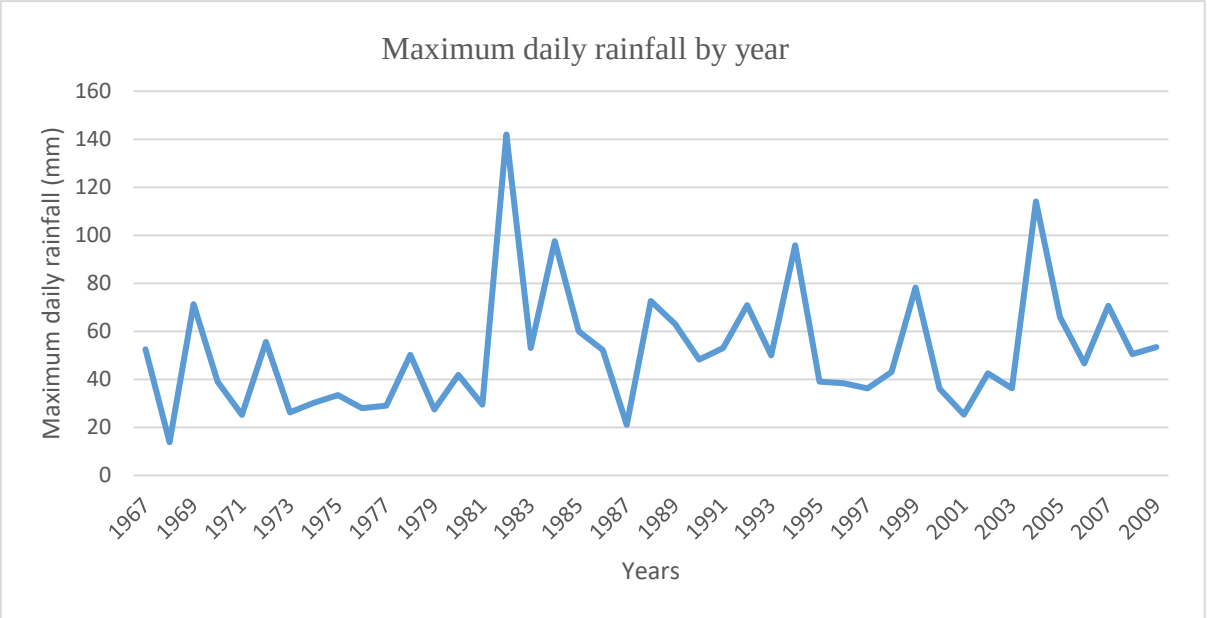

Figure II.6: Maximum daily rainfall by year (1967-2009)

The two series X and Y are therefore combined in the table below

Tableau II-10: X series of the maximum daily rainfall series

Année	Pj max (mm)	Rang
1968	13,8	1
1971	25,2	3
1973	26,2	5
1979	27,4	6
1976	28	7
1977	29,1	8
1981	29,5	9
1974	30,2	10
1975	33,4	11
1970	39,1	17
1980	41,9	18
1978	50,3	25
1986	52,3	27
1967	52,5	28
1983	53	29
1972	55,6	32
1985	60	33
1969	71,3	38
1984	97,6	42
1982	142	44

Tableau II-11: Y series of the maximum daily rainfall series.

Année	Pj max (mm)	Rang
1987	21	2
2001	25,3	4
2000	36,1	12
1997	36,2	13
2003	36,3	14
1996	38,4	15
1995	39	16
2002	42,5	19
1998	43	20
2010	44	21
2006	46,6	22
1990	48,2	23
1993	50	24
2008	50,5	26
1991	53	30
2009	53,4	31
1989	63	34
2005	66	35
2007	70,7	36
1992	70,9	37
1988	72,6	39
1999	78,3	40
1994	95,9	41
2004	114,1	43

In order to verify the homogeneity through the Wilcoxon test for the two samples, we pose the following hypotheses:

We have those: $\begin{cases} H_0: \mu_x = \mu_y \end{cases}$ H_0 null hypothesis

$\begin{cases} H : \mu_x > \mu_y \end{cases}$ H_a alternative hypothesis

We then calculated the Wilcoxon variable for both series X and Y such that:

Wx= sum of the ranks of sample X = 393

Wy= sum of the ranks of sample Y = 597

Subsequently, we calculated the critical Wilcoxon variable that separates the rejection zone from the acceptance zone and is given by the following formula:

$$W_{x,critique} = \frac{N_1(N_1 + N_2 + 1)}{2} + 1{,}64\sqrt{\frac{N_1 N_2 (N_1 + N_2 + 1)}{12}}$$

Wxc = 519

By comparing the Wilcoxon variable of the first series (series X) with the critical Wilcoxon variable we have:

$$Wx < Wxc$$

Result:

As a result, we are in the acceptance zone so we keep the first hypothesis and judge it as being true, that is to say that the means of the two series X and Y are equal and our series will be qualified as homogeneous.

4.2. Adjustment to the Gumbel law:

This is a very important law, which is used in the frequency analysis of extreme values, and will be particularly the essential ingredient, in operational hydrology, of the Gradex method for the calculation of project floods.

We rank the N values in ascending order by assigning each of them an order number n, then we calculate for each of them its non-exceedance frequency.

$$\mathbf{F(x) = (n-0.5)/N}$$

We plot the observed points and their experimental frequencies on Gumbel paper.

The distribution function of the Gumbel law is:

$$\mathbf{F(x) = \exp\left(-\exp(-a(x-x_0))\right)}$$

a: x_0 are the Gumbel adjustment coefficients.

x: is a variable of the sample.

The Gumbel line has the following equation:

$$\mathbf{X = (1/a) * Y + x0Y}$$

$$\mathbf{= -ln\ (-lnf(x))}$$

Y is the Gumbel reduced variable..

For my sample we found the following results:

$X_0 = 40.696$

$1/a = 22.264$

So the Gumbel line is written in this form:

$$X = 22.264 * Y + 40.696$$

The results of the calculation of the Gumbel law are grouped in the following table:

Table II-12: Results of the Gumbel distribution calculation.

Rang	P_{max}	F(x)	Y	Rang	P_{max}	F(x)	Y
1	13.8	0,011364	-1,49903	23	48.2	0,511364	0,399472
2	21	0,034091	-1,2175	24	50	0,534091	0,466507
3	25.2	0,056818	-1,05358	25	50.3	0,556818	0,535261
4	25.3	0,079545	-0,92878	26	50.5	0,579545	0,606032
5	26.2	0,102273	-0,82422	27	52.3	0,602273	0,679156
6	27.4	0,125	-0,7321	28	52.5	0,625	0,755015
7	28	0,147727	-0,64835	29	53	0,647727	0,834053
8	29.1	0,170455	-0,57058	30	53	0,670455	0,916792
9	29.5	0,193182	-0,49721	31	53.4	0,693182	1,003858
10	30.2	0,215909	-0,42716	32	55.6	0,715909	1,096009
11	33.4	0,238636	-0,35964	33	60	0,738636	1,194189
12	36.1	0,261364	-0,29404	34	63	0,761364	1,299588
13	36.2	0,284091	-0,22989	35	66	0,784091	1,413747
14	36.3	0,306818	-0,16678	36	70.7	0,806818	1,538714
15	38.4	0,329545	-0,1044	37	70.9	0,829545	1,677303
16	39	0,352273	-0,04244	38	71.3	0,852273	1,833528
17	39.1	0,375	0,019357	39	72.6	0,875	2,013419
18	41.9	0,397727	0,081222	40	78.3	0,897727	2,226653
19	42.5	0,420455	0,143387	41	95.9	0,920455	2,490269
20	43	0,443182	0,206071	42	97.6	0,943182	2,838793
21	44	0,465909	0,269495	43	114	0,965909	3,361432
22	46.6	0,488636	0,333884	44	142	0,988636	4,471628

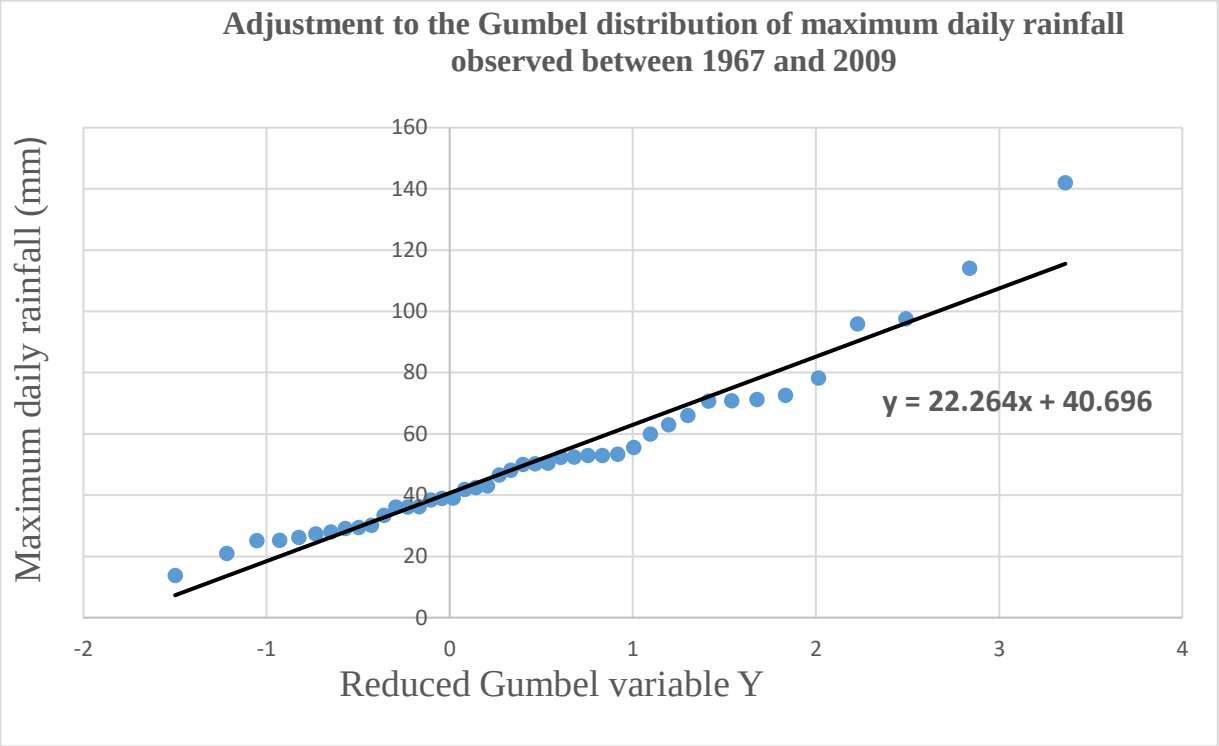

Figure II.7: The adjustment to the GUMBEL law

The maximum daily rainfall for different return periods is presented in the following table:

Tableau II.13: Result of the adjustment to the GUMBEL law

Return Period (years)	Probability (q)	XT	Standard Deviation	Confidence Interval
2	0.5	47	3.51	40.2 - 53.9
5	0.8	69.5	5.92	57.9 - 81.1
10	0.9	84.3	7.99	68.7 - 100
20	0.95	98.6	10.1	78.8 - 118
50	0.98	117	12.9	91.8 - 142
100	0.99	131	15	101 - 160
1000	0.999	177	22.1	133 - 220
10000	0.9999	222	29.3	165 - 280

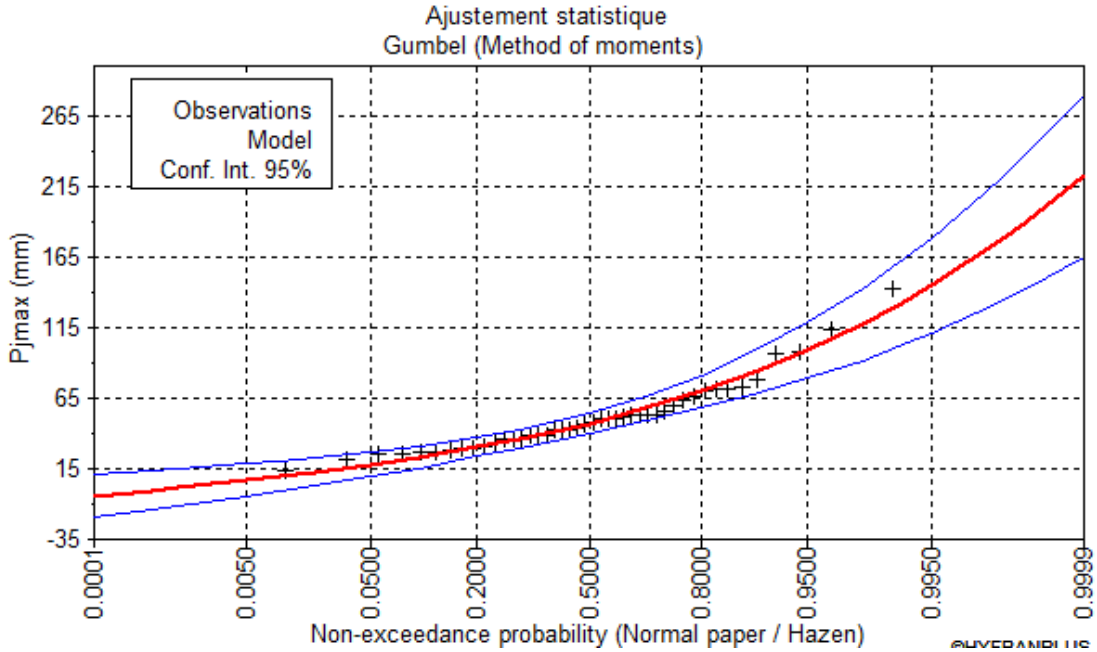

Figure II.8: Graphical representation of the results of adjustment to the Gumbel law

Result: It is clearly observed that our sample of maximum daily rainfall fits very well with the Gumbel law..

4.3. Adjustment to the Galton law:

Also known as the Log Normal law, it is considered a very powerful and very effective law for estimating extreme parameters.

The GALTON law has a distribution function that is expressed according to the following formula:

$$F(x) = \frac{1}{\sqrt{2\Pi}} \int_{u}^{+\infty} e^{-\left(\frac{1}{2}u\right)^2} dU$$

With:

$U = \frac{xi - \bar{x}}{\sigma x}$ (Gauss reduced variable)

The equation of the GALTON line is as follows:

$\log x(p\%) = \log x + б \log u(p\%)$

$$\log x = \frac{\sum^{30} \overline{\log xi}}{N}$$

The results of the adjustment by the log-normal law (Galton) are summarized in Table

Table II.14: Result of the adjustment to GALTON's law.

Return period (years)	Probability (q)	XT	Standard deviation	Confidence interval
2	0.5	46	3.23	39.7 - 52.4
5	0.8	68.1	5.57	57.2 - 79.0
10	0.9	83.6	7.95	68.0 - 99.1
20	0.95	98.9	10.7	77.9 - 120
50	0.98	120	14.9	90.4 - 149
100	0.99	136	18.5	99.6 - 172
1000	0.999	194	33	129 - 258
10000	0.9999	260	51.7	158 - 361

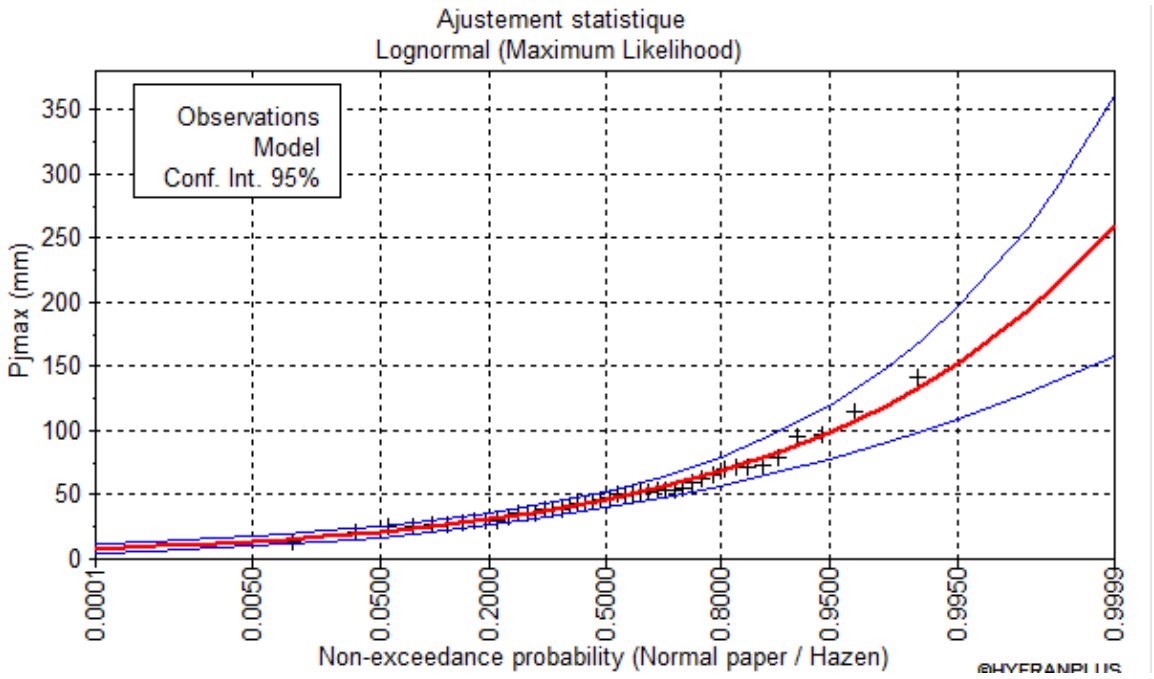

Figure II.9: Graphical representation of the lognormal distribution (Galton)

Result: We can clearly see that Galton's law is a better fit for our sample, and consequently its daily frequency rainfall will be taken into account.

5.Short-Duration Rains:

Short-duration precipitation refers to rainfall events with a duration less than or equal to 24 hours. Estimating these short-duration rains helps understand the irregularities in precipitation over time.

$$P_{T.t} = Pj\max(\%)\left(\frac{t}{24}\right)^{b}$$

The conversion from maximum daily rainfall to short-duration rainfall, which contributes to flooding, can be achieved using the Montana relation:

Where:

P_T: Represents the rainfall of duration (t) and return period (T)

Pjmax(%) : corresponds to the maximum daily rainfall frequency for return period (T).

b: is the climatic exponent (typically 0.33).

Tableau II.15: Short-Duration Frequency Rainfall, Intensity, and Characteristic Discharge of duration t, and given frequency

DESIGNATION				DURATION (hours)							
Pjmax %	**Frequency**	**PER - RET**	**Pt / It**	**1**	**2**	**4**	**8**	**12**	**24**	**48**	**72**
			Pt (mm)	14.19	17.84	22.42	28.18	32.22	40.50	50.91	58.20
40.5	50	2 ans	**It (mm/h)**	14.19	8.92	5.61	3.52	2.68	1.69	1.06	0.81
			q (L/s/km²)	3.94	2.48	1.56	0.98	0.75	0.47	0.29	0.22
			Pt (mm)	21.06	26.47	33.28	41.83	47.82	60.11	75.56	86.38
60.11	20	5 ans	**It (mm/h)**	21.06	13.24	8.32	5.23	3.98	2.50	1.57	1.20
			q (L/s/km²)	5.85	3.68	2.31	1.45	1.11	0.70	0.44	0.33
			Pt (mm)	25.61	32.19	40.46	50.86	58.15	73.09	91.88	105.03
73.09	10	10 ans	**It (mm/h)**	25.61	16.10	10.12	6.36	4.85	3.05	1.91	1.46
			q (L/s/km²)	7.11	4.47	2.81	1.77	1.35	0.85	0.53	0.41
			Pt (mm)	29.97	37.67	47.36	59.53	68.05	85.54	107.52	122.92
85.54	5	20 ans	**It (mm/h)**	29.97	18.84	11.84	7.44	5.67	3.56	2.24	1.71
			q (L/s/km²)	8.33	5.23	3.29	2.07	1.58	0.99	0.62	0.47
			Pt (mm)	35.62	44.77	56.28	70.75	80.87	101.66	127.79	146.08
101.66	2	50 ans	**It (mm/h)**	35.62	22.39	14.07	8.84	6.74	4.24	2.66	2.03
			q (L/s/km²)	9.89	6.22	3.91	2.46	1.87	1.18	0.74	0.56
			Pt (mm)	39.85	50.09	62.97	79.15	90.48	113.74	142.97	163.44
113.74	1	100 ans	**It (mm/h)**	39.85	25.05	15.74	9.89	7.54	4.74	2.98	2.27
			q (L/s/km²)	11.07	6.96	4.37	2.75	2.09	1.32	0.83	0.63
			Pt (mm)	53.84	67.68	85.07	106.93	122.24	153.66	193.15	220.81
153.66	0.1	1000 ans	**It (mm/h)**	53.84	33.84	21.27	13.37	10.19	6.40	4.02	3.07
			q (L/s/km²)	14.96	9.40	5.91	3.71	2.83	1.78	1.12	0.85

***Pt (Pluie de durée t)*:** This column represents the maximum daily rainfall for a specific duration (t) (in hours) in millimeters (mm).

***It (Intensité horaire*)**: This column represents the hourly intensity of rainfall (in mm/h) associated with the given duration (t).

***Q (Débit caractéristique*)**: This column represents the characteristic flow rate (in liters per second per square kilometer, l/s/km²). It is related to the rainfall and hydrological processes.

Part III: Study of Contributions:

This part of the study will focus on quantifying liquid contributions at the level of the Ouizert River.

We will analyze the variability of these contributions based on parameters that follow a log-normal distribution.

These analyses aim to provide maximum information for use in the subsequent stages of the project.

1.Average Annual Contribution:

In cases where direct observation data is lacking, it is customary to estimate liquid contributions using empirical methods.

The most commonly used methods include:

Samie's Formula:

Derived from a study of 12 basins with rainfall between 300 and 500 mm, Samie's formula is expressed as follows:

$$L_e = P_0^2\left(293 - 2.5\sqrt{S}\right) = 42.18mm$$

Where:

L_e: Effective runoff (mm)

S: Watershed area (km²)

Po: Average annual rainfall (mm)

Deri I Formula:

This relationship was established by the author in 1977 after studying 18 Algerian watersheds with areas ranging from 102 to 4000 km² and rainfall between 386 and 1400 mm. It is based on the correlation between average rainfall and contributions. The formula is as follows :

$$M_o = 11.8P_0^{282} = 0.82l/s/km^2$$

Where:

M_o: Specific flow rate (module spécifique) (l/s/km²)

P_o: Average annual rainfall (m)

Deri II Formula:

This formula is established for watersheds with areas ranging from 50 to 1000 km² and rainfall between 290 and 1400 mm. It is expressed as follows :

$$A = 0.915.P_0^{2.684}.S^{0.842} = 1.123hm^3$$

Where:

A: Average annual contribution (hm^3)

P_o: Average annual rainfall (m)

Urgiprovodkhoz Formula:

This relationship is based on observation data from 21 small rivers in northern Algeria. It is expressed as follows :

$$M_0 = \left(\frac{P_0}{340}\right)^{2.24} = 1.34l/s/km^2$$

Avec:

M_o: Specific flow rate (module spécifique) (l/s/km²)

P_o: Average annual rainfall (mm)

Table II.16: Results table.

Formula	Le (mm)	Mo (l/s/km²)	Cr (coef ruis)	A (Hm^3)
Samie	42.18	1.34	0.11	1.10
Deri I	25.88	0.82	0.07	0.68
Deri II	42.65	1.35	0.11	1.12
Urgiprovodkhoz	42.18	1.34	0.11	1.10
Average	38.22	1.21	0.10	1.00

Note: In Deri's formulas, the conversion from average contribution to effective runoff (lame écoulée) is obtained by dividing the former by the watershed area.

By further dividing the result by the duration of one year in seconds (T = 31.56 × 10^6 s), we obtain the specific flow rate (module spécifique, Mo).

Finally, the coefficient of runoff is given by the ratio between the effective runoff (Le) and the precipitated rainfall (Po) (388 mm).

The analysis of the obtained results clearly shows a consensus around the value of 1.10 hm^3, which will be considered for subsequent calculations..

The average annual contribution obtained using the Deri I formula deviates slightly from the results of other methods because it is based on observations from medium to large watersheds (102 - 4000 km^2).

The proposed monthly distribution of the average annual contribution is inspired by the monthly distribution of rainfall, taking into account the absence of flow during low-flow months (étiage).:

Table II.17: Results table.

Month	Sep	Oct	Nov	Dec	Jan	Feb	Mar	Apr	May	Jun	Jul	Aug	Year
A. hm^3	-	0.114	0.158	0.198	0.165	0.160	0.138	0.102	0.064	-	-	-	**1.100**
%	-	10.4	14.33	18	15	14.5	12.58	9.22	5.83	-	-	-	**100**

1.1. Variability of the Contribution:

The variability of the contribution can be considered by applying a Log-Normal (Galton) distribution, which best represents the frequency distribution of contributions in Algeria. This law is expressed as follows:

$$A(\%) = \frac{A_0}{\sqrt{Cv^2+1}} . e^{u\sqrt{LnCv^2+1}}$$

Where:

A (%): Contribution at a given frequency (hm^3)

U: Reduced Gaussian variable

A_0: Average annual contribution (hm^3)

Cv: Coefficient of variation

Various authors have proposed formulas to determine the coefficient of variation for contributions based on observation data from Algerian watersheds. Among them are :

Urgiprovodkhoz Formula :

$$Cv = \frac{0.70}{M_0^{0.125}} = 0.675$$

Where:

M_0: Specific flow rate 1.34 l/s/km².

Padoun Formula :

$$Cv = \frac{0.93}{M_0^{0.23}} . K = 0.869$$

Where:

M_0: Specific flow rate 1.34 l/s/km².

K: Reduction coefficient (assumed equal to 1 for temporary watercourses).

Sokolowsky Formula

$$Cv = 0.78 - 0.27Log(M_0) = 0.74$$

Where:

M_0: Specific flow rate 1.34 l/s/km².

For the continuation of the study, we will adopt the average value, which is:

Cv = 0.76

The frequent contributions will be as follows:

Table II.18: Results the frequent contributions calculation.

Frequency (%)	Return Period (years)	Variable (u)	Frequent Contribution (hm^3/an)
80	1.25	-0.8428	0.500
50	2	0.00	0.875
20	5	0.8428	1.548
10	10	1.2850	2.088
5	20	1.6449	2.664
4	25	1.753	2.860
2	50	2.0571	3.507
1	100	2.328	4.231
0.1	1000	3.100	7.136

Part IV: Study of Solid Transport:

1.Introduction:

Quantifying solid contributions is a crucial element in any study related to dams or reservoirs. Understanding the rate of solid material that can be transported by the river and reach the reservoir, even if it is only approximate, allows for making certain design decisions during dam sizing. These decisions ensure an acceptable operational lifespan of the structure by considering a dead storage zone specifically designated for sediment accumulation. This approach avoids any negative impact on distribution facilities and the necessary operational volume.

2.Calculation of solid transport:

Several authors have proposed formulas for estimating solid contributions, taking into account the geological and morphological characteristics of the watershed. Among the most commonly used formulas in Algeria are :

Fournier Formula :

$$Es = \frac{1}{36}\left(\frac{Pm^2}{P_0}\right)^{2.65}\left(\frac{H^2}{S}\right)^{0.46} = 267.40T/Km^2/an$$

Where:

Es: Specific Erosion (T

Pm: Rainfall in the wettest month (December 66.85 mm)

P0: Average annual rainfall (388 mm)

H: Mean elevation difference (Dénivelée) (Hmoy - Hmin = 117 m)

S: Watershed area (26.26 km²).

Gavrilovic Formula: Erosion Specific (Es) is given by:

$$Es = 3.14T.P_0\sqrt{Z^3} = 590.12T/km^2/an$$

Where : T : Temperature coefficient

$$T = \sqrt{\frac{t_0}{10}} + 0.1 = 1.37$$

to: Average annual temperature (16.2°c)

P0: pluie moyenne annuelle

Z: Relative erosion coefficient of the watershed (0.5 according to abacus)

To estimate the volume of solids, the author introduces a retention coefficient for materials in the basin calculated as follows:

$$Rm = \frac{\sqrt{P.Hmoy}}{0.2(L+10)} = 0.60$$

With

P: catchment perimeter (22 km)

Hmoy: Average altitude (183 m)

L: length of thalweg (7 km)

Tixeront (Sogréah) Formula :

Inspired by Tixeront's work in Tunisia, Sogréah proposes the following formula for Algeria, considering watersheds with low to moderate permeability:

$$Es = 350.R^{0.15} = 612.033T/km^2/an$$

Fournier's formula, which is not highly recommended for applications in Algeria, is given for information only.

For this reason, any comparison should take account of the Gavrilovic and Sogréah formula, which also give very similar results. We therefore recommend as the value for specific erosion that obtained by the Sogréah formula (Tixeront), which has the advantage of being adapted to Algerian conditions:

Es = 612 T/km²/an

Knowing the surface area of the catchment, which is 26.26 km², it is easy to deduce the abrasion rate:

Ta = Es. S . Rm = 11250 T/an

***Rm**:* Retention of materials by the basin, taken equal to 0.70, considering that the rate of sediment actually reaching the reservoir is 70% (generally accepted value).

By opting for the TIXERONT formula as the dead volume of our reservoir, this is the most suitable relationship in Algeria, so the dead volume is **Vm = 105470 m^3.**

Part V: Study of the Floods:

1.Introduction

Understanding floods is of paramount importance for designing evacuation and site protection structures.

These events can lead to submersions and destructive floods.

The aim of this study is to assess the flood flows at the site in question, in order to be able to design the structures to be built on the site to guarantee maximum safety, as well as their evolution over time as expressed by the flood hydrograph.

The parameters defining a flood are:

1- The maximum flow of the flood (peak flow).

2- The volume of the flood.

3- The shape of the flood (flood hydrograph).

4- Time of concentration.

5- Base time.

As mentioned previously, the lack of direct observation series of flows that have transited through the Ouizert wadi leaves no alternative but to resort to empirical formulas and methods:

:

2.Evaluation of flood flows:

2.1. Sokolowsky Formula:

$$Qmax = \frac{0.28.P_{Tc}.\alpha.S}{T_c} f$$

With:

Qmax: Maximum flood flow (m^3/s)

P_{Tc}*:* Rainfall corresponding to the time of concentration

□□*:* Runoff coefficient

S: Catchment watershed(km^2)

f: shape coefficient of the hydrograph taken equal to 1.2 for small watersheds.

2.2. Rational Formula:

$$Qmax = \frac{C.P_{Tc}.S}{3.6.T_c}$$

Where:

Qmax: Maximum flood flow (m^3/s)

P_{Tc}*:* Rainfall coresponding to the time of concentration

C□: Runoff coefficient

S: Watershed area (km^2)

Tc: Time of concetration

2.3. Mallet Gauthier Formula:

Although frequently used, this formula is only valid for frequencies greater than or equal to 100 years:

$$Qmax = 2.K.\log\left(1 + A + P_0\right)\frac{S}{\sqrt{L}}\sqrt{1 + 4\log T - \log S}$$

Where:

Q_{max}*:* Maximum flood flow (m^3/s)

S: Watershed area versant (km^2)

T: Return period

P_o*:* Average annual rainfall

A and K: Coefficients depending on the topographical and geological conditions of the watershed (for small watersheds with a fairly regular relief, fairly impermeable, it is recommended to use the respective values of A and K = 20 and 1).

2.4. Giandotti Formula

It is given by:

$$Qmax = \frac{A.S.P_{Tc}.\sqrt{Hmoy - Hmin}}{4\sqrt{S} + 1.5L}$$

Q_{max}: Maximum flood flow (m^3/s)

S: Watershed area (km^2)

P_{Tc}: Rainfall corresponding to the time of concentration

L: Length of main thalweg

H_{moy} *et* H_{min}: Average and minimum altitudes of the watershed respectively..

A: Coefficient depending on the topographic conditions generally taken as equal to 120-160 for small basins with fairly gentle morphology.

The results of the calculations are recorded in the following table:

Table II.19: A table summarizing the results

T	P_{Tc}	Cr	Formula Q(m^3/s)				Adopt
			Sokolows	Rationnel	Mal- Gaut	Giandotti	
5	33.28	0.27	19.14	16.39	-	42.38	**19**
10	40.46	0.37	33.02	27.80	-	51.51	**33**
20	47.36	0.46	48.05	39.73	-	59.99	**48**
50	56.28	0.51	63.31	52.35	-	71.64	**63**
100	62.97	0.55	76.41	63.16	72.70	80.15	**76**
1000	87.07	0.60	112.59	93.08	89.86	108.29	**112**

Result: There are no formulas for calculating the runoff coefficient, which depends on several factors, including:

- The nature of the soil, in particular its permeability
- The slope of the watershed
- Potential soil retention, notably vegetation cover.
- Degree of saturation (increases with return period)
- Rainoff Intensity

Choosing the runoff coefficient is a very delicate stage in any hydrological study, and one in which we need to be very cautious, especially as observations will be lacking. Consequently, in our study we will retain Cr values that best represent the averages recommended by various authors, depending on the frequency of the flood and the nature of the soil.

Conclusion:

The **Sokolowsky** method is widely used by hydrologists in the Maghreb in studies of hill reservoirs, mainly because it takes into account not only the characteristics of the catchment area, but also hydrograph parameters such as shape, flood rise time and flood-generating rainfall frequency..

Bearing in mind the uncertainties relating to the topographical coefficients of the other formulas, and the acknowledged fact that the **Mallet-Gauthier** formula tends to overestimate, and that the **Giandotti** formula is much more recommended for watersheds larger than 50 km^2.

We recommend adopting the results obtained by the **Sokolowsky** method, especially as they are close to the average results of all the methods used.

3.Flood Hydrograph:

The flood hydrograph allows you to have the distribution of the flood discharge over the time that the flood lasts, i.e. the time of concentration. It also allows you to estimate the characteristics of the flood: shape, volume, rising time and base time.

To plot the Flood Hydrograph, one must follow the SOKOLOVSKI method, which divides the Hydrograph into two non-symmetrical curve branches, one for the rising time and the other for the recession.

For the rising time:

$$Q_{montée} = Q_{max} \cdot (T/T_m)^2$$

Where:

T_m: Rising time which is equal to the time of concentration.

For the recession

$$Q_{décrue} = Q_{max}.[(T_d-T)/T_d]^3$$

Where: $T_d = \delta.T_m$ (Sokolovski)

δ : Coefficient depending on the watershed, the hydraulic regime of the watercourse, the overall permeability of the terrain, the afforestation or vegetation of the basin. It is generally taken between 2 and 4.

The results are summarized in the table below:

Table II.20: Flow of return period of 10,20,50,100, and 1000 year

Return period (years)	10	20	50	100	1000
T (hour)	Q (m^3/s)				
0	0	0	0	0	0
0.5	0.515938	0.7507813	0.9892188	1.1939063	1.7592188
1	2.06375	3.003125	3.956875	4.775625	7.036875
1.5	4.643438	6.7570313	8.9029688	10.745156	15.832969
2	8.255	12.0125	15.8275	19.1025	28.1475
2.5	12.89844	18.769531	24.730469	29.847656	43.980469
3	18.57375	27.028125	35.611875	42.980625	63.331875
3.5	25.28094	36.788281	48.471719	58.501406	86.201719
4	33.02	48.05	63.31	76.41	112.59
4.5	28.31052	41.196869	54.280411	65.512024	96.531851
5	24.07158	35.02845	46.15299	55.70289	82.07811
5.5	20.27841	29.508706	38.880254	46.925291	69.144334
6	16.90624	24.6016	32.41472	39.12192	57.64608
6.5	13.93031	20.271094	26.708906	32.235469	47.498906
7	11.32586	16.48115	21.71533	26.20863	38.61837
7.5	9.068118	13.195731	17.386509	20.984096	30.920029
8	7.13232	10.3788	13.67496	16.50456	24.31944
8.5	5.493703	7.9943188	10.533201	12.712714	18.732161
9	4.1275	6.00625	7.91375	9.55125	14.07375
9.5	3.008948	4.3785563	5.7691238	6.9628613	10.259764
10	2.11328	3.0752	4.05184	4.89024	7.20576
10.5	1.415733	2.0601438	2.7144163	3.2760788	4.8272963
11	0.89154	1.29735	1.70937	2.06307	3.03993
11.5	0.515938	0.7507813	0.9892188	1.1939063	1.7592188
12	0.26416	0.3844	0.50648	0.61128	0.90072
12.5	0.111443	0.1621688	0.2136713	0.2578838	0.3799913

13	0.03302	0.04805	0.06331	0.07641	0.11259
13.5	0.004128	0.0060063	0.0079138	0.0095513	0.0140738
14	0	0	0	0	0

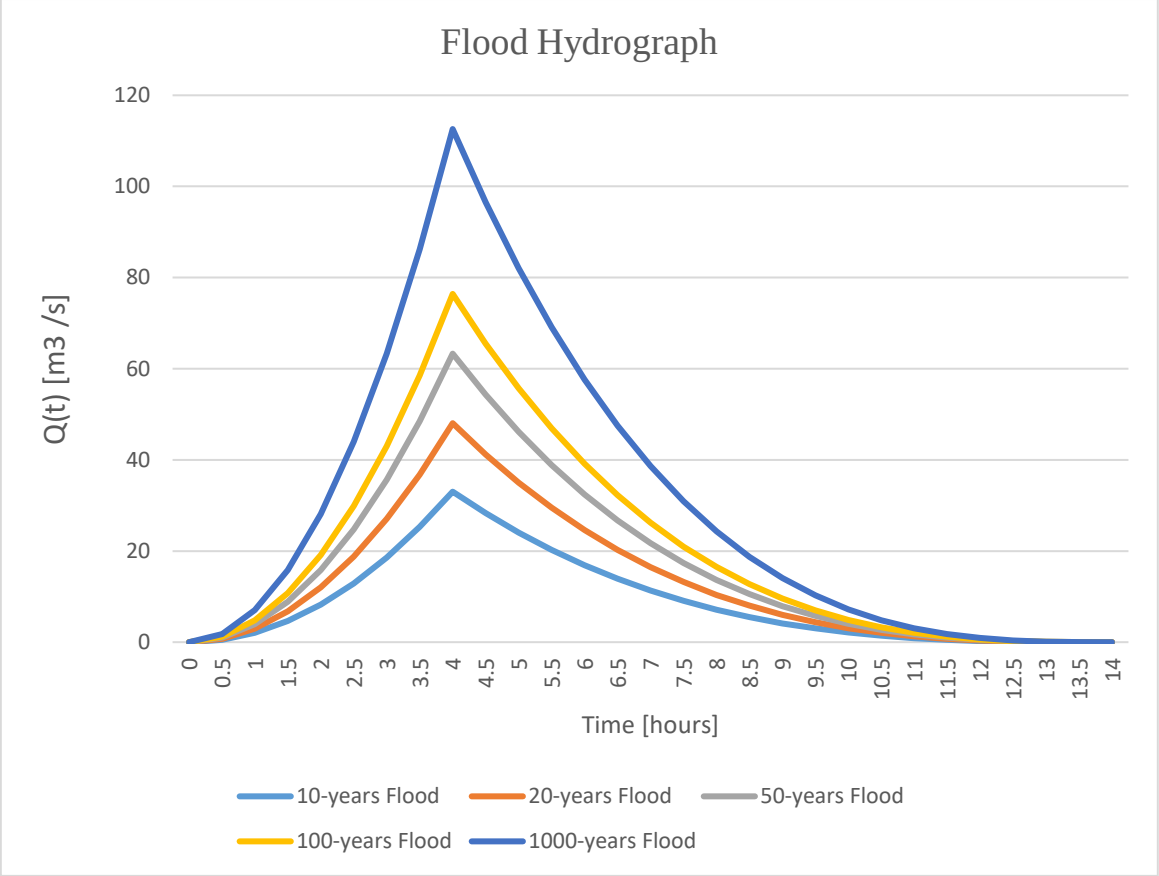

Figure II-10: Flood hydrograph.

4.Estimation of the Design Flood:

A design flood corresponds to the discharge that can be expected in the worst combination of meteorological and hydrological conditions reasonably considered characteristic of the region concerned. In other words, the design flood is the flood with the lowest frequency entering the reservoir. It is taken into account to determine the level of the highest water level (HWL), and thus the height of the dam.

Certainly, the choice of the design flood is a very important step in the study of the design of a hydraulic structure. Often the considered design flood is the flood with the maximum peak discharge. The minimum recommended return period for this flood is 100 years.

In the case of the Oued Ouizert dam, and taking into account the recently adopted

safety requirements by the INTERNATIONAL COMMISSION ON LARGE DAMS for the construction of hydraulic structures, we have opted for the millennial design flood, which is estimated at:

$$\underline{Q_{1000} = 112\ m^3/s}$$

5.Flow Regulation:

Regulation is the artificial redistribution of irregular natural river flows over time in accordance with the requirements of water consumers and users.

The capacity of regulation depends on:

- Volume demand.
- Evaporation..
-The inflow from Wadi (river).

Regulation makes it possible to rationally manage the capacity of the reservoir, determine the useful volume and therefore the useful height of the dam.

The following table summarizes the regulation calculations:

Table II-21: Results of the Flow Regulation calculation

Month	Inflow (hm^3)	Evaporation (mm)	Flooded Area (Km^2)	Evaporated Volume (m^3)	Infiltrated Volume (m^3)	Volume d of Needs (m^3)	Remaining Cumulative Volume (m^3)
Jan	165	27	0.108	2909	5425	0	621886
Feb	160	34.3	0.128	4380	7019	0	777665
Mar	138	62	0.142	8834	8467	0	905319
Apr	102	91.5	0.149	13657	9436	25300	964265
May	64	169.7	0.146	18045	9583	75900	928045
Jun	0	169.7	0.124	21033	8395	177100	453821
Jul	0	205.3	0.089	18252	6001	244600	229383
Aug	0	184.4	0.056	10304	3484	210800	229042
Sep	0	126.2	0.031	30920	1704	118020	106042
Oct	114	69.6	0.043	2991	1356	59100	162203
Nov	158	40.1	0.059	2370	1845	0	262389
Dec	198	29.4	0.086	2541	3614	0	460022

These results are interpreted by this graph:

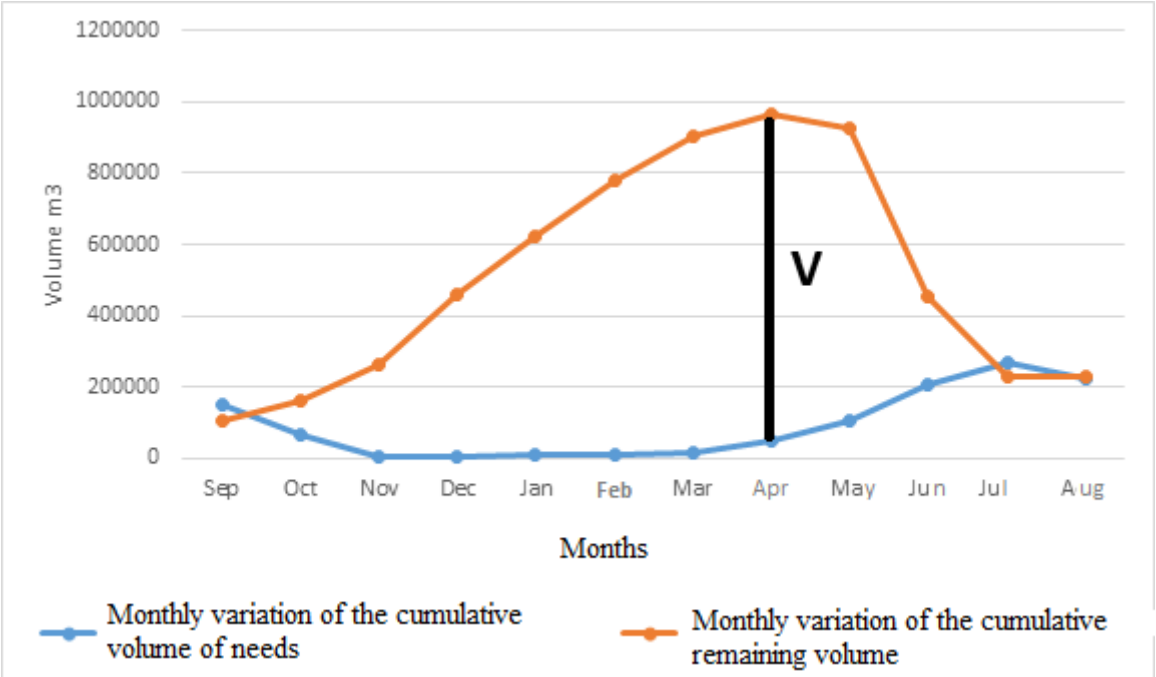

Figure II-11: Calculation of Flow Regulation.

Conclusion:

From the calculations performed and the plotted regulation curve, it appears that the optimal regulation rate is 82.8%, which allows us, after calculation, to set the volume and level of the normal retention..

- Normal Volume : 964300 m^3
- Dead Volume : 105470 m^3
- Useful Volume : 858830m^3

6.Flood Routing :

The phenomenon of flood routing is the transformation of the flood wave between an upstream point and a downstream point of a watercourse. Its effect is to reduce the peak discharge (the maximum flow) by distributing the volume of the flood over time. This is possible thanks to the temporary storage of a part of the flood volume in the major bed of a watercourse (natural routing) or in the reservoir of a dam (artificial routing).

Flood routing allows to find the dimensions of the spillway to evacuate the flood serenely and safely.

The discharge flow is calculated according to the formula:

$$\mathbf{Q = m.b.\ (2g)^{0.5}.\ H^{3/2}}$$

- m: discharge coefficient depends on the shape of the weir.

-b: width of the weir in m.

-H: water head on the weir.

Observation:

The practical weir is frequently used because of the advantages it presents, which leads to taking the value of m equal to 0.49. With an estimated width of 14 m.

Determination of the Maximum Overflowing Discharge:

$H = (Q_{max} / 30.39)^{2/3}$ $H_{d\,max} = (I^{max} / 30.39)^{2/3}$

N.A: $H_{d\,max}$= : $H_{d\,max}$= 2.39 m.

Determination of Initial Conditions :

- The initial outflow discharge:
  $O_1 = 0\ (m^3/s)$
- The initial overflowing discharge/head :
  $H_1 = (O_1 / 30.39)^{2/3}$ $H_1 = 0$ m.

Plotting the Characteristic Curve of the Reservoir Basin:

We have : $f(O)=2S\Delta t+O$

Table II-22: Results table

H (m)	S (m3*10^6)	O (m3/s)	(2S/dt)+O (m3/s)
0	0	0	0
0.2	0.2	2.718146	165.319772
0.4	0.4	7.688079	332.891331
0.6	0.6	14.1239	501.928781
0.8	0.8	21.74517	672.151675
1	1	30.3898	843.3979
1.2	1.2	39.94843	1015.5582

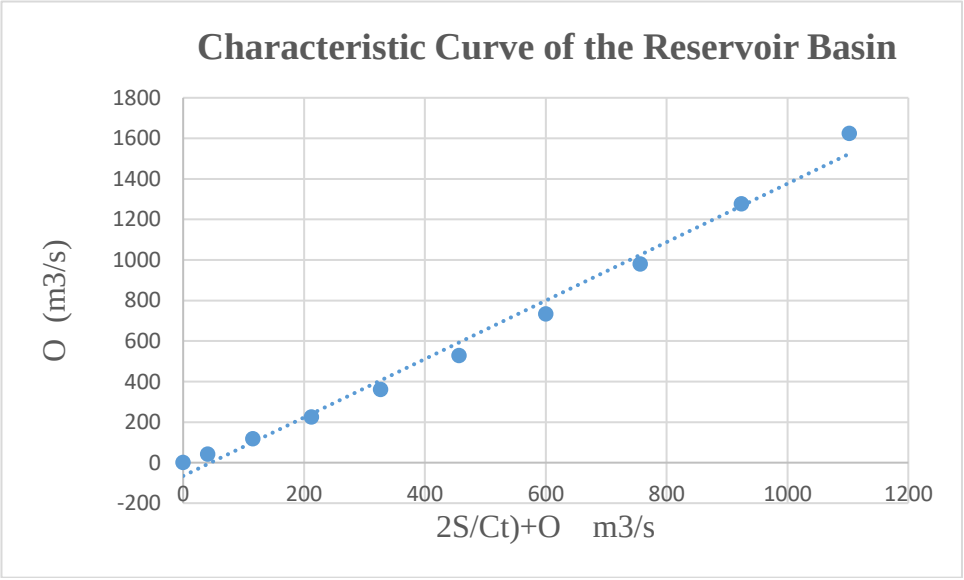

Figure II-12: Characteristic Curve of the Reservoir Basin

Determination of the Outflow Hydrograph:

We proceeded using the Muskingum method to perform the flood routing. The results of the flood routing calculation are presented in the following table:

Table II-23: Results of the Flood Routing Calculation

T (hour)	Inflow (m3/s)	I1+I2	2s/dt+O	2s/dt-O	O (m3/s)
0	0	0	0	0	0
0.5	1.759219	1.759	1.759	1.622	0.069
1	7.036875	8.796	10.418	9.603	0.407
1.5	15.83297	22.870	32.473	29.934	1.270
2	28.1475	43.980	73.914	68.134	2.890
2.5	43.98047	72.128	140.262	129.293	5.484
3	63.33188	107.312	236.606	218.103	9.251
3.5	86.20172	149.534	367.637	338.888	14.375
4	112.59	198.792	537.679	495.633	21.023
4.5	97	209.122	704.755	649.643	27.556
5	82	178.610	828.253	763.483	32.385
5.5	69.14433	151.222	914.706	843.176	35.765
6	57.64608	126.790	969.966	894.115	37.926
6.5	47.49891	105.145	999.260	921.118	39.071
7	38.61837	86.117	1,007.235	928.469	39.383
7.5	30.92003	69.538	998.008	919.963	39.022
8	24.31944	55.239	975.203	898.942	38.130
8.5	18.73216	43.052	941.994	868.330	36.832
9	14.07375	32.806	901.136	830.667	35.234
9.5	10.25976	24.334	855.000	788.139	33.431
10	7.20576	17.466	805.605	742.607	31.499
10.5	4.827296	12.033	754.640	695.627	29.506
11	3.03993	7.867	703.494	648.481	27.507
11.5	1.759219	4.799	653.280	602.193	25.543
12	0.90072	2.660	604.853	557.554	23.650
12.5	0.379991	1.281	558.835	515.134	21.850
13	0.11259	0.493	515.626	475.304	20.161
13.5	0.014074	0.127	475.431	438.252	18.589
14	0	0.014	438.266	403.994	17.136
14.5	0	0.000	403.994	372.402	15.796
15	0	0.000	372.402	343.280	14.561
15.5	0	0.000	343.280	316.435	13.422
16	0	0.000	316.435	291.690	12.373
16.5	0	0.000	291.690	268.880	11.405
17	0	0.000	268.880	247.853	10.513
17.5	0	0.000	247.853	228.471	9.691

18	0	0.000	228.471	210.605	8.933
18.5	0	0.000	210.605	194.136	8.235
19	0	0.000	194.136	178.954	7.591

The routed flood is represented by the hydrograph below:

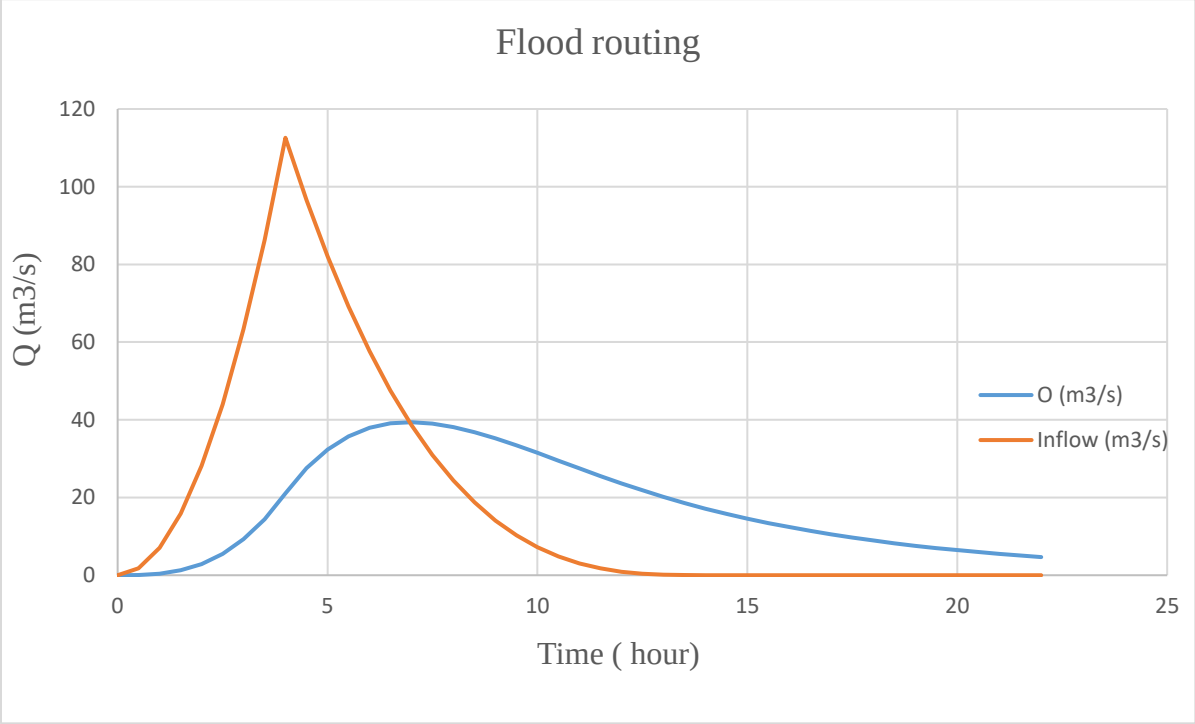

Figure II-13: Hydrograph of flood routing

Determining the maximum overflow discharge:

So in the end we have:

$Q_{laminée} = 39.383 m^3/s$

$H_{dmax} = 1.188$ m

For the sizing of the spillway, we adopted for the centennial flood Q 1% = 76 m3/s, in accordance with the standards applicable to dams of this class.

Optimization

Optimization is a technical-economic calculation whose objective is to determine the optimal width of the spillway.

The purpose of the calculation is to draw curves showing the evolution of the cost of the development as a function of different spillway widths. The optimal width will therefore be the one that corresponds to the minimum cost on the summary curve.

The volume of work was determined only for significant parts with proven influence on the overall cost of the development, namely:

- Embankment for the dike
- Spillway plus the trench with variable section
- Excavation for the spillway and the trench with variable section

The principle of the optimization calculation is based on two essential parameters:

Estimation of the project flood:

$$Q_{p5}=\frac{Q_{\max}}{f}\left(1-\frac{V_l}{V_c}\right)$$

Where:

- Qp: project flow rate
- Qmax: flood flow rate
- Vl: laminated volume of the flood (curve v = f(h))
- Vc: volume of the flood (Vc = 912,000 m3)
- F: hydrograph coefficient (f = 1.2)

Estimation of the spillway width:

$$b=\frac{Q_p}{m\sqrt{2g.H^{\frac{3}{2}}}}$$

Where:

- b: width of the spillway (m)
- m: flow coefficient (m = 0.46)
- H: water head on the sill (m)

Once these two parameters are defined, a technical-economic calculation will be carried out where the volume and cost of the dike as well as the work on the spillway will be estimated. The superposition of the curves giving the cost of the dike as a function of the spillway width and that reflecting the cost of the spillway as a function of its width will allow determining the optimal width of the latter.

Estimation of spillway widths:

Charge H (m)	**Laminated Volume VL (m^3)**	**VL/Vcr**	**Project Flow Rate Qpr**	**Spillway Width B (m)**
1.0	162.19	0.180	51.93	25.50
1.5	245.50	0.269	46.30	12.40
2.0	345.70	0.379	39.33	6.80
2.5	430.70	0.472	33.44	4.15

Estimation of work costs:

H(m)	B(m)	H_B(m)	Work Volume (10^3 m^3)			Work Cost (10^6 DA)			Total Cost MDA
			Dike	Concrete	Excavation (Fouille)	Dike	Concrete	Excavation (Fouille)	
1.0	25.5	25	107.03	0.218	0.863	64.218	3.279	0.345	67.84
1.5	12.4	25.5	103.40	1.063	0.420	62.040	1.594	0.168	63.80
1.69	10.00	25.6	106.07	0.857	0.338	63.636	1.286	0.135	65.06
2.0	6.80	26	109.70	0.583	0.230	65.820	0.877	0.092	66.79
2.50	4.15	26.5	116.45	0.357	0.140	69.870	0.536	0.056	70.46

Note: For cost estimation, the following unit prices were used:

- Price per m^3 of concrete: 15,000 DA
- Price per m^3 of embankment: 600 DA
- Price per m^3 of excavation: 400 DA

Conclusion:

The summary curve of work costs as a function of spillway width shows that the optimum (minimum cost) would be the adoption of a 14 m wide spillway.

The lamination study using the "Lamin" software developed at the National Polytechnic School of Warsaw gave the following results:

- Spillway width b = 14 m
- Water head on the spillway sill H = 1.41 m
- Discharged flow Qp = 48.02 m3/s

Highest water level:

The highest water level is defined as follows:

NPHE = NNNR + H

Where:

- NPHE: highest water level
- NNNR: normal retention level
- H: water head on the spillway

NPHE = 118.3 + 1.41 = 119.71 NGA

Conclusion :

So in the end, we only have to say that we have estimated more or less reliable dimensions of the spillway in order to contain the flood by ensuring a serene evacuation to guarantee the safety of our structure and not harm it. From a hydrological point of view, and taking into account all these calculations, we can affirm that the Oued Ouizert dam is hydrologically feasible.

Part VI: Dimensioning of the dam body

1.Dam Height and Freeboard:

The freeboard or safety reserve is calculated using the DAVIS formula, which is written as follows:

$R = 0.75H + V^2/2g$ (minimum reserve)
Where:
H: wave height (m)
V: wave propagation speed (m/s)

Several heights have established relationships for calculating the wave height. The most commonly used are:

$H = 0.75 + 0.032(WL)^{0.5} - 0.27(L)^{0.25}$ (Molitor)

$H = 0.75 + 0.34(L)^{0.5} - 0.26(L)^{0.25}$ (Stevenson)

$H = 0.5 + 0.3(L)^{0.5}$ (Mallet)

Where:
L: fetch length (0.75 km)
W: maximum wind speed (120 km/h)

The wave propagation speed is given by Gaillard's formula:

$V = 1.5 + 2h$

The calculation results are presented in the table below:

Table II.24: Summary table of dam Height and Freeboard

Parameter	H(m)	V(m/s)	R(m)
MOLITOR	0.12	1.74	0.90
STEVENSON	0.80	3.10	1.24
MALLET	0.75	3.00	1.21

Furthermore, taking into account the recommendations of the USBR (United States Bureau of Reclamation), which recommends adopting a freeboard between 1.5 and 2.0 for dam heights exceeding 20 meters, we will therefore adopt, for safety and practical reasons, a freeboard of:

$$R = 1.49m.$$

Hence, the crest elevation of the dam is thus deduced:

$$Nc = NPHE + R = 121.20$$

2.Height of the dam:

The height of the dam is given by:

$$H\,b = N\,c - N\,f + H\,d = **26\ m**$$

Where:

NC: crest elevation 76.00
Nf: foundation elevation (96)
N d: height of the exposed foundation 0.8m

3.Crest width:

The main formulas giving the crest width are:

- KNAPPEU formula :

$$Bc = 1.65\ (H\,b)^{1/2}$$

- PREECE formula:

$$Bc = 1.1 + (H\ v)^{1.2} + 1$$

- USBR formula:

$$Bc = H/5 + 3$$

- FRENCH formula:

$$Bc = 3.6(H\ b)^{1/3} - 3$$

Table II.25: Summary table of Crest width:

KNAPPEU	PREECE	USRB	FRENCH
8.41	7.6	8.2	7.66

The results obtained mostly recommend a crest width greater than 7 meters, knowing that in general all these formulas tend to slightly overestimate the results, in addition to the rather inconsistent nature of the embankment material which argues in favor of reducing the width obtained by calculation, therefore we will retain the following value of the crest width.

$$B_c = 7.0 \text{ meters}$$

4.Crest length:

The crest length of the dam is defined as the distance connecting the opposite contour lines of altitude equal to the crest elevation of the dam, it is deduced from the development plan at scale 1/500

$$L_c = 141.00 \text{ m}$$

5.Slope of embankments:

The slopes of the dam embankments depend on certain factors such as:

- The nature of the embankment materials.
- The nature of the foundations.
- The type of dam.
- The safety of the dam.

Taking into account all these elements we propose the following embankment slopes:

Variant No. 1:

· Upstream slope m1 =1/2.5
· Downstream slope m2 =1/2.3

variant No. 2:
· Upstream slope m1=1/3.0
· Downstream slope m2=1/2.5

variant No. 3:
· Upstream slope m1=1/2.5
· Upstream slope m1=1/2.0

6.Dimensioning of the core:

The core must be wide enough to reduce infiltrations as much as possible, it is generally accepted as a general dimensioning rule the following criteria:

- core width

$$L_n \geq 1/3\ L_b$$

With:

L_n: core width.

L_b: dam width.

- Core crest

The crest width must be: $C_n \geq 1$m.

The core crest must be above the PHE by 0.5 m, hence the level:

$$N_{cr} = N_{PHE} + 0.5 = 120.21 \text{ NGA}$$

Given the existence of clay in the basin in sufficient quantity in the excavation area and beyond, in its extension, the following dimensions have been adopted:

- Crest width: C_n =3m
- Base width: L_n =47.5 m
- Slopes: $m_1 = m_2 = 1$

Chapter III: GEOLOGICAL AND GEOTECHNICAL STUDY

1. Introduction:

This study falls within the framework of the contract concluded between the Directorate of Hydraulics of the Ain Témouchent wilaya and concerns the feasibility study of a reservoir on the Ouizert river in the municipality of Ouled Taoui.

This report was established based on:

Site reconnaissance and basin assessment

Geological map No. 179–180 Rio Salado / Lourmel, scale 1:50,000.

In-situ geotechnical work and tests on intact and reconstituted samples carried out by the Sersid laboratory.

The results of the investigations and mechanical tests conducted on the collected samples to determine the quantitative and qualitative characteristics of the foundations and borrow materials are documented in the following paragraphs.

2. Stratigraphic and Tectonic Overview:

The territory covered by the combined LOURMEL and RIO SALADO map sheets is topographically divided into two distinct regions:

The Great Sebkha Plain:

The plain is predominantly occupied by the Sebkha basin, with a very uniform, completely bare floor at an elevation of 80-81 meters.

To the north and west, the Sebkha is bordered by a narrow, low terrace that rises to the south and widens, continuing into the M'Léta plain, bounded by the Ain Beida and Djebel Ahmar hills.

Northern Mountain Massif:

This mountainous region to the north lacks prominent relief features. Instead, it consists of a series of plateaus, variably incised by ravines, gradually rising to elevations of 250 and 310 meters.

From a regional perspective, the sedimentary formations can be described as follows:

Current Beaches and Alluvium (A):

Represented by the Marsa Bou Zedjar beach and the mouth of the Rio Salado; current silts from the Oued El Melah.

Salt Alluvium of the Sebkhas (A5):

Comprises the salted silts within the Sebkha basin.

Current Dunes (Ad):

Highly developed along the cliffs to the south and north of the Rio Salado mouth.

Also found in several interior locations, where they form at the expense of underlying Pliocene sandstones (Turgot, Er Rahel).

Consolidated Dunes (ad):

Relatively rare among the current dunes.

These dunes are embedded in the limestone faces, particularly in the southwest of Djebel Dechera and the small pass of Djebel Touita.

Slope Debris (a): Located on the eastern flank of Djebel Touita.

Saline Border Lands of Sebkha (a^3_S): These are salted lands that are flooded in winter and covered with saltwort (salicornes) in summer.

Recent Alluvial Deposits (a^2): Found along riverbanks.

Saline Limon Deposits of Sebkhas (a^2_S): Recent limon deposits, often highly saline, from the periphery of the large Sebkha. They currently form the banks with an apparent thickness of 1-2 meters.

Lacustrine Formation - Calcareous-Sandstone (a^1): Constitutes the subsoil of the plain to the south and east of Er-Rahel at a depth of 1 meter. Also found in Brédéah, where it is more recent.

Travertines and Tuffs (T): Located near the source of Ain Béida.

Ancient Alluvial Deposits (Lower Level) (q^1): These are limited in extent and found along riverbanks. They result from runoff and form terraces between Brédéah and Rio-Salado above the Sebkha.

Sand and Sandy Basins (q^1_b): Often red sands from Pliocene deposits.

Ancient Saline Limon Deposits of Sebkhas (q^1_s): These dark grayish limon deposits mark the oldest level of the large Sebkha. They constitute El Djezira Island, the slopes of Douar Krata, and the Hammoul ridge.

Helical Sandstone (q^1_d): More or less hard sandstone, forming low cliffs and coastal islets in the Blad Chellaoua region.

Emergent Beach (0-15 meters level) (q^1_m): Rarely visible but overlaid by helical sandstone (Q1md).

Ancient Alluvial Deposits (Medium Level) (q^1): Gravel deposits around large depressions, rill cones, and always covered by a thick, hard crust.

Ancient Limon Deposits of Sebkhas (qS1): Saline, dark limons marking the oldest Sebkha level. They form El Djezira Island, the slopes of Douar Krata, and the Hammoul ridge.

Consolidated Ancient Dunes (q^d): Hidden by limons, exposed 3 km northeast of Ain Beida.

Ancient Travertines (T_i): Found upstream of the Ain Beida spring.

Sandy Alluvial Deposits (q_i): Deposits from elevated regions.

Gres-Calcareous Carapace (P^2_b): Overlies P2a marls, P1g sandstone, and the Sahelian layer, concealing their boundaries.

Red Sandstone Marls (P^2_a): Alluvial deposits transitioning to sandy marls with coarse sandstone slabs at depth. These are very ancient deposits from Rio-Salado and Djebel-Ahmar, with a potential thickness exceeding 40 meters.

Sandstone Scree (mp^1_g): Gravelly sandstone debris fallen from Pliocene cliffs onto the lower Sahelian layer of Blad Chellaoua. These disintegrate to form dunes.

Helical Sandstone (P^1_g): Dune-originated flaggy sandstone, weathering at the surface. Highly developed between Djebel Touita and the sea, forming the high cliffs at the mouth of Rio Salado. Its thickness is at least 60 meters.

Puddingstones and Shell-bearing Sandstones (P^1_a): Only rare remnants remain

Marls and Fossiliferous Sandstones (p_i): Sandy marls and white or yellow sandy sandstones, clayey, rich in small pectens. Clearly visible only at the mouth of Oued Sassel, possibly extending into the valley where it may be in contact with Sahelian marls covered in shrubs.

Massive White Limestones (Upper Sahelian) (m^4): Fossiliferous chalky coralline limestones with lithothamnium, from Brédéah to Bou Tlélis and Ouizert, Er Rahel.

Sahelian Gypsum (m^1_g): Isolated outcrops seemingly resting on m4d. Fish-bearing layers are minimal and rarely visible.

Limestone Scree (m^4_{ad}): Detached remnants from the following formation.

Chalky Limestone (m^4_d): White limestones with variable composition, often ending in rare flint layers. Typically marly limestones, hard, interbedded with softer marly limestone banks, white or yellowish. Sometimes sand-mica layers at the base (e.g., Ben Derabine to Chabet el Ateuch). Fossiliferous layers at the base indicate a transgression over the micaceous marls of the Lower Sahelian. Thickness varies (10-30 meters at Figalo, 60 meters at Ain Chellaoua, 120 meters at El Ateuch).

Micaceous Sandstones and Marls (m^1_a): Within this group:

Upper Micaceous Sandstones (m^1_a): Clearly bedded, sometimes quite hard, terminating the micaceous formation. Variable thickness, with some fossils (e.g., Figalo Promontory, Chabet Derabine).

Marls and Micaceous Sandstones (m^4_c): Variable colors (greenish, reddish, or blackish), occasionally gypsiferous, with volcanic debris. Cut by one or more blue micaceous sandstone layers. Found in Bou Zedjar. Thickness: 180 meters.

Lower Micaceous Sandstones (m^1_a): Coarse, blue or greenish, with rhyolitic tuffs. Forms the base of the Lower Sahelian, resting on Figalo and Moul El Bahar and merging with volcanic breccias of Bled el Farod. Thickness: 20-70 meters.

Neocomian (C_{IV-V}): Shales and quartzites. Clayey, gray, yellow, or greenish shales with quartzite lenses or thin beds (0.60-0.80 meters). Typical in Temakrouda.

Oxfordian Shales (J^2): Greenish and pinkish-gray shales, zoned, interbedded with twisted ferruginous calcite plaquettes and thin lenses of ochreous quartzite. Ammonite traces on the right bank of Rio, and intercalations in Djebel Touita and Déchera.

Banded Limestones (l^1): Limestones with siliceous nodules transitioning to slabs or lenses, interbedded in hard, pearly slate shales.

Massive Liasic Limestones (l^2): These limestones occur in large beds, often distinct, and are gray or blue. They have a waxy appearance and are strongly veined with calcite. Sometimes, the outer layers appear yellow, and in certain places, they exhibit a marbled texture. Their thickness is at least 30 meters.

Volcanic Rocks:

Hypersthene Andesite Breccias and Flows (**mα** and α^4): These originate from the Tifaraouine volcano. They are massive, reddish, or black (due to pyroxene) with coarse grains. The facies can vary significantly, and their thickness ranges from 2 to 300 meters.

Hornblende Andesite Breccias and Flows (α^3): These are gray, relatively clear, and contain small visible hornblende crystals. Found near Blad and Farod, forming two isolated outcrops.

Biotite Andesite Breccias and Flows (**mα**^{2} and α^2): Dark gray and rich in biotite crystals. Prominently visible at Figalo, where the flows create columnar structures on the steep cliffs.

Micaceous Andesite Breccias and Flows (α^1): Gneiss-like facies, sometimes reddish or grayish. Occurs at Moul el Bahar.

Ophite (**w**): Two small outcrops with variegated marls.

3. Regional Geology:

Triassic Outcrops: Two Triassic outcrops penetrate through the secondary shales of Djebel Touita and Dechera.

Lias Formation: The Lias is represented by the limestone formations of Djebel Touita and Déchera. Some are massive, while others exhibit banded structures. They anomalously overlie the underlying shales. These shales, likely of Neocomian age, form the Tamakrouda hill and the basement of Djebel Tita and Dechera. They extend along the right flank of Rio-Salado and occasionally emerge through the Pliocene cover, revealing Oxfordian facies.

Volcanic Deposits: Extensive volcanic rock deposits were formed by the pre-Sahelian Tifaraouine volcano.

Sahelian Formation: The Sahelian occupies a significant portion of the Lourmel sheet territory. However, it is often concealed by Pliocene sandstones or more recent sands. It rests either on shales or volcanic deposits. The Sahelian landscape is gently undulating and generally slopes southward, eventually passing beneath the Sebkha, where fine sediments level the anticlinal floor.

Pliocene Marine Deposits: Truly marine Pliocene deposits are rare. The ancient Pliocene is only typical at the mouth of the Wadi Sassel. The shell-bearing sandstones (grès coquilliers) are represented by remnants, well-characterized in the Wadi Atchane valley, where they appear at approximately 240 meters above sea level. These sandstones are discordantly overlain by Sahelian Upper Limestone in the Sasse gorges (near Chabet Nouala), although distinguishing them mineralogically can be challenging. The extensive P1g sandstones and sands spread across the western plateaus and terminate in steep coastal cliffs, where the marine formation has not yet appeared.

Pliocene Sediments at the Mouth of Wadi Sassel: At the mouth of Wadi Sassel, sandy sandstones rest on the ancient Pliocene marls. They may represent the Upper Pliocene, but their thickness and altitude (150 meters at Figalo) suggest an attribution to the Middle Pliocene.

The P2a continental formations are dispersed intermittently, reaching elevations up to 180 meters in the Djebel Hamer area.

Quaternary marine deposits are relatively rare. These deposits are found at or near the Earth’s surface in valleys, plains, seashores, and even on the seafloor. The P2a continental formations play a vital role in elucidating geological history, as they can be directly correlated and compared with contemporary sedimentary depositional environments.

In specific regions, such as the Bahia Blanca Estuary in Argentina, marine Quaternary deposits associated with transgressive-regressive processes are abundant. These deposits provide valuable insights into past environmental conditions, sedimentation patterns, and the distribution of fossils. For example, the Bahia Blanca area has experienced two significant transgressive events during the Late Pleistocene and Holocene. An examination of the

sedimentological and taphonomic characteristics of these P2a continental deposits elucidates variations in energy regimes, sediment compositions, and the preserved marine faunal assemblages across the intervals represented by these formations, shedding light on the differing environmental conditions that prevailed during their deposition.

Additionally, Quaternary rocks and sediments are essential for unraveling the Earth's geologic history and understanding landscape evolution. These continental formations not only act as important reservoirs for hydrological resources, but also preserve records of past geological hazards. Expansive dune fields and sandy areas, derived from the erosion of Pliocene sandstones (p1g) and Sahelian sandy formations (m1d), blanket vast swaths to the west, adding intricate pieces to the intricate geological mosaic characterizing this region.

4. Site and Basin Geology:

The right flank of the future reservoir basin is primarily composed of helical sandstones and sandy formations, as indicated by geological maps and geotechnical investigations, including excavation **F1**. Notably, the thickness of the formation ($\mathbf{p^1_g}$) exceeds 60 meters, suggesting that its continuity extends well beyond the limits reached by the excavation.

On the left flank of the reservoir, white limestones ($\mathbf{m^4_d}$) dominate. These limestones are typically altered and fissured, with an intercalation of sandstone beds. The surface layers consist of whitish, clayey-sandy material, while the softer white limestones below exhibit tuff-like structures with limonite-rich passages (starting from 6 meters).

Regarding the lower valley areas, which represent the riverbanks and riverbed, they consist mainly of alluvial deposits. The continental deposits comprise a surficial layer of clayey-sandy material interspersed with gravel lenses, transitioning downwards into clayey-sandy silts that retain gravel stringers at greater depths.

Geological Map

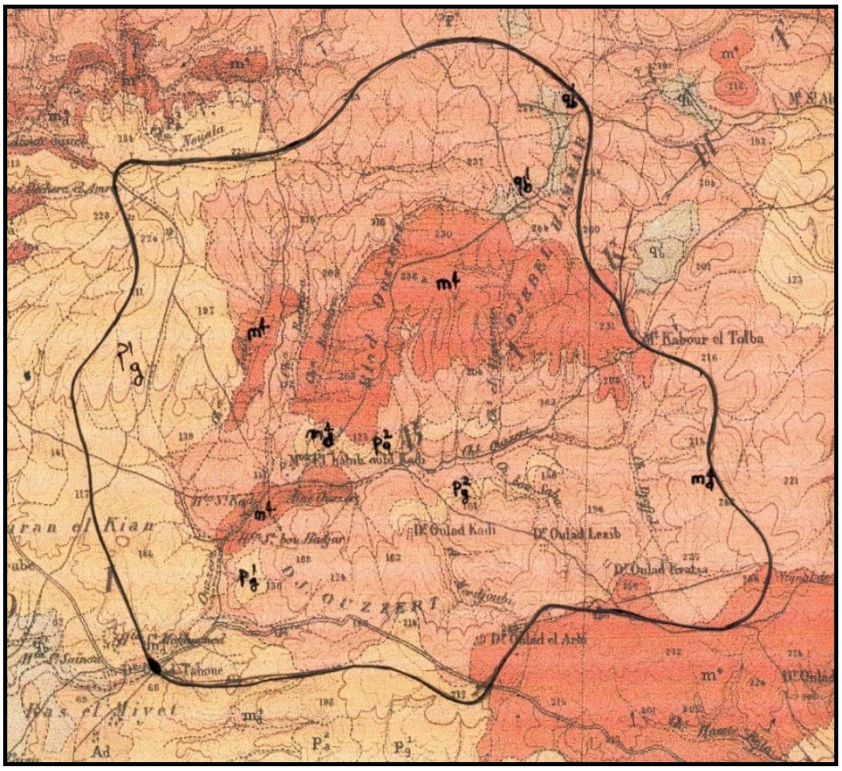

Figure III.1: Watershed of the Ouizert River Extract from Geological Map No. 180 Lourmel, scale: 1/50,000. Source: SNS

LEGEND

m4: Massive white limestones (Upper Sahelian).

m4d: Chalky limestones.

p1g: Sandstones and helical sands.

p2a: Red sandy marls.

q1b: Sandy and liassic river sands.

5. Site and Basin Waterproofing:

The laboratory investigations, including tests conducted on collected samples and in situ observations, suggest the presence of impermeable foundations composed of clayey alluvium with a thickness of approximately 8.0 meters.

Interestingly, the increase in permeability beyond 8.0 meters at the S1 borehole is attributed to the presence of a more permeable layer with a sandy-silty texture near the formation (p1g) constituting the right bank (excavation F1). This layer likely extends beyond the limits reached by the excavation.

The results of permeability tests conducted on S1, S2, and F1 indicate that between the valley floor and the 1001 contour level (at the site), the terrain benefits from good impermeability. However, beyond this elevation, permeability becomes more significant due to the nature of the fissured sandy left bank and the prevailing sandy conditions on the right bank.

The obtained permeabilities are as follows:

Bed materials (clayey-sandy): $K = 1.02 \times 10^{-6}$ m/s to 2.25×10^{-8} m/s.

Left bank materials (sandstone limestones): $K = 1.70 \times 10^{-5}$ m/s to 2.50×10^{-5} m/s.

Right bank materials (sandy-silty): $K = 2.0 \times 10^{-5}$ m/s.

Borehole S2 reveals a rapid loss between 4.50 and 6.0 meters, attributed to the alteration of sandstone limestones at that depth. These findings underscore the need for further verification and assessment to determine if waterproofing measures would be necessary in this area during any subsequent field campaign, should the project progress to the execution study phase.

6. Seismicity:

The current documents used for defining seismic risk in Algeria, specifically the DTR B C 2 48 (related to the Algerian seismic regulations RPA 99), developed by the CGS (Center for Applied Research in Seismic Engineering), divide the national territory into four distinct seismicity zones:

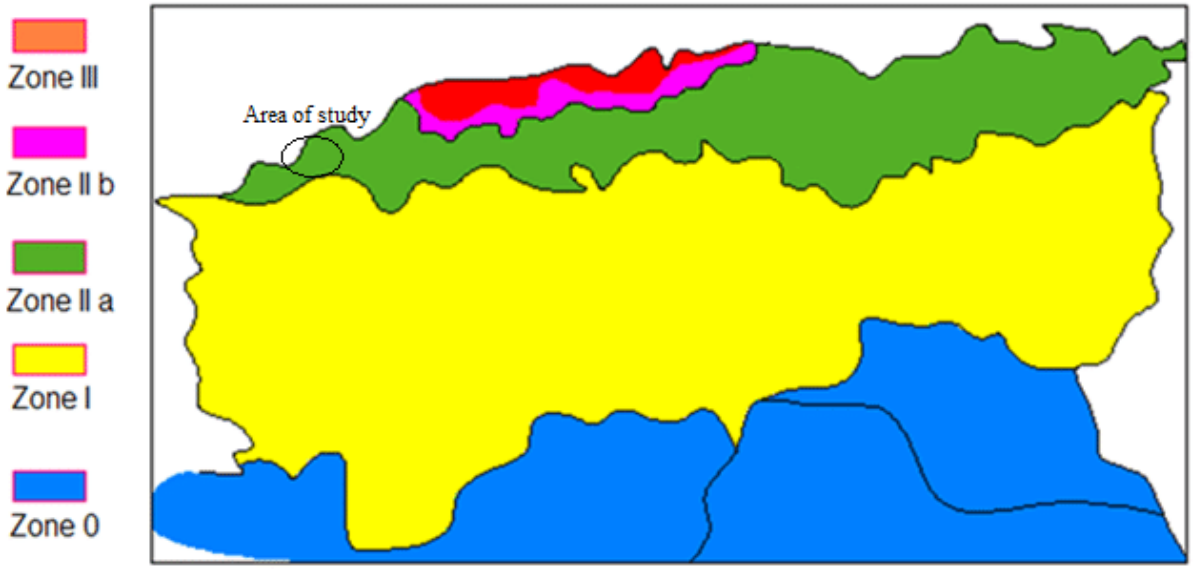

Figure III.2 : Seismic zoning map of the national territory-RPA99. Source: Regles Parasismiques Algeriennes RPA 99

The minimum level of seismic protection granted to a structure depends on its purpose and significance in relation to the community's protection objectives.

Table III.1: Seismic classification of zones.

Zone 0	Negligible seismicity
Zone I	Low seismicity
Zone II	Moderate seismicity
Zone III	High seismicity

Source : Regles Parasismiques Algeriennes RPA 99

Any structure falling within the scope of the Algerian seismic regulations RPA 99 must be classified into one of the following four groups:

Group 1A: Vital structures

Group 1B: High-importance structures

Group 2: Common or moderately important structures

Group 3: Low-importance structure

The sites have also been classified based on their geological nature and the mechanical properties of the soils constituting them. The following categories are distinguished:

Category S1: Rocky site characterized by an average shear wave velocity, Vs ≥ 800 m/s.

Category S2: Firm site characterized by an average shear wave velocity, Vs ≥ 400 m/s, starting at a depth of 10 meters.

Category S3: Loose site characterized by an average shear wave velocity, Vs ≥ 200 m/s, starting at a depth of 10 meters.

Category S4: Very firm site characterized by an average shear wave velocity, Vs < 200 m/s, within the first 20 meters.

Based on the above, the studied site falls within Zone II, corresponding to a region of moderate seismicity, and can be classified as Category S1.

In accordance with Usage Group No . 1B, the seismic acceleration coefficient to consider is **A = 0.201.**

7. Geotechnical Reconnaissance :

7.1. In-Situ Investigation :

The in-situ investigation program includes:

Two core-drilled boreholes along the axis of the dam, with water tests. These works are carried out to identify the geological nature of the foundation soil and its mechanical characteristics and permeability. The goal is to assess its suitability for supporting the construction of an earth dam.

A 5-meter-deep excavation on the right bank, replacing the originally planned borehole. The difficult access for the drilling rig and the cultivated land it would have to traverse made the initial borehole challenging.

Five excavations downstream of the site, following research in the reservoir and its immediate surroundings. The goal is to assess the availability of borrow materials suitable for embankment construction, both quantitatively and qualitatively.

7.2. Results of the Investigations:

All boreholes and excavations yielded sufficient samples for laboratory testing to evaluate their nature and mechanical properties.

Core-Drilled Boreholes and Trench (F1) on the Right Bank:

The boreholes and the F1 excavation on the right bank revealed the following geological formations forming the foundation of the future Ouled Taoui reservoir:

Borehole S1, conducted on the riverbed, revealed clayey materials, specifically a silty-sandy clay, down to a depth of 8 meters. These clays rest on clayey-silty sands with some gravels, likely representing a continuation of the sandy formation identified on the right bank. According to information recorded in the explanatory note accompanying the 1:50,000 geological map, this formation's thickness is at least 60 meters. The surface clay layer, containing plant debris and shells down to 3 meters, constitutes the alluvial terrace of the watercourse, formed by slope deposits and stream transport.

Borehole S2 on the left bank revealed, beneath the surface silts (20 cm thick), a formation consisting of fissured sandy-clayey limestones, followed by whitish and friable sandy limestones in the form of tuff. These limestones are sometimes highly altered starting from 6 meters deep.

On the right bank, there is an approximately 1.5-meter-thick vegetative layer, likely artificially modified by local farmers. It rests on sands containing some gravels and light brown siltThe stratum in question likely belongs to the expansive P1g geologic formation prevalent in the area, stretching all the way to the marine environment.

Permeability Tests:

Core-drilled boreholes are subjected to Lefranc water tests, commonly used for loose soils. This in-situ test aims to determine a local permeability coefficient and is conducted following the French standard NFP 94-132 (June 1992).

The test procedure is as follows:

Drilling into the Soil: A borehole is drilled to the depth of the test.

Casing the Borehole: The borehole is cased.

Introduction of Filter Material: Gravel is introduced at the bottom of the borehole.

Lifting the Casing: The casing is lifted to the desired cavity height.

Before the actual test, certain parameters are measured:

Height of Casing Above Ground (HT) (meters)

Static Water Level Height Above Casing (HP) (meters)

Cavity Diameter (B) and Length (L) (meters)

Cavity Depth Relative to Casing Top (meters)

These parameters are associated with a topographic reference point (NGA or local) :

The test begins by injecting water into the casing up to the top. Then, the water level decline relative to the casing top (He) is measured every minute during the first 20 minutes, followed by measurements every five minutes until three successive readings show a difference of approximately 1 cm or less between them.

In all cases, the test is terminated after one hour.

All time measurements (t in minutes) and water level measurements (He in meters) are recorded on the borehole log.

Given the water level drop (ΔH) over a time interval (Δt), we calculate the percolation flow rate Q(t) through the cavity wall at time t.

$$Q = \frac{\Delta H}{\Delta t} xS \text{ (cavity cross-section)}$$

We also compute h(t), which corresponds to the hydraulic head at a given instant:

h = Hp – He (meters)

Based on the obtained results, a graph representing flow rate versus hydraulic head is plotted.

The permeability coefficient is then expressed as follows:

$$KL = \frac{\Delta Qt}{m.\Delta h(t).B}$$

m being a form factor depending on the dimensions of the cavity.

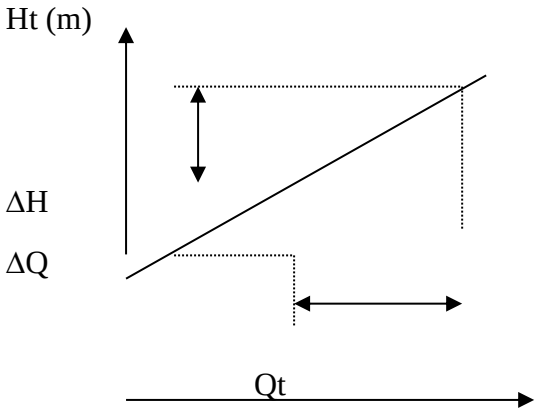

Regarding the F1 trench on the right bank, which represents essentially sandy terrain, the permeability was evaluated using a permeameter.

Table III.2: Results of laboratory tests on Ouled Taoui dam foundation soil

Borehole N°		S1	S1	S1	S1	S1	S2	S2	S2	S2	S2	S2	F1
Depth (m)		2.73	6.08	7.60	8.05	9.57	3.04	4.56	6.08	7.60	9.12	10.64	5.00
Classification		CL	CL										SM
Natural moisture content : **W%**			18		27.8	10.8							8.20
Wet Density : ρ_h **(t/m^3)**		1.85	1.79	2.09	1.92	1.50	1.81	1.60			2.17	2.67	1.87
Specific weight:ρ_s **(t/m^3)**		2.66	2.65	2.65	2.65	2.66							2.61
Sieving Sediment	G %	1.51	0.85	2.53	2.79	0.98	79.07		50.92	35.94	19.76	1.82	11.20
	S %	44.32	28.75	26.81	42.30	55.72	15.32		44.62	52.87	78.88	80.12	81.27
	F %	54.17	70.40	70.66	54.91	43.30	5.61		4.46	11.19	9.36	8.06	7.53
Atterberg Limits	Liquid Limit: WL %	33.50	37.00	35.00	28.40	35.10							19.50
	Plastic Limit: Wp %	16.26	21.40	19.09	14.32	15.01							8.55
	Plasticity Index: Ip %	17.24	15.60	15.91	14.08	20.09							10.95
Organic Matter Content %		12.17	6.14	7.04	4.17	4.17	Traces						Trace
Carbonate Content		12.17	11.30	13.00	34.00	13.00	49.13	57.39	62.65	47.82	39.13	33.48	12.20
Chloride Content		No traces											
Sulfate Content		No traces											
	Pc (bars)		1.40										
	Cc		0.17										
Direct Shear parameters	C (bars)		0.45						0.15				0.21
	φ °		12.10						46				35
Permeability: K (m/s)		1.75 .10^{-7}		2.25 .10^{-8}		1.02 .10^{-6}	2.5 . 10^{-5}			1.7 . 10^{-5}			2.10^{-5}

Oedometric Consolidation

The average permeability obtained for the tested materials is as follows:

Foundations: 1.70×10^{-7} m/s (impermeable)

Left bank: 2.0×10^{-5} m/s (low permeability)

Right bank: 2.0×10^{-5} m/s (low permeability)

Result:

In general, it can be concluded that the valley has good impermeability in its lower parts (below elevation 100, which apparently represents the limit of fine alluvial materials). The banks are relatively impermeable ($K < 10^{-4}$ m/s). Therefore, even if leaks through the foundations and banks are relatively significant, they should not pose a catastrophic risk.

However, during the next phase (execution study), it would be useful to conduct further investigations on the left side of the reservoir to understand the behavior of the altered limestone band, which experienced total loss during water tests. Adequate measures to reduce leaks should be planned accordingly.

Laboratory Tests:

The foundation material samples underwent laboratory testing. However, due to the powdery nature of the bank materials, only the fine samples from borehole S1 were suitable for identification and consolidation tests.

The results indicate clayey soils from 0 to 8 meters at the S1 level, transitioning to sandy materials at greater depths. The fine fraction is present in proportions ranging from 43% to 70%, the sandy fraction from 26% to 55%, and the gravel fraction from 0.85% to 2.8%. These materials exhibit a plasticity index ranging from 14% to 20%, suggesting the presence of clay with relatively low plasticity.

7.3. Borrow Zones:

Following site and surrounding prospecting, two types of materials have been identified: sands with traces of silt and gravel (excavations F2, F3, F4, and trench F1), as well as low-plasticity clays (F5 and F6). Considering the high organic content of the clayey materials within the reservoir impact area and the risk of preferential infiltration zones due to quarry openings within the reservoir space, it was deemed useful to search for borrow zones downstream of the development.

The excavations are located as follows:

-F2 and F3 approximately 300 m and 400 m downstream on the left side of the road leading to Ouled Taoui.

-F4 approximately 450 m downstream from the watercourse on the right bank.

-F5 approximately 1 km downstream from the site at the exit of Ouled Taoui.

-F6 approximately 200 m upstream from the reservoir axis on the left bank, outside the reservoir impact area.

Except for well F1, intended for foundation reconnaissance on the right bank (with a depth of 5 m, which can still be considered in the analysis of borrow materials), the other excavations are all at depths ranging from 2.50 to 3.0 m.

Laboratory Tests:

Atterberg Limits:

Excavations F1 to F4:

Liquid Limit (WL): 15.2 to 22.0%

Plastic Limit (Wp): 7.12 to 12.77%

Plasticity Index (Ip): 8.08 to 11.0%

Excavations F5 and F6:

Liquid Limit (WL): 30.2 to 35.7%

Plastic Limit (Wp): 14.45 to 17.43%

Plasticity Index (Ip): 15.75 to 18.27%

Granulometric and Sedimentometric Analyses:

This analysis involves measuring the distribution of soil particles based on their dimensions and determining their relative importance. The results are expressed in a curve called the granulometric curve, which reflects the cumulative percentage of elements with dimensions smaller than each diameter.

The granulometric curves obtained for excavations F1 to F4 show a relatively narrow grain size distribution, where the sandy fraction dominates, varying between 73% and 86%. The

remaining percentage is shared between silt and gravel in the following proportions: silt (7.53% to 11.12%) and gravel (2.80% to 15.60%).

Excavations F5 and F6 indicate a tendency toward silty-sandy behavior (according to the unified classification), as 54% to 56% of the elements have diameters smaller than 0.08 mm. The plasticity indices are 15.75% and 18.27%.

Based on the above, we can say that the materials available around the site are:

-Sandy soils with traces of gravel

-Low-plasticity clays

Proctor Compaction Tests:

The standard Proctor compaction test determines the optimal water content corresponding to the maximum compacted density.

The laboratory-obtained maximum density varies from 1.79 to 1.89 T/m³, with an optimal water content of 12.08% to 14.14%.

A soil is considered suitable for use as compacted fill if:

-Dry Density (Proctor): The dry density (Proctor) is greater than 1.6 T/m³.

-Optimal Water Content: The optimal water content is less than 20%.

Direct Shear Test:

The direct shear tests using the Casagrande box were conducted on reconstituted samples at the Proctor optimal density and water content. The obtained results indicate a cohesion ranging from 0.21 to 0.82 bars and an average internal friction angle of 15 to 42 degrees, which aligns with the sandy nature of the samples.

Permeability Determination:

Given the existence of two different soil types, permeability was determined using two types of equipment, each suitable for a specific soil type. For sandy soils, permeability was determined using a constant head permeameter, while for clayey soils, an oedometer was used.

The results reveal impermeable soils for samples from excavations F5 and F6, with permeability coefficients ranging from 1.51×10^{-7} m/s to 1.79×10^{-7} m/s. The soils are also slightly permeable, with permeability coefficients ranging from 1.4×10^{-5} m/s to 2.0×10^{-5} m/s.

Chemical Analyses:

Chemical tests aimed to determine the soil's content of organic matter, which could affect the quality of fill soil, as well as the carbonate content (beneficial for crops). Additionally, chloride and sulfate levels were assessed, as they can impact both soil quality (solubility) and water quality (salinity).

Results of these tests are as follows:

Table III.3: Results of chemical analyses

Chemical Elements	Contents in %					
	F1	F2	F3	F4	F5	F6
Organic matter	traces	12.8	11.7	traces	traces	traces
Carbonates	12.2	13.04	20.8	32.17	7.83	4.34
Chlorides	No traces					
Sulfates	No traces					

The high organic matter content in excavations F2 and F3 exceeds the maximum allowable limit for fill soils (which should not exceed 5%). Consequently, their use is compromised. The lack of chlorides and sulfates signifies no risk of material dissolution, while the existence of insoluble carbonates suggests favorable water quality concerning salinity.

Table III.4: Results of laboratory tests on Ouled Taoui dam Borrow areas

Borehole N°		F2	F3	F4	F5	F6
Depth (m)		3.00	3.00	3.00	2.50	2.50
Classification		SM	SM	SM	CL	CL
Natural Moisture content **: W%**		9.30	1.94	3.27	6.72	12.67
Dry Density **: ρ_d (t/m^3) (OPN)**		1.89	1.85	1.80	1.79	1.90
Moisture Content W_{opt} (**OPN)**		12.34	12.29	12.08	14.14	12.26
Specific weight: **ρ_s (t/m^3)**		2.62	2.63	2.62	2.66	2.66
Sieving Sediment	G %	15.60	2.80	14.54	13.80	0.00
	S %	73.66	86.08	77.22	31.55	44.00
	F %	10.74	11.12	8.24	54.65	56.00
Atterberg Limites	Liquid Limit: WL %	20.00	22.00	15.20	35.70	30.20
	Plastic Limit: Wp %	9.00	12.77	7.12	17.43	14.45
	Plasticity Index: Ip %	11.00	9.23	8.08	18.27	15.75
Organic Matter Content %		12.18	11.70	Traces		
Carbonate Content		13.04	20.80	32.17	7.83	4.34
Chloride Content		No traces				
Sulfate Content		No traces				
Oedometric Consolidation	Pc (bars)					
	Cc					
Direct Shear parameters	C (bars)	0.51	0.65	0.28	0.67	0.82
	φ°	36	34	42	16	14
Permeability: K (m/s)		$1.45.10^{-5}$	$1.48.10^{-5}$	$1.72.10^{-5}$	$1.51.10^{-7}$	$1.79.10^{-7}$

8. Influence of geological conditions on the dam:

8.1. Characteristics of the Dam Body:

Considering the availability of construction materials in the vicinity of the site and their mechanical characteristics obtained from laboratory tests (as reported in the previous pages), the geological conditions of the site are as follows:

-The foundations at the valley floor level exhibit moderate compressibility (alluvial layer) with a coefficient of compressibility (Cc) ranging from 0.10 to 0.20.

-The available materials in sufficient quantity are silty sands, with slightly fewer clayey materials.

-The height of the embankment (26 m) does not favor homogeneous clayey fill materials from both an economic perspective (larger volume of fill) and stability considerations (development of interstitial pressures). Additionally, the borrow zones are relatively distant (the F6 excavation indicates a shallow exploitable potential of approximately 1 m depth).

-There are risks associated with the poor behavior of clays in seismic regions.

Three alternative dam designs can be proposed:

-*Clayey Core Dams with Sand Recharges* .

-*Sand Material Dams with an Upstream Clayey Seal.*

-*Sand Material Dams with a Flexible Waterproof Membrane (Geomembrane)* .

8.2. Characteristics of the Reservoir Basin:

Although the permeability of the reservoir basin may be relatively high compared to desired standards, it should not jeopardize the feasibility of the project. Ensuring that the left side of the basin is better understood during the next study phase will allow for the adoption of appropriate measures (especially considering the permeable layer identified at 6 m depth by borehole S2).

The slopes of the reservoir do not present specific problems related to instability risks such as slip initiation or detrimental gravitational movements.

The existence of a well upstream of the reservoir axis indicates the presence of the aquifer at a probable depth of about fifteen meters. However, this aquifer was not reached by borehole S1.

8.3. Ancillary Structures:

When considering the feasibility criteria for evacuation structures, including:

-Topographical conditions

-Economic considerations (e.g., length of the structure)

-Restitution requirements

-Discharge volumes

-Geological nature of the banks

Our recommendation is to construct a surface drainage facility on the left embankment.

9. Conclusion and Recommendations:

At the end of this study, it is evident that the geological nature of the foundations and banks of the reservoir on the Ouizert River is suitable for the construction of an earth dam with a height of 26 meters from the foundations. However, the following remarks should be considered in the next phase, which is the execution study:

The right flank of the basin requires better understanding for evaluating percolation risks, especially concerning the permeable band identified during drilling at location S2. The significance and inclination of this band can influence percolation.

The compression coefficient of the foundations at location S1 indicates moderately compressible soil. Therefore, this fact must be taken into account during settlement calculations.

The materials that could be used for embankment construction have better mechanical properties than those of the foundations at location S1. It is crucial to verify the stability

of the foundations during the execution study once the selected dam variant is determined. The mechanical characteristics of both the foundations and the embankment support the occurrence of deep-seated slip circles.

While the mechanical characteristics of materials from excavations F2 and F3 do not exhibit significant deficiencies justifying their rejection, their high organic content is sufficient reason to consider them unsuitable for use as borrow materials.

For construction materials, we propose the following:

Fill Materials: Zone of excavation F4 and downstream of F1.

Impermeable Materials: Zones of excavations F5 and F6, or geomembranes available in the national market.

Filter Materials: Locally available if needed or sourced from approved quarries in the region (such as El Maleh Quarry, Terga Quarry, Chaabet El Ham Quarry), or geotextiles available in the national market.

Riprap: Hard limestone from the m4d formation, with deposits located on the summits of the right flank of the site, approximately 3 km upstream along the river, as well as on the southern summits of the reservoir, about 1.5 km away.

Aggregates for Concrete: Quarries in the region can meet the requirements for such materials.

Chapter IV: PRESENTATION OF MODELING SOFTWARE

Part I: Presentation of PLAXIS:

1.Introduction:

The safety of dams is a major issue. It is present implicitly or explicitly in all decisions made during the design, construction and operation of a dam. It depends on many factors, both technical and human. The constant concern for safety must be at the heart of the action of engineers and dam managers. The aim is to avoid both catastrophic failures and failures that could compromise the operation of the structure. The analysis of geotechnical projects is possible thanks to many finite element codes. Nowadays, the use of numerical methods has become common for the analysis of slope stability. Among these codes are Plaxis, Abaqus, ANSYS, COMSOL, Multiphysics, Phase2, and Slide. The Plaxis code is a finite element method (FEM) software developed by Plaxis BV. It is used in a wide range of applications. Plaxis allows us to go from a complex real project to a numerical model and to easily and quickly carry out parametric studies. The modeling of soil behavior is an approach that takes into account the composition and properties of the soil, as well as the size and type of the structure.

It is a software commonly used in engineering firms today. Designed by numerical geotechnicians from the University of Delft in the Netherlands in the 1980s, the finite element calculation code PLAXIS is a practical tool for analyzing geotechnical structures and tests. While this code was initially developed to analyze dikes and soft soils, its field of application now extends to a wide range of geotechnical problems. It allows the analysis of elastic, elasto-plastic, elasto-viscoplastic problems in 2D or 3D and with large displacements using the updated Lagrangian method. Very reliable from a numerical standpoint, this code uses high-precision elements, such as 15-node triangles, as well as recent solution driving techniques like the arc-length method.

PLAXIS is a two- and three-dimensional finite element program specially designed to perform deformation and stability analyses for various types of geotechnical applications. This software, developed by Professor Vermeer's team, allows us to represent real situations.

Figure IV.1: PLAXIS 2D icon

The finite element models can be either plane strain or axisymmetric:

Plane strain models are used for structures whose section is uniform and whose stresses and loading are uniform over a sufficient length in the z direction. Displacements perpendicular to the section are considered to be zero. However, normal stresses in the z direction are fully taken into account.

Axisymmetric models are used for circular structures having a (more or less) uniform radial section, with a loading pattern distributed around the central axis and identical stress and strain states in the radial directions. Note that for axisymmetric problems, the x coordinate represents the radius and the y coordinate corresponds to the axis of symmetry. In this case, negative x coordinates should not be used. For a two-dimensional finite element model, the choice of plane strain or axisymmetric models results in only two translational degrees of freedom per node in the x and y directions.

2. Constitutive Models Used in PLAXIS:

There are numerous soil behavior models: from the Mohr-Coulomb elastic-plastic model to the most sophisticated constitutive laws, allowing to describe almost all aspects of the elasto-plastic behavior of soils, under both monotonic and cyclic loading. These models have been developed with the aim of being integrated into finite element calculations. In this scheme, finite element modeling allows solving the boundary value problem by taking into account, through a realistic constitutive law, the actual behavior of the soil. Two major difficulties have prevented the complete realization of this scheme: on the one hand the constitutive laws that describe soil behavior well are complex, the second difficulty is the integration of these constitutive laws

into bi or three-dimensional finite element calculation codes. Currently, few codes are operational, with sophisticated laws. The constitutive models available in PLAXIS are:

- Linear elastic model
- Mohr-Coulomb model
- Hardening Soil Model
- Soft Soil Model (SSM)
- Soft Soil Creep Model (SSCM)

The PLAXIS software has had (since version 8.0) an option allowing the user to implement their own material constitutive laws.

2.1. Linear Elastic Model:

This model represents Hooke's law for linear and isotropic elasticity. The model includes two elastic stiffness parameters: Young's modulus, E, and Poisson's ratio, ν. The linear elastic model is very limited for simulating soil behavior. It is mainly used for massive rigid structures placed in the ground. The relationship between Young's modulus E and the other moduli is given by the equations:

$$G=\frac{E}{2(1+\nu)}$$

$$K=\frac{E}{3(1+\nu)}$$

$$E_{oed}=\frac{(1-\nu)E}{(1-2\nu)(1+\nu)}$$

2-2: The Mohr-Coulomb Model:

The Mohr-Coulomb model requires the determination of five parameters (figure 4.2). The first two are E and ν (elasticity parameters). The other two are c and φ, respectively, the cohesion and the friction angle. These are classic geotechnical parameters, certainly often provided by laboratory tests, but necessary for deformation or stability calculations.

Stiffness		
E'	kN/m²	0.000
ν' (nu)		0.000
Alternatives		
G	kN/m²	0.000
E_{oed}	kN/m²	0.000
Strength		
c'_{ref}	kN/m²	0.000
φ' (phi)	°	0.000
ψ (psi)	°	0.000

Figure IV.2: Mohr-Coulomb Parameters Window.

2.2.1 Young's Modulus:

Young's Modulus, commonly referred to as the soil elastic modulus, is a fundamental parameter that characterizes the stiffness of soil. It quantifies how much a soil deforms (stretches or compresses) under an applied load. Specifically, Young's Modulus relates the stress (force per unit area) to the strain (relative deformation) in the range of elastic soil behavior.

The choice of a deformation modulus is one of the most difficult problems in geotechnics. The deformation modulus varies with strain and mean stress. In the Mohr-Coulomb model, the modulus is constant. It seems unrealistic to consider a tangent modulus at the origin (which would correspond to Gmax, measured in dynamic tests or at very small strains). This modulus requires special tests. It is advisable to take an "average" modulus, for example the one corresponding to a level of 50% of the failure deviatoric stress (see Figure 4.3). The user must remain aware of the importance of the choice of modulus they will take into account. This is not surprising and the same question arises, for example, in any classic foundation calculation.

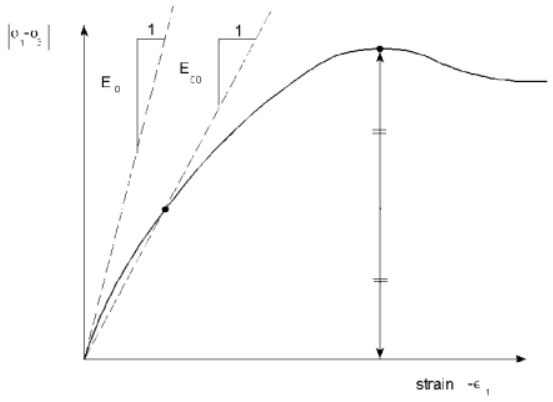

Figure IV.3: Definition of the modulus at 50% of failure.

In the dialog boxes, you can also enter the gradient giving the variation of the modulus with depth.

2.2.2. Poisson's Ratio:

The Poisson's ratio is a material property that describes the ratio of lateral strain (strain perpendicular to the applied load) to axial strain (strain along the applied load) in an elastic material.

It quantifies how a material deforms laterally when subjected to axial loading.

A value of 0.2 to 0.4 is recommended for Poisson's ratio. This is realistic for the application of self-weight (K0 procedure or gravity loading). For certain problems, especially during unloading, lower values can be used. For incompressible soils, Poisson's ratio approaches 0.5, although this value cannot be used.

2-2-3: Friction Angle:

PLAXIS does not account for variation of the friction angle with the mean stress.

The friction angle to be entered is either the "peak" friction angle or the residual friction angle. Attention is drawn to the fact that friction angles greater than 35° can considerably increase calculation times. It may be advisable to start calculations with reasonable friction angle values, and then increase them later. This value of 35° is compatible with the constant volume friction angles CV (at residual).

2-2-4: Cohesion:

It may be useful to assign, even to purely frictional materials, a very low cohesion (0.2 to 1 kPa) for numerical reasons. For undrained analyses with u = 0, Plaxis offers the option to vary the undrained cohesion with depth: this corresponds to the linear increase of cohesion with depth observed in vane shear or cone penetration resistance profiles. This option is implemented with the c depth parameter. A zero value gives a constant cohesion. The units must be consistent with those chosen for the problem (typically in kPa/m). This option also allows the deformation modulus E to vary with depth.

2.2.5: Dilation Angle:

The last parameter is the "dilation" angle noted ψ, which is the least common parameter. However, it can be easily evaluated by the following (rough) rule:

$\psi = \phi - 30°$ for $\phi \geq 30°$

or $\psi = 0°$

The latter case corresponds to very loose sands (often called metastable state, or static liquefaction). The value $\psi = 0$ corresponds to a perfectly elastic-plastic material, where there is no dilation when the material reaches plasticity. This is often the case for clays or for low to medium density sands under fairly high stresses.

2.3. Hardening Soil Model (HSM):

This type of model is well-suited for modeling the excavation of underground structures, where loading and unloading phenomena occur simultaneously. This phenomenon is accounted for by having a higher unloading/reloading stiffness Eur higher compared to the loading stiffness E_{50}.

The model aims to improve the Mohr-Coulomb model in several areas:

- To account for the evolution of the deformation modulus as stress increases: oedometer curves plotted in stress-strain are not straight lines;
- To consider the nonlinear evolution of the modulus as shear increases: the modulus E50 is unrealistic as there is curvature in the stress-strain curves before reaching plasticity;
- To distinguish between loading and unloading;
- To account for limited dilatancy.

Parameters of the HSM:

- Mohr-Coulomb Parameters:

c: (effective) cohesion [kN/m²]

φ: effective friction angle [°]

Ψ: dilatancy angle [°]

- Stiffness Parameters:

E_{50}^{ref}: secant modulus in a triaxial test [kN/m²]

E_{oed}^{ref}: tangent modulus in an oedometer test [kN/m²]

m: power (Janbu-type, 1963; approximately 0.5 for sands, while Von Soos (1990) introduced different values for mmm: 0.5 < m < 1.0) [-]

- Advanced Parameters:

E_{ur}^{ref}: unloading modulus (default $E_{ur}^{ref}=3E_{50}^{ref}$) [kN/m²]

νur\nu_{ur}νur: Poisson's ratio for unloading/reloading (default νur=0.2) [-]

$p^{ref:}$ reference stress (default $p^{ref}=100$) [kN/m²]

k_0^{nc}: coefficient of earth pressure at rest for normally consolidated soil (Jaky, 1944)

R_f: failure ratio q_f/q_a (default Rf=0.9) [-]

$\sigma_{tension:}$ tensile strength (default σtension=0) [kN/m²]

$c_{increment}$: as in the Mohr-Coulomb model (default $c_{increment}=0$) [kN/m³]

The definition of the tangent oedometer modulus is given in Figure 5.6, and that of the (possibly truncated) dilatancy is shown in Figure V.5.

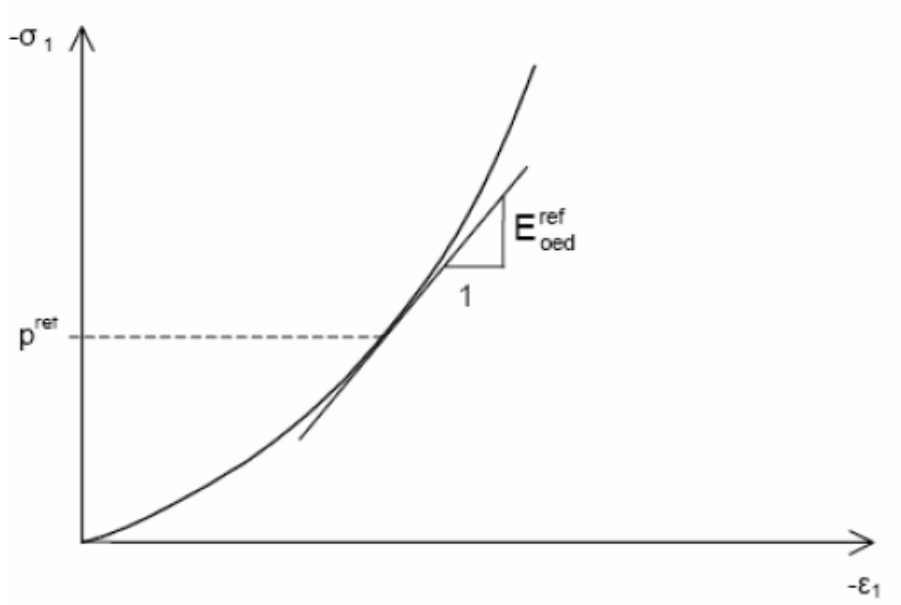

Figure IV.4: Oedometric modulus

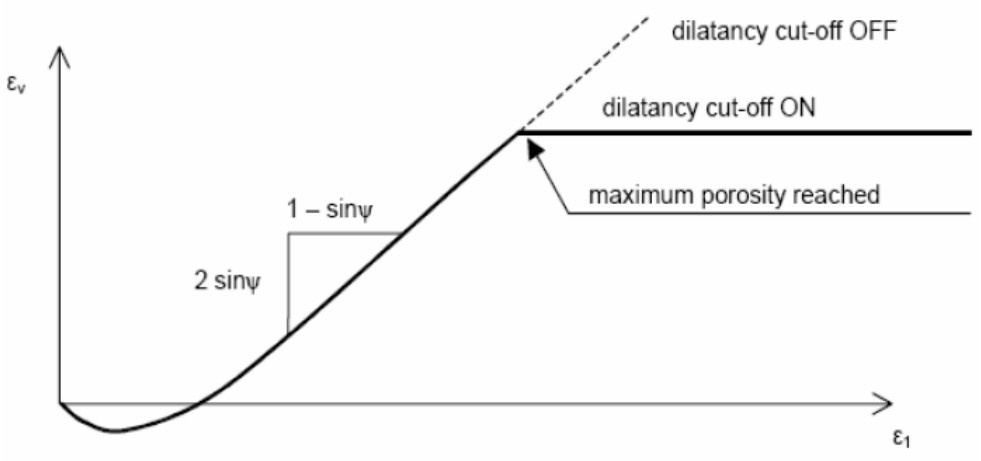

Figure IV.5: Dilatation angle

Part II: The Modeling Approach

1 Data Input:

a. Model Geometry:

Start PLAXIS 2D by double clicking the icon of the Input program. The Quick select dialog box appears in which you can create a new project or select an existing one (Figure IV.6).

Figure IV.6: *Quick select* dialog box

Click Start a new project. The Project properties window appears, consisting of three tabsheets, Project, Model and Constants (Figure IV.6 and Figure IV.7).

Project properties

The first step in every analysis is to set the basic parameters of the finite element model. This is done in the Project properties window. These settings include the description of the problem, the type of model, the basic type of elements, the basic units and the size of the drawing area.

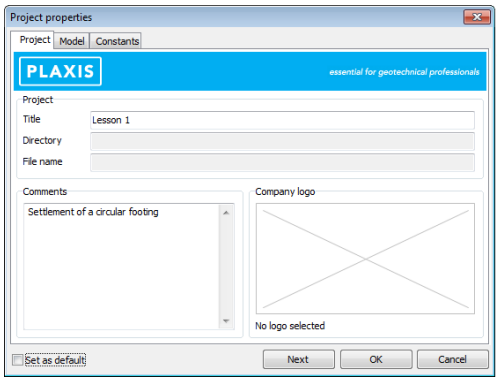

Figure IV.7 *Project* tabsheet of the *Project properties* window

To enter the appropriate settings for the footing calculation follow these steps:

- In the Project tabsheet, enter "Lesson 1" in the Title box and type "Settlement of a circular footing" in the Comments box.
- Click the Next button below the tabsheets or click the Model tab.
- In the Type group the type of the model (Model) and the basic element type (Elements) are specified. Since this tutorial concerns a circular footing, select the Axisymmetry and the 15-Noded options from the Model and the Elements

drop-down menus respectively.

- In the Contour group set the model dimensions to xmin = 0.0, xmax = 5.0, ymin = 0.0

and ymax = 4.0.

- Keep the default units in the Constants tabsheet.

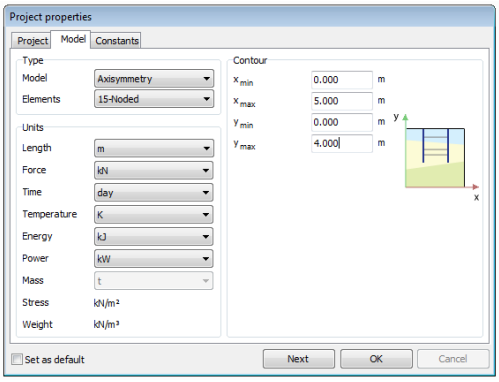

Figure IV.8: Model tabsheet of the Project properties window

b. Material Properties:

In order to simulate the behaviour of the soil, a suitable soil model and appropriate material parameters must be assigned to the geometry. In PLAXIS 2D, soil properties are collected in material data sets and the various data sets are stored in a material database. From the database, a data set can be assigned to one or more soil layers. For structures (like walls, plates, anchors, geogrids, etc.) the system is similar, but different types of structures have different parameters and therefore different types of material data sets. PLAXIS 2D distinguishes between material data sets for Soil and interfaces, Plates, Geogrids, Embedded beam rows and Anchors.

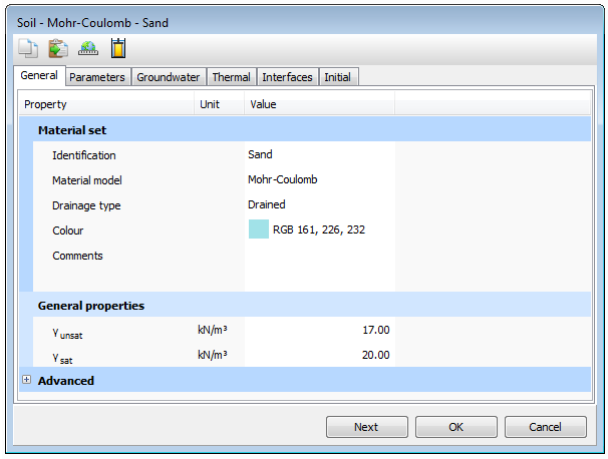

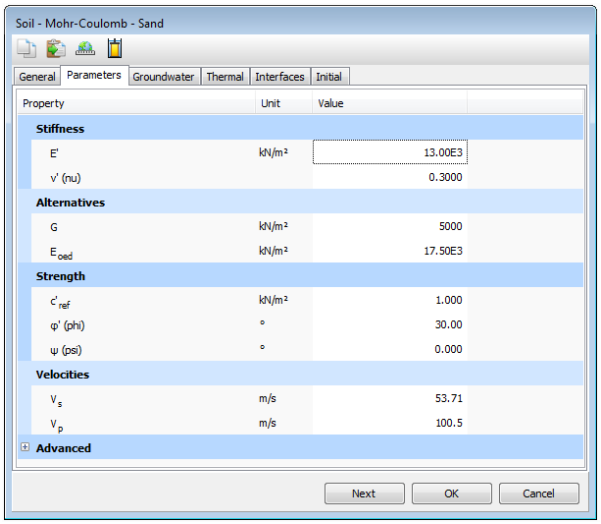

Figure IV.9: Example of the material properties

c. Boundary Conditions:

"Fixities" are imposed zero displacements. These conditions can be applied to lines or points defining the model geometry, in the x or y directions. An option allows the application of standard support conditions valid in most cases.

d. Loading:

Two independent loading systems are proposed to apply point loads or distributed loads. Point loads can be applied to any point of the geometry, distributed loads to any line of the geometry, not limited to the outer boundary. The load values can be modified in the "Staged Construction" mode and/or by using multipliers.

e. Automatic Mesh Generation:

Plaxis offers fully automatic generation of unstructured finite element meshes, with options to refine the mesh, globally or locally. The mesh can contain thousands of elements.

Proceed to the Mesh mode.

- Create the mesh. Use the Fine option for the Element distribution parameter.
- View the generated mesh.

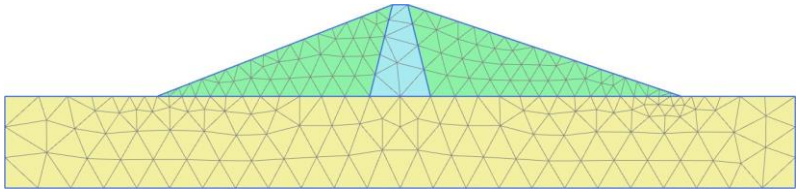

Figure IV.10: Example of mesh generation for an earth dam

f. Initial Conditions:

Once the geometric model is created and the finite element mesh is generated, the initial stress state and initial configuration must be specified. This is done in the part dealing with the initial conditions of the data input program. The initial conditions consist of two different modes, one to generate the initial pore pressures (hydraulic conditions mode) and the other to specify the initial geometric configuration and generate the initial effective stress field (geometric configuration mode).

2.The Calculation:

The calculation program performs deformation analyses either by plastic calculation, consolidation calculation, or large deformation calculation, and safety factor calculation. For each project, several calculation phases can be defined before starting the calculation.

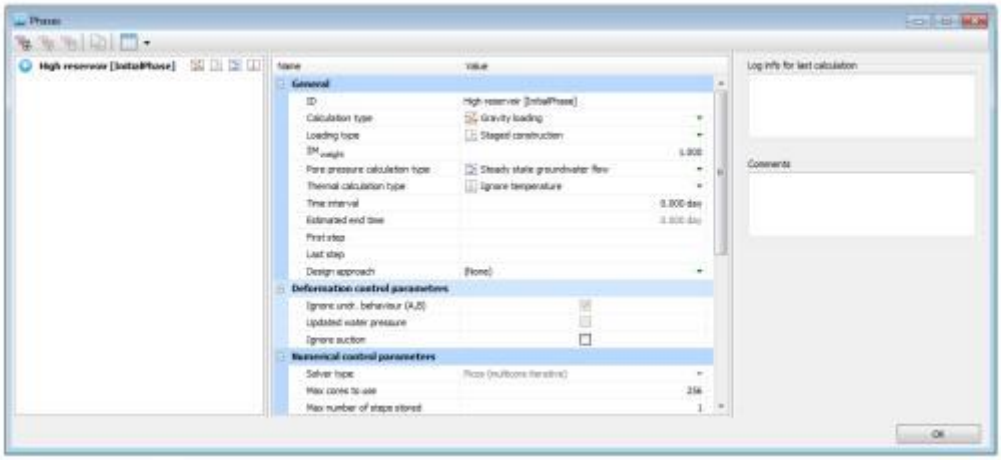

Figure IV.11: Example of calculation phases

3.Result Analysis:

The main results of a finite element calculation are the displacements at the nodes and the stresses at the stress points. Additionally, when a finite element model includes structural elements, forces are calculated in these elements.

a. Déformations:

The graphical representation of deformations can be done in the form of deformed mesh, total or incremental displacement maps, or total or incremental strain maps.

b. Stresses:

The representation of stresses can be done in effective stresses, total stresses, pore pressures, and excess pore pressures.

4.Conclusion:

Like all software, Plaxis is an easy-to-use tool that allows the analysis of 2D geotechnical problems. The toolbar contains icons for actions related to the creation of the geometric model. These icons are placed in an order that generally allows the complete definition of the model by following the buttons on the toolbar from left to right. It is characterized notably by the "staged construction" function (Staged construction) which is the most important type of loading (Loading input). Thanks to Plaxis' special features, it is possible to change the geometry and loading configuration by deactivating or reactivating loads, soil layers, or structural elements created during the definition of the geometric model. Staged construction allows an accurate and realistic simulation of different loading, construction, and excavation processes. The Plaxis calculation code has been used in this thesis as a modeling support for the remainder of the work.

Chapter V: Stability study of dam using Plaxis software

1. Introduction:

A significant factor that can impact the stability of a dam is the reduction of water levels, often called drawdown. Drawdown is a classic scenario in slope stability, whether partial or total reservoir drawdown, rapid or slow. The latter, known as slow drawdown, is a common operating procedure that may be necessary for maintenance, safety, or water resource management reasons, in case of extreme events. Our study focuses on calculating the stability of earth dams during their end of construction, normal operation, and determining displacements using numerical methods. We use the PLAXIS V20 calculation code. The objective of this study is to investigate the stability and displacements of a real dam using two behavior models: the Mohr-Coulomb model (PLAXIS).

The value of the safety coefficient indicates the degree of stability of a slope. This value measures the possible reduction in the soil's shear strength before the soil slips along the most critical surface.

The final safety coefficient depends on several factors:

- The mechanical characteristics of the soil, determined by the geotechnical investigation,

which correspond to the load conditions to be considered when designing the embankment.

- The stability calculation method used to assess the safety coefficient.

- The precision with which the values of pore pressures are estimated

and how they are applied in the chosen stability analysis method.

The aim of the slope stability calculation is to find the minimum safety coefficient that will

ensures the correct operation of the structure and is the most economical.

2. Modeling of the Dam using PLAXIS:

The modeling was established and calculated using the PLAXIS V.20 software to verify the sensitivity of earth dam deformations to the soil behavior model. Each finite element software has its own algorithms: resolution methods, modeling parameters. Uninformed users are not always aware of these implicit numerical assumptions.

3. Assumptions for modelling:

The main assumptions:

- 2D plane model
- 15-node elements
- Refined mesh at the dam
- Lowering of the "hydrostatic" water table. Initially, the foundation is modeled without the dam. The complete model will be prepared in Plaxis.
- Filters, being small compared to the dam, are not taken into account in the modeling, nor are the gallery and other hydraulic structures.
- However, the elasticity modules are fixed at a realistic value to approximately calculate the failure mode and the distribution of principal stresses under static loading in normal retention.

4. The geometry and characteristics of the dam construction materials:

First, we go to “Structures” to add geometry of our dam dike:

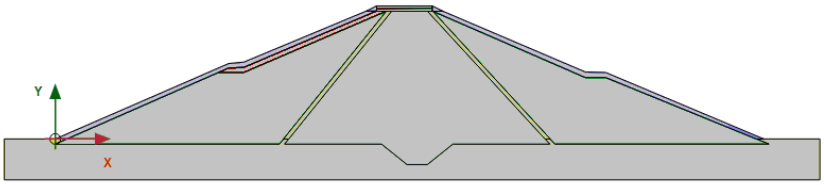

Figure V.1: Dam geometry.

Next,we go to “Soil” to add materiales:

The Mohr-Coulomb model was used in this study

The model is characterized by the following parameters:

Internal Friction Angle : This angle describes the shear strength of the soil due to friction between the grains of the material. A high friction angle indicates a material with greater shear strength.

Cohesion: Cohesion is a measure of the inter-particle attraction that allows the material to resist shear forces without any normal pressure. Cohesion is particularly important for clayey soils.

Young's Modulus: Young's modulus is a measure of the stiffness of the material in response to axial stress. A high Young's modulus means the material is stiffer.

Poisson's Ratio: This coefficient measures the lateral deformation of a material when it is subjected to axial stress. It describes the elasticity of the material.

Dilatancy Angle: This angle describes the tendency of the material to expand or contract under shear conditions. For many soils, this angle is often close to the internal friction angle.

Material set			Stiffness		
Identification		Fill	E'	kN/m²	20.00E3
Material model		Mohr-Coulomb	ν' (nu)		0.3300
Drainage type		Drained	**Alternatives**		
Colour		RGB 46, 239, 101	G	kN/m²	7519
Comments			E_{oed}	kN/m²	29.63E3
			Strength		
General properties			c'_{ref}	kN/m²	5.000
γ_{unsat}	kN/m³	16.00	φ' (phi)	°	31.00
γ_{sat}	kN/m³	20.00	ψ (psi)	°	1.000

Figure V.2: Set parameters of fill.

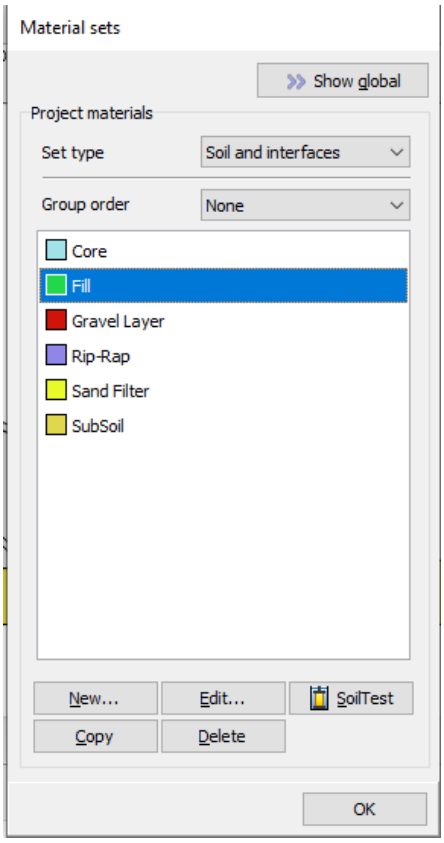

Figure V.3: Materials table.

Then we add to each part the material suitable for it:

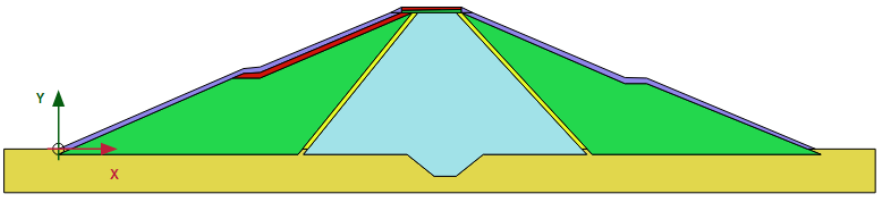

:

Figure V.4: The structure of the first variant.

Then we go to mesh and view in Plaxis Output:

The mesh is generated automatically, which is a strong point of Plaxis. The operator can set the mesh fineness among different options (very coarse, coarse, medium, fine, very fine). The user can also choose to mesh a certain region of the soil and the vicinity of an element more finely using the refine options in the mesh menu.

We chose 15-node elements. For greater precision, the mesh is refined at the dam.

Regarding the mechanical boundary conditions, Plaxis automatically imposes a standard setting for the general boundary conditions of the geometric model.

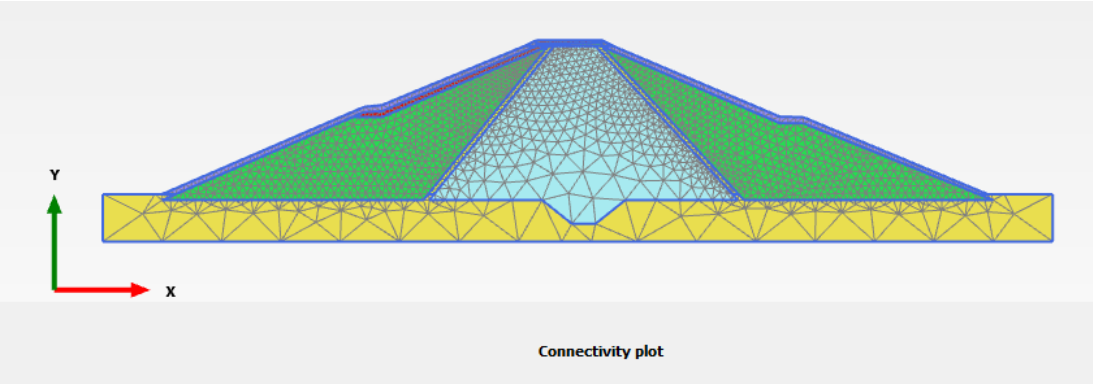

Figure V.5: Generated mesh output.

5. Initial Conditions:

Once the geometric model is created and the finite element mesh is generated, the initial stress state and initial configuration must be specified. This is done in the initial conditions section of the data input program.

The initial conditions consist of two different modes: one to generate the initial pore pressures (hydraulic conditions mode) and the other to specify the initial geometric configuration and generate the initial effective stress field (geometric configuration mode).

6. Stability factor:

First, we go to “Staged construction” then “Phase explorer”:

Phase 1: End of Construction (Under the Effect of the Dam's Self-Weight) This is a plastic calculation, and in the Parameters tab, we need to select Reset displacements to zero in the Control Parameters area. This will eliminate non-physical displacements resulting from the first calculation phase. However, this operation does not affect the stresses.

Phase 2: Stability Factor Calculation

In a stability analysis (Phi-c reduction), the value of the safety factor is an indicator of the stability of a structure. However, the pattern of the incremental displacement field also provides

important information about the failure mechanism. This pattern is typically obtained through a traditional limit equilibrium analysis for circular failure surfaces.

This step can be performed using the c/phi reduction method. The reduction in strength parameters is controlled by the total multiplier ∑Msf. This parameter is incrementally increased until failure occurs. The safety factor is then defined as the value of ∑Msf at failure, provided that a more or less constant value is obtained at failure for a certain number of successive loading steps.

7. Results of the safety factor before filling:

We observe that the displacement of the dam is 1.288m before filling, and the safety factor is 1.525.

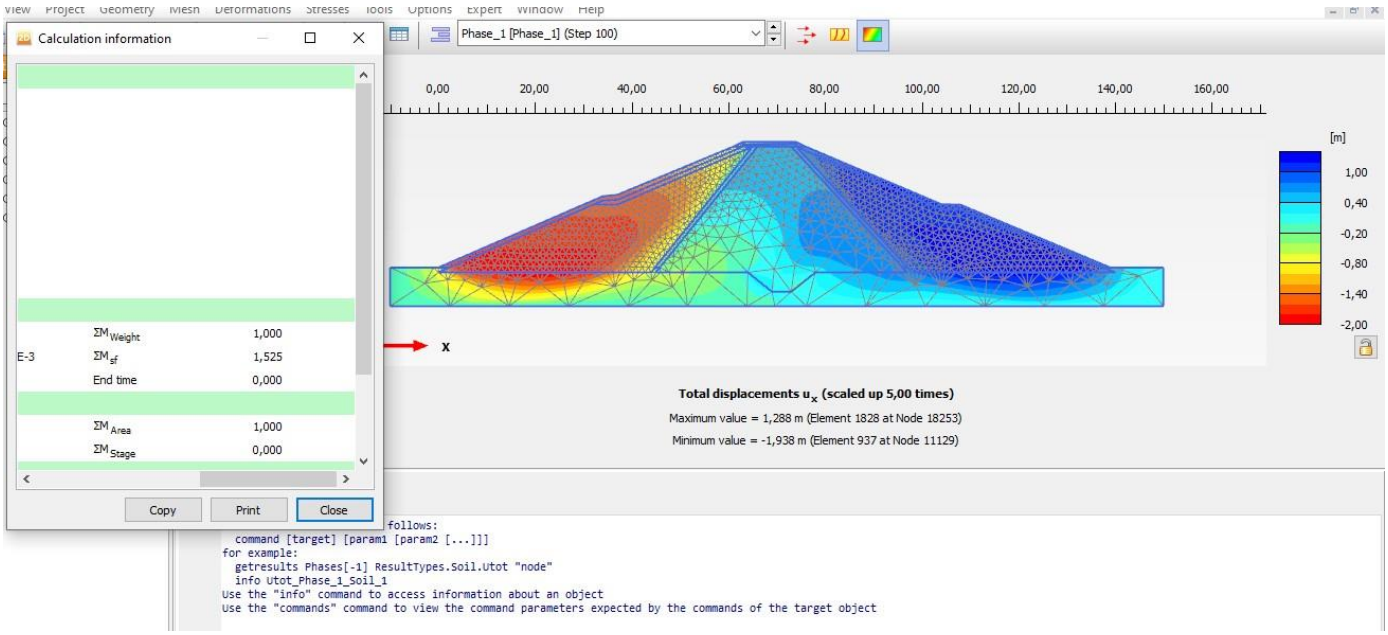

Figure V.6: Value of safety factor

8. Results of the safety factor after filling:

Pour H=10m:

We observe that the displacement of the dam is 1.335m before filling, and the safety factor is 1.450.

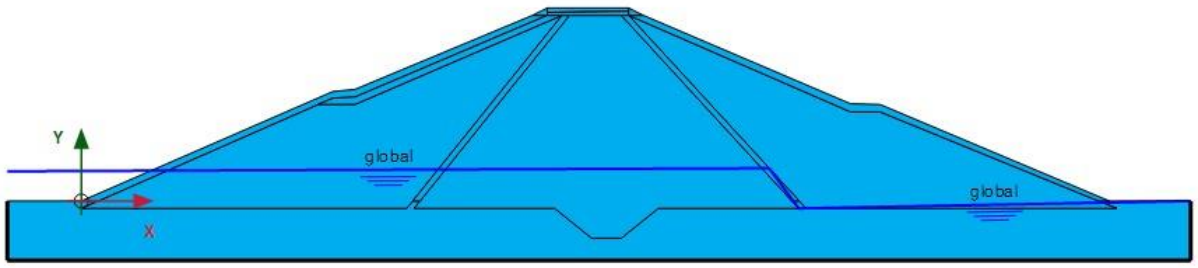

Figure V.7: Phreatic water level H=10m

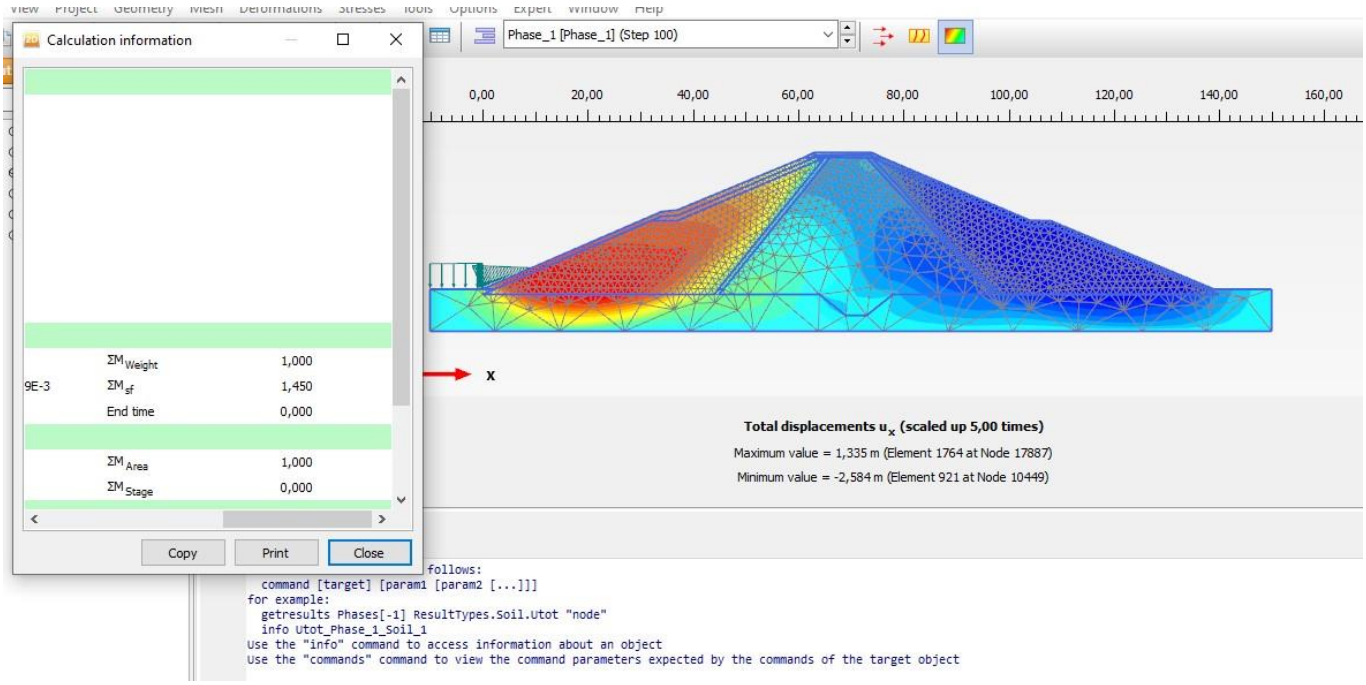

Figure V.8: Value of safety factor H=10m

H=26m:

We observe that the displacement of the dam is 1.758m before filling, and the safety factor is 1.079.

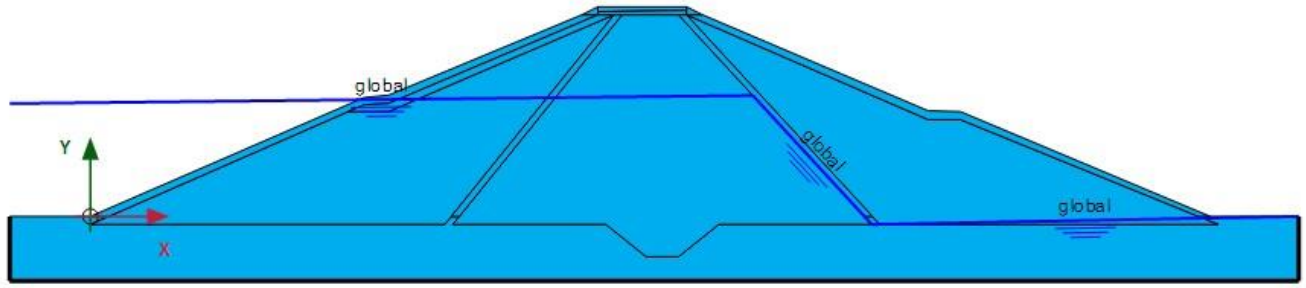

Figure V.9: Phreatic water level

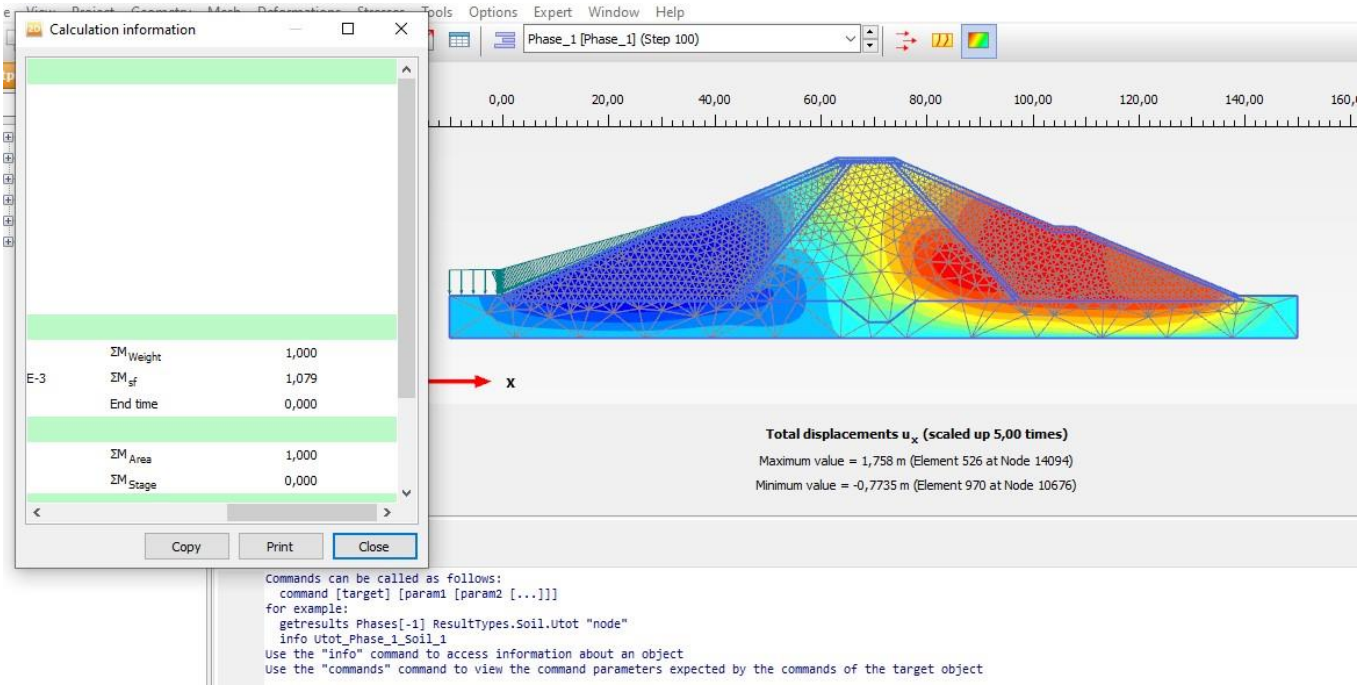

Figure V.10: Value of safety factor H=26m

9. Values of safety factor for different scenarios:

To assess the stability of the dam, the results of stability analyses of the dam facings in terms of static safety factors must be compared to the minimum permissible regulatory values for each stability case.

Our results indicate that the dam is stable under static conditions

Table V.1: Results of Safety factor for variant 1.

	Before filling	**H=10m**	**H=26m**
Displacement	1.288	1.335	1.78
Safety factor	1.525	1.450	1.079

The same way with other variant :

Table V.2: Results of Safety factor for variant 2.

	Before filling	**H=10m**	**H=26m**
Displacement	1.302	1.483	1.977
Safety factor	1.495	1.421	1.057

Table V.3: Results of Safety factor for variant 3.

	Before filling	**H=10m**	**H=26m**
Displacement	1.286	1.333	1.760
Safety factor	1.520	1.435	1.068

10. Safety factor under earthquake:

The numerical simulation investigated the response of the earth dam to dynamic loading conditions by employing the pseudo-static approach, which simplifies dynamic effects into equivalent static forces. The study assessed the stability of the dam, and the results indicated that the dam remained unstable Fs=0.732 under these dynamic conditions. This analysis reveals that the dam is unable to withstand seismic or other dynamic events with the applied loading. It provides valuable insights into the dam's performance and safety under dynamic scenarios, highlighting the need for reinforcement and supporting informed engineering decisions regarding its design and construction.

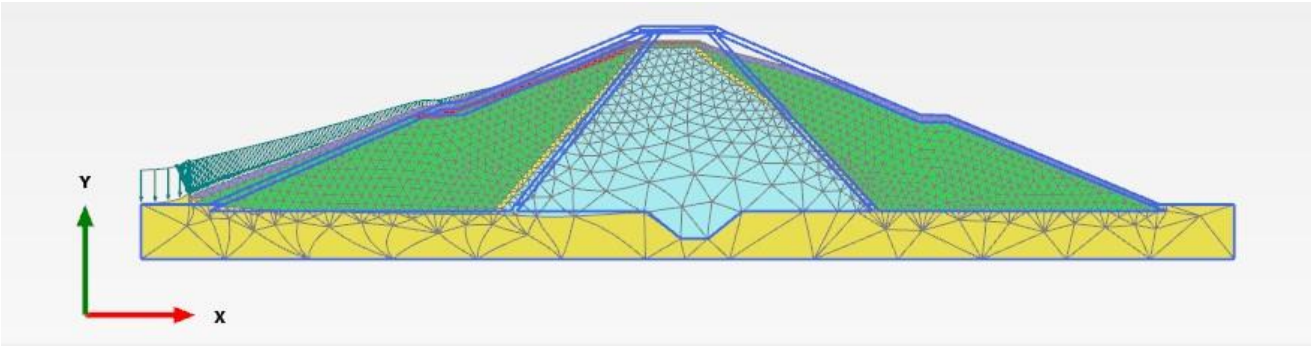

Figure V.11: Deformed mesh under dynamic condtions

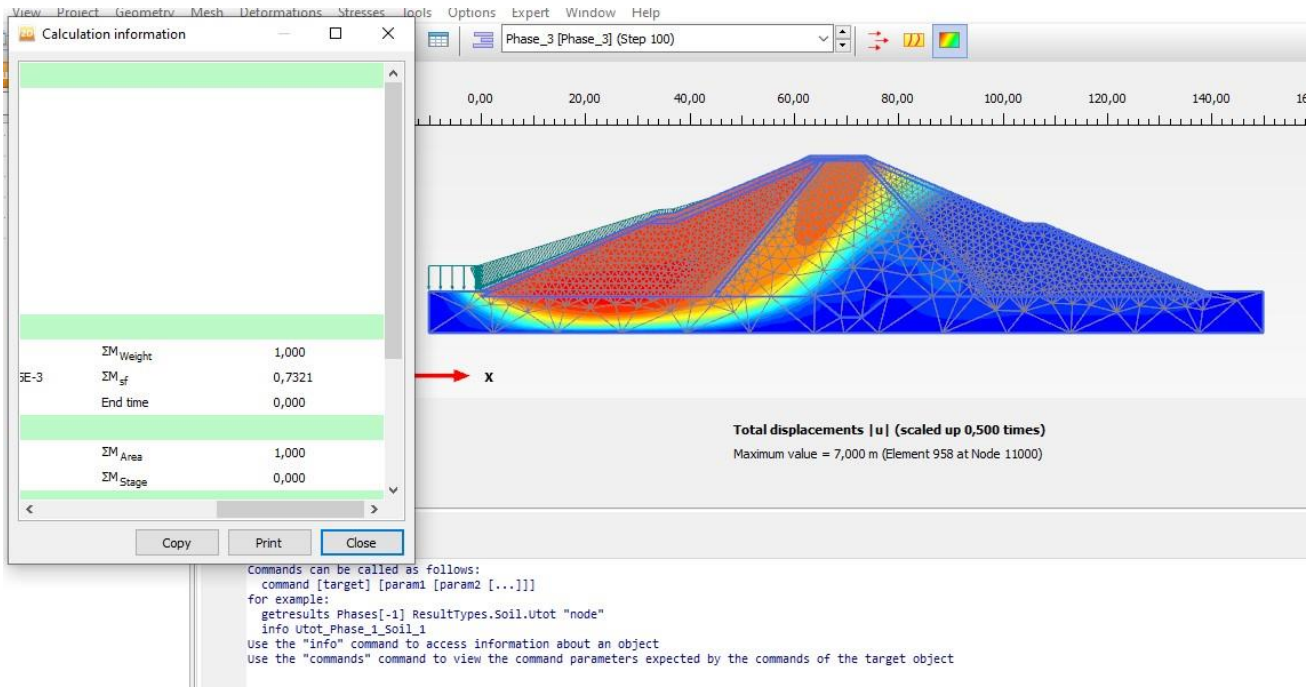

Figure V.12: Value of safety factor under dynamic conditions

11. Conclusion:

Based on the chapter you have completed, here is a general conclusion:

The numerical simulation using the Mohr-Coulomb model in PLAXIS for an earth dam provided valuable insights into its stability under varying water levels. The simulation progressed from an empty reservoir to full saturation, demonstrating that the dam remains stable under all conditions tested. Throughout the analysis, it was observed that as the water level increased, the safety factor decreased while displacements increased. This indicates that the dam's stability is closely linked to the water level, with higher water levels exerting more critical stresses on the structure. Overall, the study underscores the importance of comprehensive numerical modeling in assessing and ensuring the safety of earth dams under different loading scenarios. In addition, a dynamic study was conducted, demonstrating that the stability of the dam under dynamic loading conditions was less than 1.

Recommandations:

It is recommended to reinforce the dam so that it can withstand seismic forces.

Foundation Reinforcement: Improve the foundation of the dam using techniques such as soil compaction, cement grouting, or the use of piles to increase the bearing capacity and reduce the risk of liquefaction.

Coatings and Protections: Add geotextile or concrete coatings to protect the dam slopes against erosion and landslides during an earthquak

Chapter VI: Technical-economic Study

1.Introduction:

This chapter presents a comprehensive techno-economic study of the Ouled Taoui commune dam project, a significant water infrastructure development located in Aïn Témouchent/Algeria. The study aims to evaluate the technical feasibility and economic viability of this ambitious hydraulic engineering project.

The Ouled Taoui dam represents a major investment in the region's water resources management. As such, a thorough analysis of its technical aspects and economic implications is crucial for informed decision-making and effective project planning.

Through this techno-economic study, we aim to provide a holistic understanding of the Ouled Taoui dam project's feasibility. The analysis will draw upon engineering data, economic models, and relevant case studies to offer insights into the project's potential success and its broader implications for regional development.

This chapter will serve as a crucial component in evaluating the overall viability and sustainability of the Ouled Taoui dam project, contributing to the broader discourse on water resource management and infrastructure development in Aïn Témouchent/Algeria.

2. Estimated cost of variants:

Table VI.1: Bill of quantities.

Description of works (Dike)	UNIT	QUANTITY		
		Variant 1	Variant 2	Variant 3
Uncovering of the site	m^3	6267.2	8645.6	5997.5
Excavation of trenches (Anchor key)	m^3	3873.5	4760.0	3295
Backfilling of excavations (anchor key)	m^3	3873.5	-	3295
Rock fill (prism + Rip-rap)	m^3	3464.82	5669.69	5543.08
Gravel (crest + upstream face)	m^3	1221.19	1318.8	2346.28
Sand	m^3	5668.36	8780.7	8876.75
Dam embankment (fill zones)	m^3	52989.47	88990.47	61071.63
Clay fill (core - mask)	m^3	36808.7	12477.83	-
Flexible membrane	m^2	-	-	7400

Table VI.2: Estimated quote for the construction of the Ouled Taoui dam (Var 1).

No	Description of works	Unit	Quantity	Unit Price	Amount
	Dike				
1	Site installation	FFT	FFT	FFT	6 000 000
2	Clearing of the base	m^3	6267.2	250	1 566 800
3	Excavation (anchoring key)	m^3	3873.5	300	1 162 050
4	Backfilling of excavations	m^3	3873.5	650	2 517 775
5	Rip-Rap rockfill	m^3	3464.82	2500	8 662 050
6	Gravel for crest and facing	m^3	1221.19	2200	2 686 618
7	Sand	m^3	5668.36	2200	12 470 392
8	Dam embankment (recharges)	m^3	52989.47	500	26 494 735
9	Clay fill	m^3	36808.7	650	23 925 655
	Total amount (AD/ET)	85 486 075			

Table VI.3: Estimated quote for the construction of the Ouled Taoui dam (Var 2).

No	Description of works	Unit	Quantity	Unit Price	Amount
	Dike				
1	Site installation	FFT	FFT	FFT	6 000 000
2	Clearing of the base	m^3	8645.6	250	2 161 400
3	Excavation (anchoring key)	m^3	4760	300	1 428 000
4	Backfilling of excavations	m^3	4760	650	3 094 000
5	Rip-Rap rockfill	m^3	569.69	2500	1 424 225
6	Gravel for crest and facing	m^3	1318.8	2200	2 901 360
7	Sand	m^3	8780.7	2200	19 317 540
8	Dam embankment (recharges)	m^3	88990.47	500	44 495 235
9	Clay fill	m^3	12477.82	650	8 110 583
	Total amount (AD/ET)	88 932 343			

Table VI.4: Estimated quote for the construction of the Ouled Taoui dam (Var 3).

No	Description of works	Unit	Quantity	Unit Price	Amount
	Dike				
1	Site installation	FFT	FFT	FFT	6 000 000
2	Clearing of the base	m^3	997	250	249 250
3	Excavation (anchoring key)	m^3	3295	300	988 500
4	Backfilling of excavations	m^3	3295	650	2 141 750
5	Rip-Rap rockfill	m^3	5543.08	2500	13 857 700
6	Gravel for crest and facing	m^3	2346.28	2200	5 161 816
7	Sand	m^3	8876.75	2200	19 528 850
8	Dam embankment (recharges)	m^3	61071.63	500	30 535 815
9	Flexible membrane	m^3	7400	3500	25 900 000
	Total amount (AD/ET)	104 363 681			

3.Final results:

After all calculations, it is easy to deduce the economic parameters of the development for each variant, namely:

Variant 1: Core Dam

- Total embankment volume: 101,766 m3.
- Useful water volume in the reservoir: 868,830 m3
- Total cost of development: 148,431,475.00 DA
- Degree of profitability: R = 8.54
- Price of water per m3 at the foot of the dam: Pe = 170.84 DA/m3

Variant 2: Core Dam

- Total embankment volume: 112,718 m3.
- Useful water volume in the reservoir: 868,830 m3
- Total cost of development: 151,877,743.00 DA
- Degree of profitability: R = 7.71
- Price of water per m3 at the foot of the dam: Pe = 174.81 DA/m3

Variant 3: Core Dam

- Total embankment volume: 97,762 m3.
- Useful water volume in the reservoir: 868,830 m3
- Total cost of development: 167,309,081.00 DA
- Degree of profitability: R = 8.89
- Price of water per m3 at the foot of the dam: Pe = 192.57 DA/m3

Conclusion:

The prices used were obtained from the ANB based on an analysis of ongoing hill reservoir construction projects.

From the above, it is easy to deduce that Variant No. 1 presents better advantages both from an economic and safety perspective (behavior of the core in the face of potential earthquakes).

Chapter VII:
Data Analysis of Feasibility River Using Python

Introduction:

In recent years, the effects of climate change on the world have been observed in Algeria through the emergence of heat waves that sometimes lead to fires and the drying up of some dams.

Because we used the 1967-2009 rainfall series during a hydrological study before the drought years started in Algeria.

Therefore, this chapter consists of two parts: first, we need to analyze satellite images using machine learning (Python language) to determine if the river is affected by climate change. Second, it is interpretation about if we will assess the feasibility of constructing a dam in the area at this time.

Part I: Data Analysis using Python

1. Definition: Python data analysis is gathering, converting, and arranging data in order to provide predictions and judgments that are well-informed. The following are the main actions in a Python data analysis workflow:

- Acquire Data: Use Python libraries like pandas to read and load data into memory.
- Cleanse Data: Obtain and ensure data consistency from various sources.
- Explore Data: Visualize data using libraries like Matplotlib or Seaborn.
- Analyze Data: Apply statistical techniques, regression models, or machine learning algorithms.
- Communicate Findings:

  Present results through visualizations, reports, or dashboards.

  Make data-driven decisions based on your analysis.

2.Workflow steps:

- **Step 0:** Import libraries.

```python
from pathlib import Path
from IPython.core.display import Video

import numpy as np
import pandas as pd
import geopandas as gpd  # Vector data handling
import osmnx as ox       # Downloading data from OSM

from shapely.geometry import box
from scipy.spatial import cKDTree as KDTree # For Inverse Distance Weight calculation

import xarray as xr
import xrspatial    # Hillshading
import rioxarray    # Working with geospatial data in xarray

import matplotlib.pyplot as plt
from datashader.transfer_functions import shade, stack
```

FigureVII.1 : Import libraries's code.

- **Step 1:** Obtain and Ensure Data.

For this step, our data is series of satellite images from 1985 – 2024 (this summer).

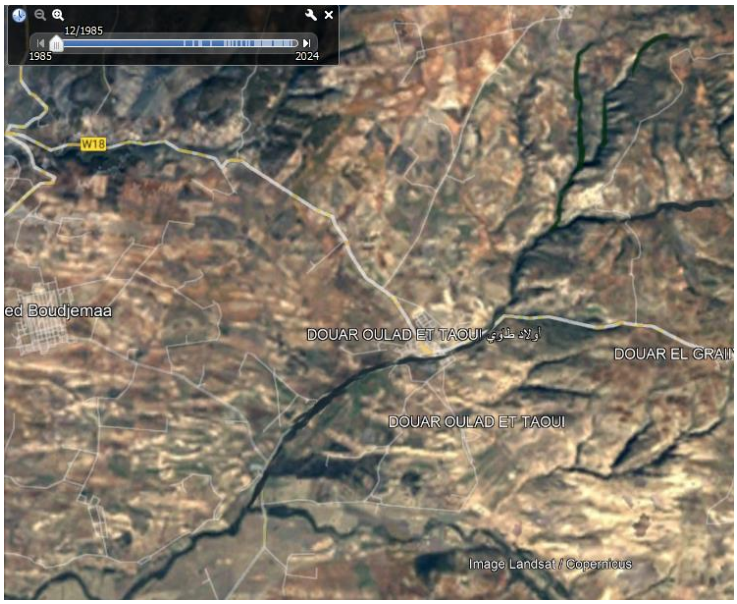

FigureVII.2 : Satellite images 1985-2024.Source : Google Earth Pro.

- **Step 2**: Download data.

The code of the downloaded data can be combined using the convenience function combine_by_coords.

```
path = Path('data').joinpath('ivalo', 'ivalo.nc')
dem = rioxarray.open_rasterio(path)

osm_id = 'W34406947'

river = ox.geocode_to_gdf(osm_id, by_osmid=True)
river = river.to_crs(dem.rio.crs)
```

FigureVII.3: Code of Download & Load DEM and Fetch coordinates of the river.

Thanks to OSMnx, we can automatically obtain a GeoPandas DataFrame from OSM data.

- **Step 3**: Visualize data.

We need to cut area of intertest by detect only data river to analyse in next step

The code:

```
fig, ax = plt.subplots()
dem.squeeze().plot.imshow(ax=ax)
river.plot(ax=ax, color='red')
```

FigureVII.4 : Code for detection the river and show it in red

The visualize

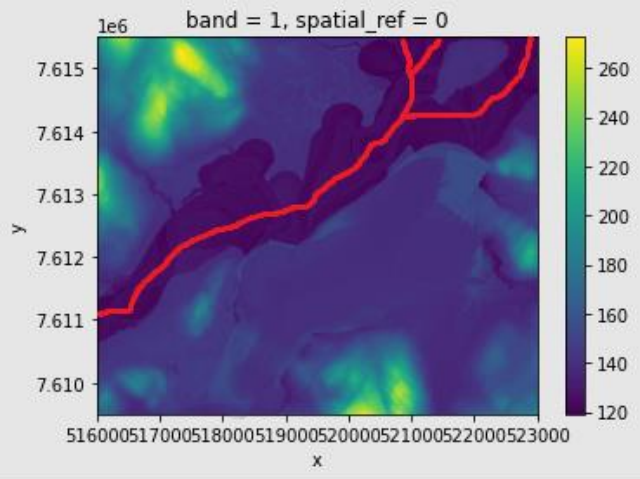

FigureVII.5: Cut to area of interest showing the river in red

- **Step 4**: Analyse data:

Now, we make REM visualizations.

```
colors = ['#f2f7fb', '#81a8cb', '#37123d']


shade(rem.squeeze(), cmap=colors, span=[0, 10], how='linear')
```

FigureVII.6 : Relative Elevation Model's code

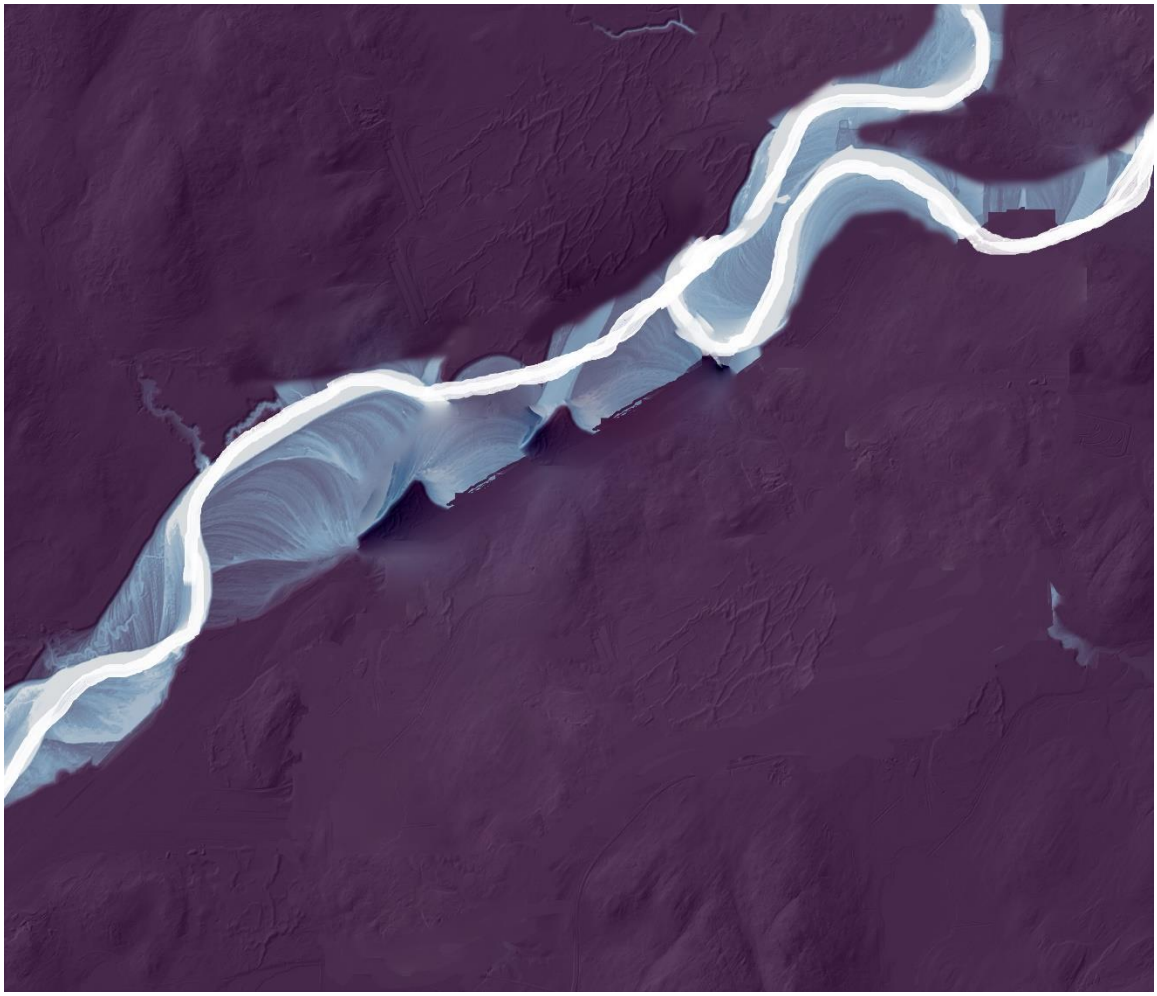

FigureVII.7: REM visualizations

Part 2: Data-driven decisions

1.Interpritation of REM visualization:

The dark blue color represents places that have not changed, such as topography and geography, while the light blue color represents the path of the Ouizert's river over the years, and the closer the color is to white, this indicates that it is more modern and close to our time.

It is normal for a river to change its course, but we notice that in the case of the Ouizert's river in Oueled Taoui commune, the white line is shrinking, this indicates that the river is undergoing some changes, which is a decrease in water levels, this is a visualization that indicates that the river has begun to dry out by a small percentage, but it can be observed over the years.

2.Expilaction:

The Algeria territory and in particular its Western part has experienced several droughts over the last century, during the 1940s and 1970s to the present day (Meddi and Hubert, 2003; Meddi et al., 2009; Taibi et al., 2013, 2017, 2019; Zeroual et al., 2017,2020).

In addition to the location of the river in a rural area such Oueled Taoui commune where the water of the Ouizert's river is consumed in agriculture without any significant regulation, this contributes to accelerating the drying process more quickly.

3.Decision:

Based on the rigorous data analysis of the river elevation model, which reveals a consistent decline in water levels attributed to climate change, it is prudent to reconsider the feasibility of constructing a dam on the Ouizert River in the Oueled Taoui commune.

The diminishing water resources pose substantial challenges to the long-term viability and sustainability of such an infrastructure project.

Instead, alternative water management strategies, adaptive measures, and comprehensive environmental impact assessments should be prioritized to address the evolving hydrological conditions and mitigate potential risks.

GENERAL CONCLUSION

General conclusion:

A study on the execution of the Oued Ouizert dam has been carried out thanks to this work and we have the following results: The chosen site is geologically and geotechnically suitable for dam construction, with no major threat to the foundations or the anchoring of the dam. The selected dam design incorporates materials available on site from three variables, ensuring embankment stability under all loads. After a comprehensive technical and economic optimization study, the topographical conditions allowed for the design of a dam with a height of 26 meters, crest width of 7 meters, and crest length of 140 meters. Complementary structures to the dam have been appropriately dimensioned to meet technical requirements. Based on the dimensioning and stability calculations developed in this work, it can be concluded that the proposed site for this development is technically favorable.

Climate change is leading to declining river water levels over time, posing challenges for infrastructure projects like dams. Prioritizing alternative water management strategies and conducting thorough environmental assessments are essential to address evolving hydrological conditions and mitigate risks.

Finally, leveraging theoretical knowledge acquired during academic studies, along with advanced technologies such as Plaxis software for numerical modeling using the Mohr-Coulomb model and the C phi reduction method to calculate safety factors under static and dynamic conditions before and during dam filling, as well as utilizing Python-based machine learning for satellite image analysis to determine the impact of climate change on the river, this study has comprehensively addressed various aspects of dam design and execution.

Bibliography

Bibliographic references

A Zeroual, AA Assani, M Meddi, R Alkama (2019)Assessment of climate change in Algeria from 1951 to 2098 using the Köppen–Geiger climate classification scheme .

Jacob Montiel &AL (2021) River: machine learning for streaming data in Python .

Meddi, M. et Zeroual, A. (2018) Formules empiriques d'estimation de débit de pointe. In : Introduction à la modélisation en hydrologie.

Mihoubi, M.K. (2014) Manuel de dimensionnement d'un barrage réservoir en remblai, ENSH, Blida.

Mohamed Meddi, , Gil Mahé, Ali Hadour (2020) Watershed based hydrological evolution under climate change effect: An example from North Western Algeria, a National High School of Hydraulics.

Moslem Ouled Sghaier &AL (2018) A Multiscale Based Approach for River Extraction from SAR Images Using Attribute Filters.

PLAXIS 2D Tutorial Manual: CONNECT Edition V20, Bentley .

Rodriguez, R. and La Rosa, C. (2004). "Design of Filters in Earth Dams." Dams and Reservoirs: Concepts, Engineering, and Management. Edited by A. E. Scheidegger and M. A. Celia. New York: Springer.

Touabia, B. (2001) Régularisation des débits, ENSH Blida.

Touaibia, B. (2004) Manuel pratique d'hydrologie. ENSH Blida.

Touabia, B. et Benlaoukli, B. (2004) Introduction au dimensionnement desretenues collinaires. ENSH Blida.

Touaibia, B. (2015) Manuel Pratique d'Hydrologie, 2 eme éd, Ecole Nationale Supérieure d'Hydraulique Blida.

United States Department of the interior. (1987) Design of small dam, 3 eme éd.

Analyse chimique d'eau

TRAVAUX GEOETECHNIQUES
EPE SERSID SPA

11, RUE BENGOUA ABDELKADER ES-SEDDIKIA –ORAN
DEPARTEMENT LABORATOIRE

A la demande de l'entreprise , une analyse chimique a été réalisée sur deux échantillons d'eaux de puits et d'oued au niveau du laboratoire central SERSID, pour la détermination de ses qualités chimiques .

Résultats d'analyse chimique d'eau

L'échantillon / Les paramètres		Puits	Oued
PH		6.8	6.7
TH "dureté totale		38.5°F	48° F
Titre Alcamétrique	**TAC**	31.66° F	33.33° F
	TA	nulle	nulle
Les chlorures « Cl^- »		745.5 mg/l	274.5 mg/l
NaCl		1228.5 mg/l	243.36 mg/l
Les sulfates « SO_4^{2-} »		160.17 mg/l	82.64 mg/l
H_2SO_4		163.52 mg/l	133.32 mg/l
NaOH		253.28 mg/l	279.97 mg/l
$NaHCO_3$		532 mg/l	166.51 mg/l
$CaCO_3$		316.6 mg/l	259.43 mg/l
$Ca(HCO_3)_2$		512.89 mg/l	339.94 mg/l
$Mg(HCO_3)_2$		462.24 mg/l	234.04 mg/l

UNITE TRAVAUX GEO - TECHNIQUE Dépt. Laboratoire Entreprise SERSID

CONCLUSION

Les deux échantillons d'eau analysés présentent une dureté moyenne et une faible teneur en chlorures et en sulfates .

A cet effet et conformément aux normes , les deux échantillons ont une faible Agressivité et chimiquement potable.

INGENIEUR CHIMISTE.
M^{ELLE} BELKALLOUCH. N

Situation géographique du site de le barrage
Sur oued Ouizert

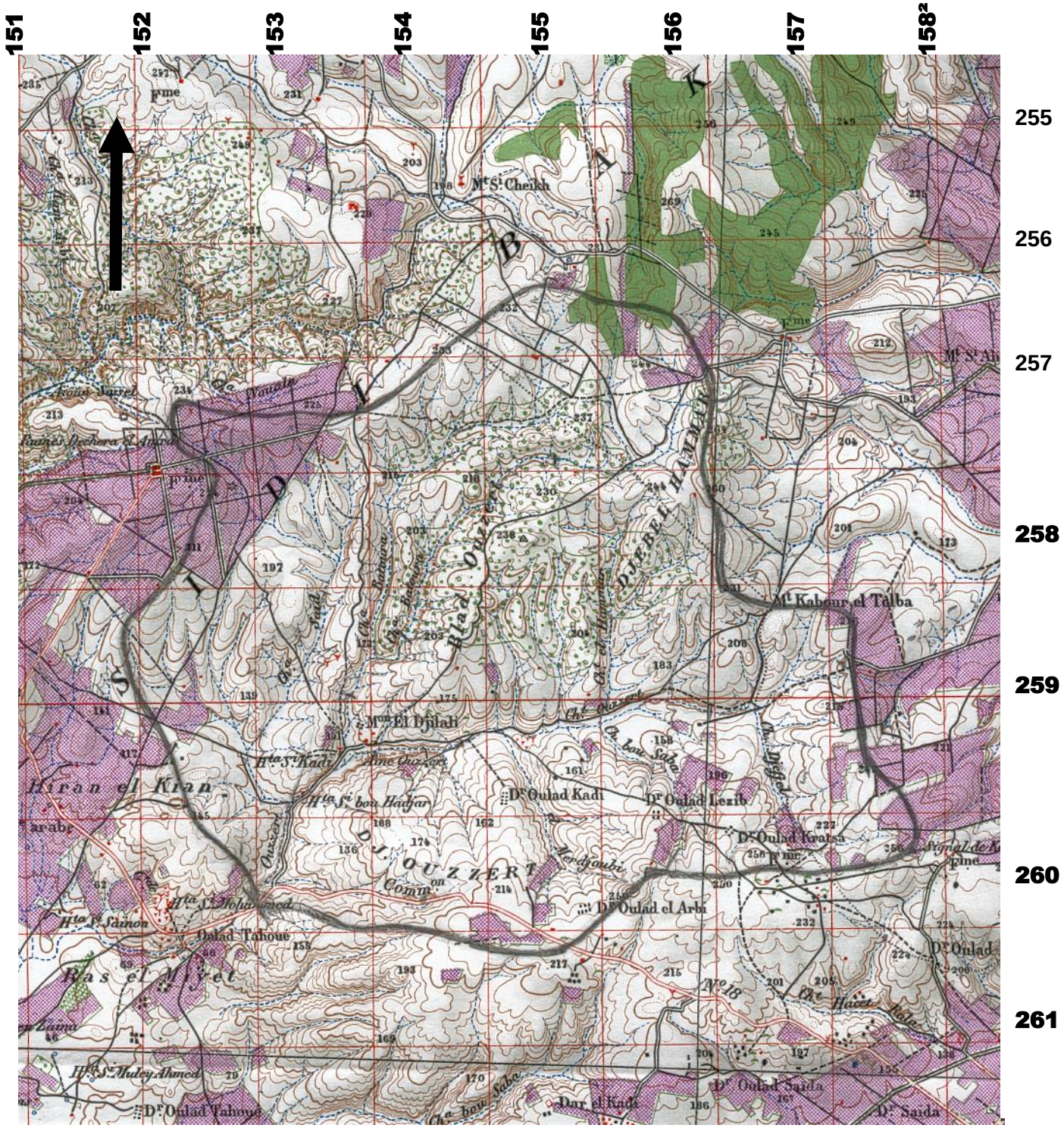

Extrait de la carte d'état major N° 180 LOURMEL

Echelle 1 /50.000 è

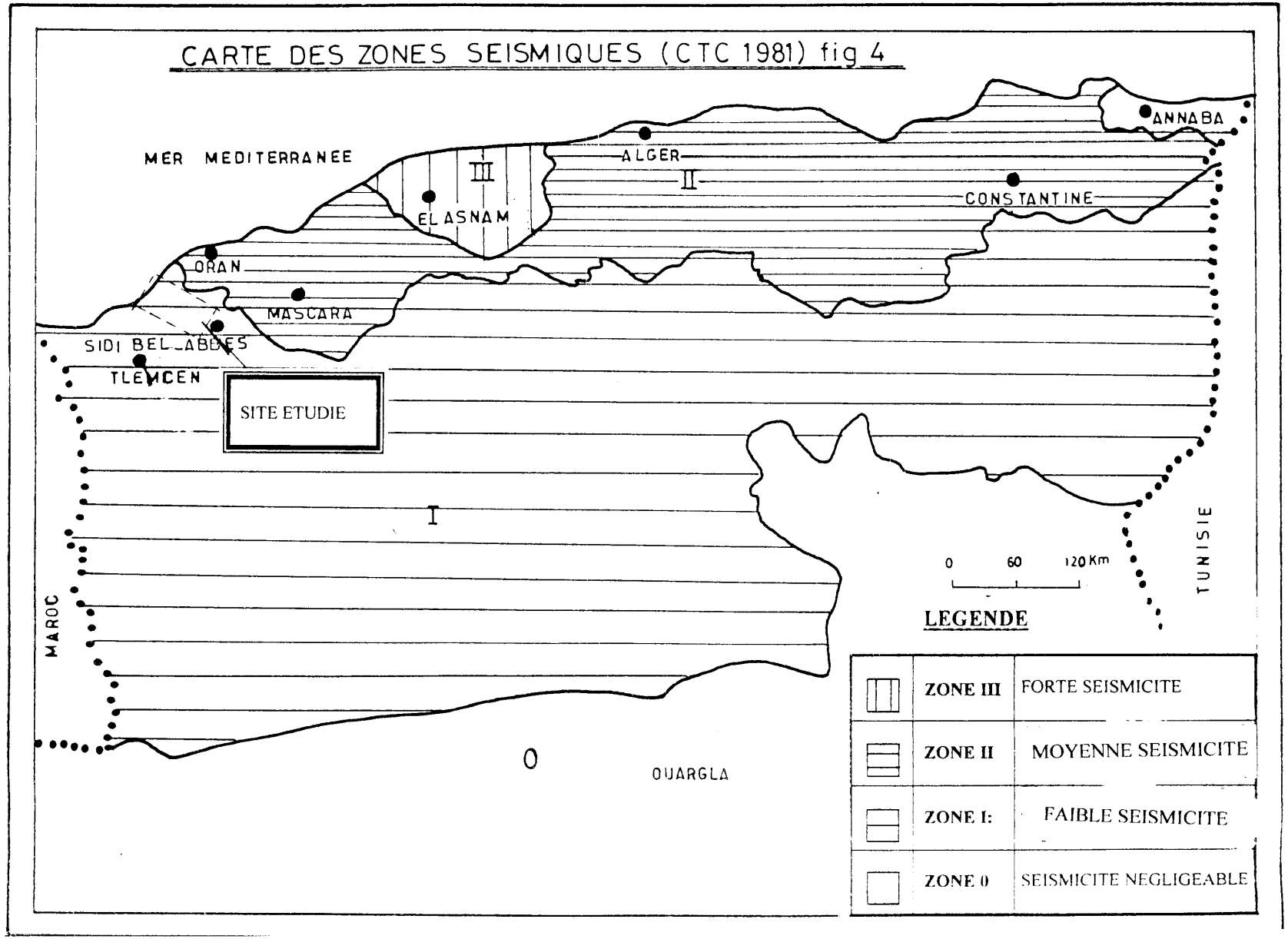
CARTE DES ZONES SEISMIQUES (CTC 1981) fig 4
MER MEDITERRANEE
ALGER
ANNABA
CONSTANTINE
EL ASNAM
ORAN
MASCARA
SIDI BEL ABBES
TLEMCEN
SITE ETUDIE
MAROC
TUNISIE
OUARGLA
III
II
I
0
0 60 120 Km
LEGENDE
ZONE III FORTE SEISMICITE
ZONE II MOYENNE SEISMICITE
ZONE I: FAIBLE SEISMICITE
ZONE 0 SEISMICITE NEGLIGEABLE

G '94^ O(" ED TAO"'
RETENUE COLLINAIRE

HA^S(-^"-^'TA^
FOUILLES

L^ 08 ^7; 00
ECHELLE 1/100

F1 (S3)

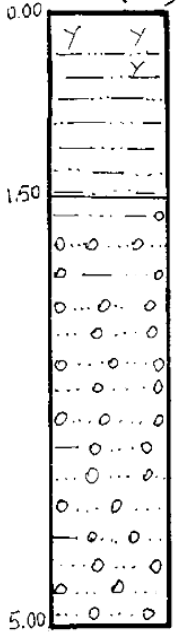

TERRE VEGETALE : LIMON BRUN MARRON, PEU CONSOLIDE.

SABLE, TRACES DE GRAVIER ET DE LIMON, MARRON-CLAIRE.

F2

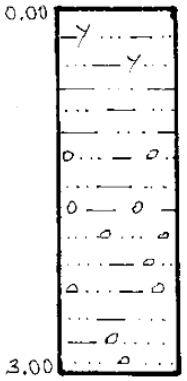

SABLE, TRACES DE GRAVIER ET DE LIMON, NOIRATRE.

F3

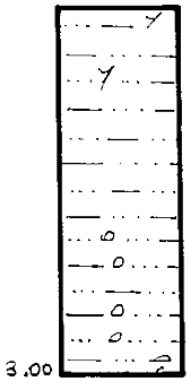

SABLE, TRACES DE LIMON ET GRAVIER NOIRATRE.

F4

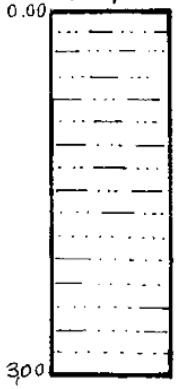

SABLE, TRACES DE GRAVIER ET DE LIMON, BEIGE.

F5

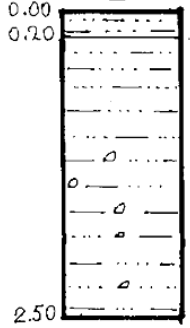

TERRE VEGETALE

ARGILE LIMONEUSE SABLEUSE, AVEC TRACES DE GRAVIER MARRON FONCE.

F6

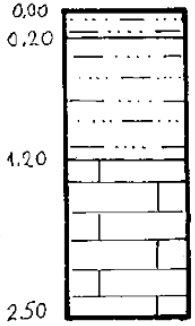

TERRE VEGETALE.

ARGILE LIMONEUSE SABLEUSE, MARRON.

CALCAIRE BLANC GRESEUX INDURE.